



TRACE ELEMENT CONTENT OF HUNGARIAN ACACIA HONEYS

Nikolett Czipa^{[a]*}, Zita Burján^[a], Dávid András^[a] and Béla Kovács^[a]

Paper was presented at the 4th International Symposium on Trace Elements in the Food Chain, Friends or Foes, 15-17 November, 2012, Visegrád, Hungary

Keywords: Honey, Trace element content, ICP-MS, ICP-OES

Forty-four acacia honey samples from beekeepers and hypermarkets were collected examined in our laboratory. Five elements (Al, Cu, Fe, Li, Sr, Zn) were analysed by ICP-OES and seven elements (As, Ba, Cd, Cr, Ni) were also determined by ICP-MS. Aluminium, iron and zinc were the most abundant elements found in our samples under study. The concentration was ranging between 100.0 and 4910 $\mu\text{g kg}^{-1}$ for Fe, 319.0 and 4440 $\mu\text{g kg}^{-1}$ for Zn and 242.0 and 3095 $\mu\text{g kg}^{-1}$ for Al. The lowest values were $4.648 \pm 4.184 \mu\text{g kg}^{-1}$ for Cd, $27.12 \pm 13.62 \mu\text{g kg}^{-1}$ for Cr and $42.49 \pm 20.37 \mu\text{g kg}^{-1}$ for As. The element concentration increased in the following order: Cd < Cr < As < Li < Ni < Ba < Cu < Sr < Al < Zn < Fe.

* Corresponding Authors

Fax: +36.52.417574

E-Mail: czipa@agr.unideb.hu

[a] Institute of Food Science, Quality Assurance and Microbiology, Centre for Agricultural and Applied Economic Sciences, University of Debrecen, 138. Böszörményi Str. Debrecen, H-4032, Hungary

Introduction

Honey is a very important and healthy food product that is defined by the EU (Eu Council Directive 2001/110/EC) as "The natural sweet product produced by *Apis Mellifera* bees from the nectar of plants from secretions of living plants, which bees collect, transform by combining with specific substances of their own, deposit, dehydrate, store and leave in honeycombs to ripen and mature." In the year 2010 the honey production of the world was 1.540.242 tons and in EU was 202.871 tons. Hungary was the fourth biggest honey producer in EU with 16.500 tons. Hungarian acacia honey is widely known famous due to his purity.

Quality of honeys depends on various parameters such as sugar, moisture, vitamin, amino acids, element content, enzyme activity, electrical conductivity, solid corpuscles, etc. Mineral content of honey is very low.¹ Some of the metals such as chromium, copper, iron, manganese and zinc are essential for human body,² but at the same time these elements can be toxic to human beings in high doses.³

Mineral content of a honey may be the indicator of the environment.⁴ The collecting area of the honey bees is about 7 km². Due to this large surface area the honey bees and their products is suitable to show the status of this area (e.g. chemical pollution).⁵

Methods

Samples

Examined acacia honey samples were collected from beekeeper and hypermarkets, the collecting area was Hungary. Ten samples each collected in the year 2007, 2008

2011 and 14 samples in 2009 respectively and stored in glass jars at room temperature in dark until analysis.

Reagents and solutions

All chemicals were of analytical-reagent grade or better. Nitric acid 69% and hydrogen peroxide 30% were purchased from VWR. Ultrapure water (Milli-Q[®] Integral 3/5/10/15 System, Millipore, France) was used to the preparation of solutions and dilutions.

Instrumentation

Samples were prepared according to the method of Kovács et al. ⁶ Determination of aluminium, copper, iron, lithium, strontium and zinc was carried out by inductively coupled plasma-optical emission spectrometry (ICP-OES) (Thermo Scientific iCAP 6300, England). Measuring of arsenic, barium, cadmium, chrome and nickel concentration was carried out by inductively coupled plasma-mass spectrometry (ICP-MS) (Thermo Scientific X Series 2, England). All measurement was performed in triplicate.

Results and discussion

The results are shown in Table 1. and Table 2. Iron was the most abundant element presented in most of the honey samples where as the cadmium was found at the lowest amount in all samples.

The quantity of iron was the highest in samples of the year 2007 and 2008. This value was four times higher in the year 2007 ($1787\text{--}4913 \mu\text{g kg}^{-1}$) as compared to year 2011 ($100\text{--}1781 \mu\text{g kg}^{-1}$). Zinc concentration was very high in 2009 ($2190\text{--}4440 \mu\text{g kg}^{-1}$) and 2011 ($319.1\text{--}3924 \mu\text{g kg}^{-1}$) samples which was two to three times higher than in other years. The zinc concentration in 2009 and 2011 samples was higher than the iron concentration. Aluminium content was nearly same in all years. The content of this element was higher in 2011 than the iron concentration.

Table 1. Trace element content by ICP-OES

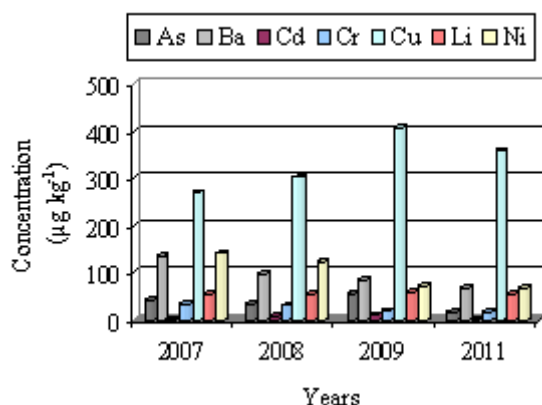
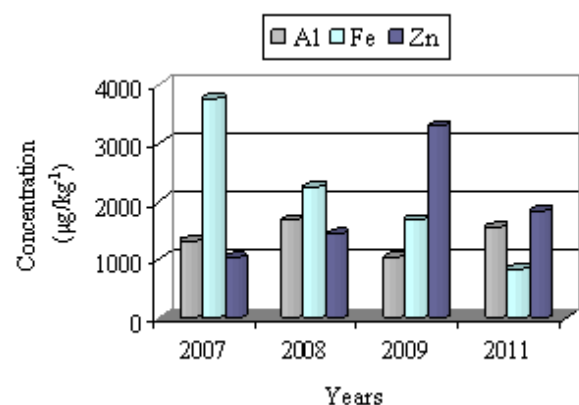
	Al	Cu	Fe	Li	Sr	Zn
2007	1324±262	269.2±56.9	3771±571	56.18±2.13	283.7±22.3	1032±472
2008	1678±273	302.6±42.3	2238±568	56.28±2.08	249.1±41.6	1442±4212
2009	1027±224	406.2±44.3	1696±609	58.53±0.89	350.0±51.8	3294±560
2011	1552±255	358.6±63.9	844±262	54.88±3.04	550.6±161.8	1838±423
Average	1463±211	324.9±59.9	2178±772	56.32±2.41	340.5±119.1	1747±471

Table 2 Trace element content by ICP-MS

	As	Ba	Cd	Cr	Ni
2007	40.98±9.46	135.6±40.5	2.294±0.291	34.66±15.44	141.5±32.4
2008	33.97±12.25	97.98±18.91	6.995±0.307	31.56±10.96	123.6±32.8
2009	55.75±11.91	84.60±17.57	10.45±3.94	19.20±6.75	71.88±36.81
2011	17.61±7.71	67.35±9.14	1.773±0.368	17.76±11.21	68.31±26.18
Average	42.49±20.37	98.07±47.37	4.641±4.184	27.12±13.62	98.19±47.69

Concentration of other elements was lower than $1000 \mu\text{g kg}^{-1}$. Lithium content wasn't shown any change during the four years. Nickel and barium were found in the samples in the same level. Copper concentration was the highest in 2009 ($338.2\text{-}454.3 \mu\text{g kg}^{-1}$) and the lowest in 2007 ($210.7\text{-}374.5 \mu\text{g kg}^{-1}$). Strontium content was two times higher in 2011 ($327.2\text{-}831.3 \mu\text{g kg}^{-1}$) than 2007 and 2008 ($261.4\text{-}319.3$ and $185.2\text{-}400.7 \mu\text{g kg}^{-1}$).

The three elements in the lowest concentration were cadmium, chromium and arsenic. Cadmium level was very low, its value ranged between 0.112 and $15.5 \mu\text{g kg}^{-1}$. The concentration of this element was more times higher in 2009 ($6.49\text{-}15.5 \mu\text{g kg}^{-1}$) than 2011 ($0.11\text{-}4.07 \mu\text{g kg}^{-1}$). Chrome content was higher in 2007 and 2008 than 2009 and 2011, this value was nearly duplex. The lowest arsenic concentration ($5.65\text{-}26.5 \mu\text{g kg}^{-1}$) was measured in 2011 and the highest ($33.8\text{-}69.1 \mu\text{g kg}^{-1}$) in 2009

**Figure 1.** Element content of acacia honeys I.**Figure 2.** Element content of acacia honeys II.

The average concentration of the examined elements decreased in the following order: $\text{Fe} > \text{Zn} > \text{Al} > \text{Sr} > \text{Cu} > \text{Ni} > \text{Ba} > \text{Li} > \text{As} > \text{Cr} > \text{Cd}$. In 2009 the barium concentration of the honey samples was higher than the nickel content (Figure 1.). The iron concentration was the highest in 2007 and 2008 but in 2009 and 2011 the zinc content was the higher. In 2007 and 2008 the zinc content was followed by aluminium concentration that was lower than the iron content in 2009. The concentration of aluminium and iron was inverse of the previous year (Figure 2.).

Among the elements examined so far there was no significant relation found. The nearest correlation was $r^2=0.536$ between the cadmium and arsenic content. This was followed by cadmium and lithium concentration with $r^2=0.511$.

Table 3. Comparison of trace element content of honey types from different country

	Tuzen et al.	Pisani et l.	Terrab et al.	Our results
Al	83-325	No data	445-25400	242-3095
As	No data	2.78-20.20	0.00-1930	5.65-69.12
Ba	No data	218-2634	280-1116	18-302
Cd	0.90-17.90	1.00-15.30	0.00-50.00	0.11-15.52
Cr	No data	No data	20.0-440.0	3.3-48.4
Cu	230-2410	172-5900	2620-7800	139-552
Fe	1800-10200	970-13700	4920-24100	100-4912
Li	No data	No data	11700-27700	53-61
Ni	5.3-29.9	77.0-2760.0	170.0-660.0	4.5-392.6
Sr	No data	850-2010	0-1010	185-831
Zn	1100-12700	720-3660	70-16800	319-4440

Compared to our results Terrab et al.⁷ reported higher element concentrations of avocado honeys from Spain. Tuzen et al.¹ measured lower aluminium concentration in the multifloral honeys from Turkey, but determined iron, nickel and zinc content was higher than our values. The barium, copper, iron, nickel and strontium content in the honey samples from Siena County⁸ showed higher concentrations (Table 3).

The lithium content in Spain honeys samples was more than two times higher than our values. In case of cadmium concentration, the difference among the countries was not very important.

From our results it can be concluded, that the concentration of some element may alter year after year, but in case of main toxic elements (As, Cd) this alteration does not mean much as regards to food-safety instance - these elements are found in a very low concentration.

Acknowledgements

The research work was supported by the TÁMOP 4.2.1./B-09/1/KONV-2010-0007 and TÁMOP-4.2.2/B-10/1-2010-0024 projects. The project was co-financed by the European Union and the European Social Fund.

References

- ¹Tuzen, M.; Silici, C.; Mendil, B.; Soylak, M. *Food Chem.* **2007**, *103*, 325-330.
- ²Falco, G.; Gomez-Catalan, C.; Llobet, J.M.; Domingo, J.L. *Trace Elements and Electrolytes* **2003**, *20*, 120-124.
- ³Domingo, J.L. *J. Toxicol. Environ. Health* **1994**, *42*, 123-141.
- ⁴Przybylowski, P.; Wilczynska, A. *Food Chem.* **2001**, *74*, 289-291.
- ⁵Leita, L.; Muhlbachova, G.; Cresco, S.; Barbattini, R.; Mondini, C. *Environ. Monitoring and Assessment* **1996**, *43*, 1-8.
- ⁶Kovács, B.; Györi, Z.; Prokisch, J.; Loch, J.; Dániel, P.; *Commun. soil sci. plant anal.*, **1996**, *27*(5-8), 1177-1198.
- ⁷Terrab, A.; Recamales, A.F.; González-Miret, M.L.; Heredia, F.J. *Food Chem.*, **2005**, *92*, 305-309.
- ⁸Pisani, A.; Protano, G.; Riccobono, F. *Food Chem.*, **2008**, *107*, 1553-1560

Received: 15.10.2012.
Accepted: 12.11.2012.



LEAD AND ZINC IN THE SUSPENDED PARTICULATE MATTER AND SETTLED DUST IN BUDAPEST, HUNGARY

Péter Sipos^{[a]*}, Viktória Kovács Kis^[b], Emő Márton^[c], Tibor Németh^[a], Zoltán May^[d] and Zoltán Szalai^[e]

The paper was presented at the 4th International Symposium on Trace Elements in the Food Chain, Friends or Foes, 15-17 November, 2012, Visegrád, Hungary

Keywords: air pollution, heavy metals, magnetite, clay minerals, urban geochemistry

Urban airborne particulate matters and dusts can be both ingested and inhaled, causing health damage due to their size, shape and nature of toxic components. Our aim was to characterize the concentration, enrichment and host phases of lead and zinc in total suspended particulate matter (TSP) and settled dust (SD) samples from Budapest, Hungary. TSP samples were collected from the air filters placed in the respiration channels of thermal power stations, while SD samples were collected in glass pots next to a busy street. Detailed mineralogical, chemical and magnetic susceptibility analyses were carried out on these samples. The concentrations of both elements were generally higher in the TSP (330-3597 mg kg⁻¹ for Pb and 1342-19 046 mg kg⁻¹ for Zn) than in the SD samples (58-474 mg kg⁻¹ for Pb and 399-1140 mg kg⁻¹ for Zn). Additionally, they showed moderate contamination in the SD samples, while moderate to heavy contamination in TSP samples with enrichment factors up to 4.9 for Pb and 5.3 for Zn. Transmission electron microscopy (TEM) analyses showed that magnetite may contain significant amount of Zn (up to 2.60 wt%) and Pb (2.50 wt%). However, Zn could be also associated with layer silicates (up to 5.06% by wt) and Ca-carbonates. Moreover, Zn also appeared as major phase constituent in carbonates and oxides. Magnetite particles are resistant to weathering releasing its toxic components slowly to the environment, while layer silicates (and carbonates, Zn-oxides) may be the potential source of mobile toxic metals in the studied materials.

Corresponding Author

Fax: +36-1-319-3137

E-Mail: sipos@geochem.hu

- [a] Institute for Geological and Geochemical Research, Research Centre for Astronomy and Earth Sciences, Hungarian Academy of Sciences, H-1112 Budapest, Budaörsi út 45., Hungary
- [b] Institute of Technical Physics and Materials Science, Research Centre of Natural Sciences, Hungarian Academy of Sciences, H-1121 Budapest, Konkoly-Thege Miklós út 29-33, Hungary
- [c] Paleomagnetic Laboratory, Geological and Geophysical Institute of Hungary, H-1145 Budapest, Columbus utca 17-23, Hungary
- [d] Institute of Materials and Environmental Chemistry, Research Centre of Natural Sciences, Hungarian Academy of Sciences, H-1025 Budapest, Pusztaszeri út 59-67, Hungary
- [e] Geographical Institute, Research Centre for Astronomy and Earth Sciences, Hungarian Academy of Sciences, H-1112 Budapest, Budaörsi út 45., Hungary

Lead and zinc are among the most frequent heavy metal pollutants in the urban environment⁵. Soils, road dusts and airborne particulate matter generally show significant enrichment in their Pb and Zn contents there. The most important source of these metals is the traffic but they may also originate from domestic and industrial combustion for heating purposes and are the common component of construction materials of the built environment, too⁶.

Studies on sources, compositions, and distribution of dust and particulate matter components are necessary for their risk assessment to atmospheric quality, ecology and human health. This is especially true for the urban environment, where population and traffic density are relatively high, and human exposure to hazardous substances has expected to be significantly high⁷. In this study detailed mineralogical, as well as geochemical and magnetic analyses were carried out on total suspended particles and settled dust samples from Budapest Hungary.

Introduction

Airborne particulate matter has been widely associated with health disorders as presented by various studies. The settled dust (SD) sediment is created by particles with great sedimentation power and their retention time in the atmosphere is very short, while the total suspended particles (TSP) may travel great distances due to their small particle size causing contamination far away from their sources¹. Recent attention has focused on the characterization of their size fractions below 10 µm as they may cause the most intense health damage due to their easy penetration to the innermost regions of the lung². However, particles with a diameter of up to 100 µm can be inhaled by nose or mouth, and those below 32 µm may reach the bronchial tubes too³. These particles, after their sedimentation, can also contaminate soils, groundwater (and even the food chain) by their mobile toxic components⁴.

Our aim was (1) to study the concentrations of and the degree of enrichment for lead and zinc, and (2) to identify and characterize the mineral phases associated with these chemical elements in such materials.

Materials and Methods

Settled dust (SD) samples were collected according to the Hungarian standard (MSZ 21454/1-83 1983)⁸. Two parallel sampling pots were placed at the front and the backsides of a building at a busy road and at 2 meters height. The number of crossing vehicles and trains are over 50,000 and 250 per day respectively. The seasonal sampling was carried out for two continuous years. Samples were not collected in winter due to potential freezing and breaking of the sampling pots.

Total suspended particle (TSP) samples were collected from the air filters placed in the respiration channels used for the air supply of the methane-heated turbines in four thermal power stations (Csepel – CS, Kelenföld – KF, Kőbánya – KB, Újpest – UP). The filters are in use until their transmission is high enough (up to even a year). During this time such a filter may filter more than one million m³ of air monthly. They are generally placed at 5-15 m height so the contribution of soil to TSP material is minimal. However, contribution of soot and carbonaceous particles may be overrepresented with this sampling method due to the result of methane combustion in the thermal power stations. Samples were removed from the filters mechanically. Large plant and animal debris were removed by passing them through a 2 mm sieve.

A Fritsch Analysette Microtech A22 laser diffraction analyser determined particle size distribution of the samples. Magnetic susceptibility (MS) measurements were carried out using a KLY-2 Kappabridge instrument operating with one frequency. The bulk samples were characterized for their mineralogical composition by a Philips PW 1710 X-ray diffractometer (XRD).

Concentrations of Pb and Zn in the bulk samples were analysed by a Thermo Niton XL3 type X-ray fluorescent spectrometer (XRF). Enrichment factors were calculated after Ji et al.⁹ and using the geochemical background values from the geochemical map of Hungary¹⁰.

High resolution transmission electron microscopy (HR-TEM) and selected area electron diffraction (SAED) analyses were carried out to characterize the mineralogical and chemical composition of individual mineral particles in the samples with special emphasis on those containing Pb and Zn. The dust samples were suspended in ethanol, and then they were dropped onto a holey carbon coated Cu grid for the analyses. The measurements were performed on a Philips CM 20 TEM with a LaB6 filament, equipped with a Noran energy dispersive spectrometer (EDS). For the chemical analyses a 20 nm spot size and counting times of 100 s were used. The relative standard deviations of the EDS analyses are below 2.5%, 10% and 50% for element concentrations >10%, 1-10%, and <1%, respectively. We pretended to analyze only one discrete particle in each case, which could be confirmed from the corresponding diffraction pattern.

Results and Discussion

Samples characterization

The settling dust (SD) samples consist of particles with a size generally below 100 μm with two maxima (Figure 1): a higher one at around 35 μm and a lower one at around 11 μm. Between 10 and 30% of the particles are below 10 μm. In contrast, total suspended particulate (TSP) samples consist of much smaller particles as it is expected. Their particles are generally lower than 50 μm, and can be characterized mostly with one maximum at around 11 μm. Between 45 and 80% of their particles are below 10 μm. TSP samples from the UP thermal station, however, show a secondary maximum at around 35 μm. A slight shoulder at around 3 μm is characteristic of each sample types.

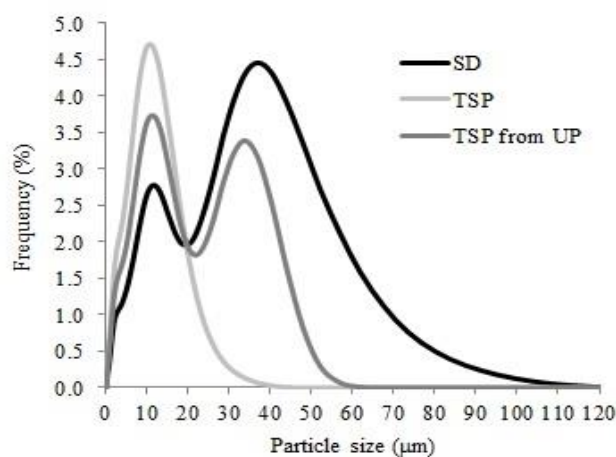


Figure 1. Characteristic particle size distribution types of the studied samples

The bulk mineralogical composition of the samples reflects primarily the geological characteristics of the sampling areas. The main components of the SD samples are in the order of their frequency: quartz (60-90%), dolomite (2-20%), calcite (1-15%), feldspar (3-6%), mica (1-5%), chlorite (1-5%). Such phases also appear in the TSP samples with different ratios: quartz (20-30%), carbonates (dolomite and calcite 10-20%), clay minerals (5-15%) and feldspars (around 5%). These phases are characteristic natural components of urban dusts¹¹. However, Zhao et al.¹² found that some portion of these phases (quartz, feldspar, carbonates) could appear also in amorphous forms in the urban settled dust that suggest their anthropogenic origin. Significant amount of amorphous (organic?) material was found in the summer SD samples, probably due to increased contribution of plant materials (debris, pollen etc.) and the unfortunate presence of algae in the sampling pots. The presence of amorphous materials may be as high as 40% in the TSP samples, which is composed both of soot and debris of plant and animal remains. Trace amounts of gypsum also appear in the autumn SD samples. It also appears in the TSP samples (up to 5%) together with halite (up to 10%). Gypsum is general component of the construction materials, but it may form also due to the reaction between sulfuric acid and calcic material in several anthropogenic processes, while halite is common deicing agent¹³. Additionally, both XRD and MS analyses showed the presence of large amounts of magnetite (up to 15%) in the TSP samples. This mineral was detectable in the SD samples only by magnetic analyses. Such particles have long been recognized to be associated with atmospheric particulates in the urban environment¹⁴. They are mainly derived from combustion processes, such as industrial, domestic and vehicle emissions or from abrasion products from asphalt and from vehicles brake systems¹⁵.

Magnetic properties of the studied samples show large variation. Apparent susceptibility values for SD samples were found to be between 6 and 253 10⁻⁶ SI, while their mass susceptibility values varied between 0.7 and 9.4 10⁻⁶ m³ kg⁻¹. These values were found to be much higher for the TSP samples, as it was expected from their much higher magnetite content. Their apparent and mass susceptibility values were in the ranges of 383 - 2316 10⁻⁶ SI and 7.7 - 45 10⁻⁶ m³ kg⁻¹, respectively. These latter values are similar to those of PM10 samples.

Table 1. Concentrations, monthly deposition rates and enrichment factors of Pb and Zn in the settled dust (SD) samples.

SD sample	Concentration, mg kg ⁻¹		Monthly deposition, mg m ⁻²		Enrichment factor	
	Pb	Zn	Pb	Zn	Pb	Zn
Spring/2009/Front	293 ± 25	546 ± 50	4.1	7.6	2.4	1.8
Spring/2009/Back	99 ± 14	462 ± 48	0.3	1.2	1.4	1.6
Summer/2009/Front	79 ± 15	553 ± 52	0.6	4	1.1	1.8
Summer/2009/Back	58 ± 13	399 ± 44	0.1	0.8	0.8	1.4
Autumn/2009/Front	135 ± 18	812 ± 62	0.6	3.3	1.7	2.2
Autumn/2009/Back	474 ± 33	1095 ± 74	0.6	1.3	2.9	2.4
Spring/2010/Front	119 ± 20	525 ± 47	1.7	7.7	1.5	1.7
Spring/2010/Back	352 ± 29	555 ± 52	0.6	1	2.6	1.8
Summer/2010/Front	200 ± 21	613 ± 54	0.7	2	2.1	1.9
Summer/2010/Back	209 ± 23	1140 ± 78	0.3	1.4	2.1	2.4
Autumn/2010/Front	162 ± 19	692 ± 57	1.1	4.8	1.9	2.0
Autumn/2010/Back	304 ± 28	592 ± 57	0.1	0.3	2.5	1.8

Metals concentrations and enrichment

The average Pb (207 mg kg⁻¹) and Zn (665 mg kg⁻¹) concentrations and their ranges (Table 1) in the SD samples are in the similar range as found in 12 Polish towns¹⁶. There is no significant linear relationship between Pb and Zn concentrations in these samples ($r = 0.49$; $p = 0.05$). Both metals show moderate contamination in these samples with similar ranges and averages (EF=1.9) of their enrichment factors. The TSP samples show much higher metal concentrations (Table 2) with averages of 846 mg kg⁻¹ for Pb and 4837 mg kg⁻¹ for Zn. Consequently, they can also be characterized by much higher enrichment factors suggesting generally heavy contamination for both metals (EF=3.5 for Pb and 3.9 for Zn). During a study concerning to 15 Chinese cities, it was found that the total fraction of the urban dusts (<100 μm) is practically uncontaminated, while the fine fractions (<10 μm) were mostly heavily contaminated with Pb, Zn and other metals (Cr, Co, Cu)¹⁷. So the higher concentration and enrichment of the studied metals in TSP than in SD samples is not unexpected as the former samples can be characterized by much greater ratio of PM10 particles.

Interestingly, metal concentrations are often higher in the backside SD samples than in the front-side ones in spite that the intense traffic should affect primarily the front-side of the building. As the mass of SD samples could be also affected by the contribution of algae or remnants of algacide, monthly deposition values are much more useful for comparison. These values are much higher at the front-side for both metals than at the backside as it is expected (Table 1). These values were found to be in the characteristic range for urban areas¹⁸.

The deposition rates of the studied metals show significant linear relationship to each other ($r = 0.83$; $p = 0.05$) suggesting the similar deposition characteristics of their host phases. Our unpublished data on the deposition characteristics of the dust around the study building suggest the dominance of re-suspension of roadside dust and soil in dust deposition. Threshold limit value is only given for Pb in Hungary that is 1.2 mg m⁻²¹⁹. This value is exceeded only in two times in the spring samples at the front-side of the building.

Table 2. Concentrations and enrichment factors of Pb and Zn in the total suspended particle (TSP) samples.

TSP sample	Concentration, mg kg ⁻¹		Monthly deposition, mg m ⁻²	
	Pb	Zn	Pb	Zn
KF 06-08/2010_1	2785 ± 88	5297 ± 152	4.7	4.0
KF 06-08/2010_2	1782 ± 59	2679 ± 91	4.2	3.3
KF 06-11/2010_1	3533 ± 87	4902 ± 128	4.9	3.9
KF 06-11/2010_2	3597 ± 89	4837 ± 128	4.9	3.9
KB 07/2009-07/2010	496 ± 32	1463 ± 69	3.0	2.7
KB 04-09/2010	559 ± 35	1342 ± 67	3.1	2.7
UP 01-12/2010	846 ± 41	19046 ± 237	3.5	5.3
UP 03-08/2010	434 ± 29	12880 ± 189	2.8	4.9
CS 03/2010-08/2011	330 ± 20	2340 ± 90	2.6	3.2

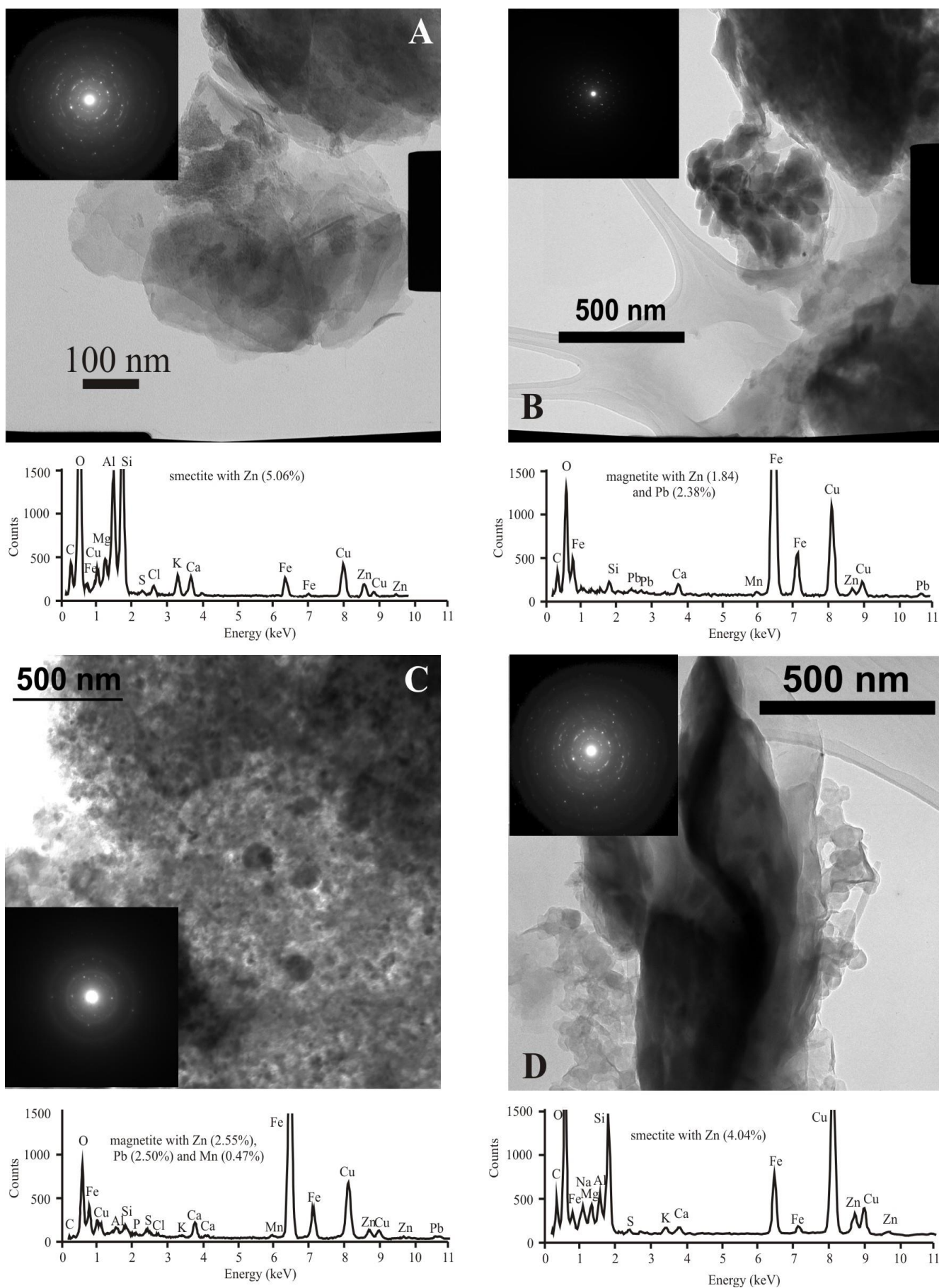


Figure 2. Characteristic Pb and Zn bearing phases in the studied samples. Transmission electron microscopy micrograph, diffraction pattern and EDS spectra of a smectite with Zn (A) and a magnetite with Pb and Zn (B) from a settled dust sample, as well as that of a magnetite with Pb and Zn (C) and smectite with Zn (D) from a total suspended particulate sample.

Either apparent or mass susceptibility values do not show any linear relationship with Pb and Zn concentrations both in the SD and TSP samples. Although these metals are often associated with magnetic particles in urban environment²⁰, several studies showed that significant proportion (up to 60%) of total metal concentration in dust could be dissolved by weak acids, which did not mobilize them from magnetite²¹. In contrast, apparent susceptibility and metal deposition values show strong linear correlation both for Pb ($r = 0.89$; $p = 0.05$) and Zn ($r = 0.92$; $p = 0.05$). Both apparent susceptibility and metal deposition values are not influenced by the possible errors in weight measurements of SD samples. This suggests that these metals travel together at least partly with magnetic particles primarily in case of re-suspension of road dust and roadside soils.

Host phases for Pb and Zn

TEM analyses showed that the most significant components of the SD samples are different mineral phases. The most frequent particles are gypsum, quartz, feldspar, layer silicates, calcite, dolomite as well as Fe and Ti oxides as XRD analyses also showed partly. The most characteristic size range is between 10 and 20 μm for most of the particles, but its dominance may be affected by the samples preparation technique. The most important Pb and Zn bearing phases are magnetite and clay minerals in these samples (Figure 2a. and b.). Additionally, Zn was found to be associated with a calcite particle in one case. This metal could be associated both with clay and Fe-oxide particles, while lead primarily to the latter ones. The silicate and oxide particles are often form aggregates with each other. The Zn content of clay minerals can be as high as 5 wt%, while Fe-oxides are characterized by a slightly lower Zn content (up to 2.5 wt%). The Pb content of the latter one phases is generally between 2 and 3 wt% and they also contain other trace metals (~0.5 wt% Mn). Among Fe-oxide particles both magnetite and hematite were identified. Additionally, ilmenite and titanite were also found in the samples but they do not contain detectable amount of Pb and Zn.

The soot aggregates consisting of nano-sized (few tens of nm) soot particles are the dominant phases in the TSP samples. This is in good agreement with the presence of high amounts of X-ray-amorphous (organic) material found in the samples by XRD analyses. The most important Pb and Zn bearing mineral phases were found to be spherular or xenomorphic magnetite particles (Figure 2c). They sometimes contain 2-3 wt% Pb and Zn. These magnetite particles often form aggregates and are closely associated with soot and/or clay minerals. In samples with high magnetite content metal-free magnetite spherules up to a few μm sizes also appeared. Samples also contain ferrihydrite and probably hematite, but their amount is much lower than that of magnetite. Clay minerals and mica particles were found to contain significant amount of Zn (up to 5 wt%) and also Pb in much smaller amount (up to 0.41 wt%) (Figure 2d). Additionally, single ZnO and ZnCO₃ (smithsonite) particles were also found in the sample with highest Zn content (collected at the UP thermal station). Again a single aggregate consisting of iron oxide and calcium carbonate was also found to contain significant amount of Pb (4.88 wt%) suggesting the presence of Pb also in carbonates. However, more direct data is needed to support this latter supposition.

Anthropogenic magnetite particles often contain Pb and Zn as showed by the close relation between their concentrations in the urban particulate matter and magnetic properties²⁰. Additionally, Zn mostly associated to layer silicates both in natural and contaminated soils²². Magnetite, metal-carbonate and Zn-oxide particles in the dust may be primarily originated from anthropogenic emissions, while clay particles derived rather from the re-suspension of roadside dust and urban soils. Magnetite particles are resistant to weathering releasing its toxic components slowly to the environment²³. However, layer silicates, carbonates and oxides are much less resistant than magnetite²⁴ so they may be the potential source of mobile Pb and Zn metals in the studied samples.

Conclusions

TSP characterized by smaller particle sizes contain much higher ratio of potentially anthropogenic phases (amorphous phases, salts, magnetite), while they can be hidden by the large amount of coarse particles of soil origin in the SD samples. Accordingly, the concentrations and enrichment of the studied metals is also higher in the TSP samples as compared to SDs. Lead and zinc concentrations do not show any linear relationship with magnetic susceptibilities in both types of the samples. Only the close correlation between the metal deposition and apparent susceptibility values suggests the partial association of Pb and Zn with magnetic particles in the SD samples where the particles from soil re-suspension dominate.

Although trace-metal-free magnetite particles also appear in the studied samples, this phase is the most important host-phase for Pb and it often contains also Zn supporting the relation between metal deposition and apparent susceptibility of settling dust samples. On the other hand, highest amounts of Zn were found to be hosted with clay minerals. This latter metal also associated with carbonates and Zn-oxide phases in much smaller rate. Magnetite particles are resistant to weathering releasing its toxic components slowly to the environment, while layer silicates (and carbonates, oxides) may be the potential source of mobile toxic metals in the studied materials.

Acknowledgements

The project was financially supported by the OTKA (K76317, K75395 and PD 75740). B. Major (Budapesti Erőmű Zrt.) is thanked for the TSP samples. P. Sipos also thanks for the support of the János Bolyai Research Scholarship of the Hungarian Academy of Sciences.

References

- Remeteiova, D., Smincakova, E., Florian, K., *Microchim. Acta*, **2007**, *156*, 109.
- Samet, J. M., Dominici, F., Curriero, F. C., Zeger, S. L., Coursac, I., *New Engl. J. Med.*, **2000**, *343*, 1742.
- UNEP & WHO, *Urban Pollution in Megacities of the World. Earth Watch: Global Environment System. Blackwell, Oxford*, **1992**.

- ⁴ Seiler, H., Sigel, H., Sigel, A., *Handbook on Toxicity of Inorganic Compounds*. Marcel Dekker INC, New York, **1988**.
- ⁵ Li, X. D., Poon, C. S., Pui, S.L. *Appl. Geochem.*, **2001**, *16*, 1361.
- ⁶ Sutherland, R.A., *Environ. Geol.*, **2000**, *39*, 611.
- ⁷ Vardoulakis, S., Fisher, B. E. A., Pericleous, K., Gonzalez-Fresca, N., *Atmos. Environ.*, **2003**, *37*, 155.
- ⁸ MSZ 21454/1-83, *Test of solid impurities in ambient atmosphere. Determination of settling dust mass. Hungarian Standards Institution*, **1983**, G 23.
- ⁹ Ji, Y., Feng, Y., Wu, J., Zhu, T., Bai, Z., Duan, C., *J. Environ. Sci.*, **2008**, *20*, 571.
- ¹⁰ Ódor, L., Horváth, I., Fügedi, U., *J. Geochem. Explor.*, **1997**, *60*, 55.
- ¹¹ Farkas, I., Weiszbürg, T., *Földtani Közlöny*, **2006**, *136*, 547.
- ¹² Zhao, J., Peng, P., Song, J., Ma, S., Sheng, G., Fu, J., *Air Qual. Atmos. Health*, **2010**, *3*, 139.
- ¹³ Panigrahy, P.K., Goswami, G., Panda, J.D., Panda, R.K., *Cem. Concr. Res.*, **2003**, *33*, 945.
- ¹⁴ Hunt, A., Jones, J., Oldfield, F., *Sci. Total. Environ.*, **1984**, *33*, 129.
- ¹⁴ Gautam, P., Blaha, U., Appel, E., *Atmos. Environ.*, **2005**, *39*, 2201.
- ¹⁵ Gautam, P., Blaha, U., Appel, E., *Atmos. Environ.*, **2005**, *39*, 2201.
- ¹⁶ Krolak, E., *Pol. J. Environ. Stud.*, **2000**, *9*, 517.
- ¹⁷ Ji, Y., Feng, Y., Wu, J., Zhu, T., Bai, Z., Duan, C., *J. Environ. Sci.*, **2008**, *20*, 571.
- ¹⁸ Shahin, U., Yi, S. M., Paode, R. D., Holsen, T. M., *Environ. Sci. Technol.*, **2000**, *34*, 1887.
- ¹⁹ Bartófi, I., *Environmental technology (in Hungarian)*, Mezőgazda Kiadó, Budapest, **2000**.
- ²⁰ Filipelli, G. M., Laidlaw, M. A. S., Latimer, J. C., Raftis, R. *GSA Today*, **2005**, *15*, 4.
- ²¹ Duong, T. T. T., Lee, B.K. *Atmos. Environ.*, **2009**, *43*, 3502.
- ²² Manceau, A., Lanson, B., Schlegel, M.L., Harge, J. C., Musso, M., Eybert-Berard, L., Hazemann, J. L., Chateigner, D., Lambelle, G. M., *Am. J. Sci.*, **2000**, *300*, 289.
- ²³ Graham, R. C., Weed, S. B., Bowen, L. H., Buol, S. W., *Clay. Clay. Miner.*, **1989**, *37*, 19.
- ²⁴ Vogelein, A., Pfister, S., Scheinost, A. C., Marcus, M. A., Kretzschmar, R., *Environ. Sci. Technol.*, **2005**, *39*, 6616.

Received: 15.10.2012.

Accepted: 13.11.2012.



STRUCTURE STABILITY OF OPTIMALLY- PRASEODYMIUM-DOPED-123- $Y_{0.85}Pr_{0.15}Ba_2Cu_3O_7$ SUPERCONDUCTOR

Khaled M. Elsabawy^{[a,b]*} and Morsy M. Abou-Sekkina^[a]

Keywords: Superconductor; Solution Synthesis; Visualization; X-ray; Scanning Electron Microscopy; Praseodymium-doped YBCO

The pure YBCO ($YBa_2Cu_3O_7$) and optimally praseodymium containing superconductors with general formula; $Y_{1-x}Pr_xBa_2Cu_3O_z$, where $x = 0.15$ mole respectively, were synthesized by solution route and characterized by XRD, SEM and Raman spectra. X-ray analyses indicated that both of pure and Pr-doped-123-YBCO has orthorhombic superconducting phase. Visualization investigations were made depending upon crystallographic data of pure and Pr-doped 123-YBCO. Both crystals are formed via DIAMOND IMPACT CRYSTAL visualizer. Comparison of structural parameters such as bond length, angles and torsion on angles of pure and Pr-doped 123-YBCO was performed to find out why this ratio of doping ($x \sim 0.15$ mole) in most cases is reported to be optimum one in literatures.

* Corresponding Authors

E-Mail: ksabawy@yahoo.com

[a] Chemistry Department, Faculty of Science, Tanta University- 31725-Tanta-Egypt)

[b] Faculty of Science-Chemistry Department-Taif University-Taif -Alhawyah-888-Saudi Arabia)

Introduction

Cuprate compounds of perovskite structure have formed a big group. In recent years a research field of perovskite and related oxide materials has emerged. Because of complicated structure, it is difficult to understand the properties of cuprate. The relationship between T_c value and carrier concentration in the high T_c systems has been understood well based on an electronic phase diagram. But, the change of the carrier concentration simultaneously causes the change of the structure of the superconductors. The effect of the structural change on the T_c value has not been studied in detail. Xiao et al.¹ observed the existence of two subtle thermal transitions in $YBa_2Cu_3O_{7-\delta}$ (YBCO) and the Bi-system compounds. Some workers even reported the existence of more than forty different phases in Bi-system compounds^{2,3}. However, it is noticed that few detailed reports about the effect of Zn- and Pr-doped on the structural change of YBCO are available in literature. In the present paper, we report the subtle structural changes of the Zn- and Pr-doped YBCO, and analyze the different roles of Zn and Pr. We also suggest that the structural change has some relation with the T_c value.

The cuprate layered 123-YBCO is considered the most interesting superconducting materials for various reasons, such as their high critical temperature T_c and high critical current density J_c . Many researchers have investigated the effect of metal cation dopants on the 123-YBCO superconducting system⁴⁻⁸. Delamare et al.⁹ have studied the effect of CeO_2 and PtO_4 mixed oxide additives on the microstructural and critical current density J_c . They reported that (Ce + Pt) oxides added to the melt-textured YBCO have significantly improved the value of $J_c \sim 4.3 \times 10^4$ A cm^{-2} . The role of additives as impurity phases like (silver, silver oxide) to improve processing magnetization and microstructure of YBCO system was studied by many authors¹⁰⁻¹⁶. Tomita et al.¹⁷ investigated effect of Nd-substitution partially for yttrium sites on Raman spectra of

YBCO system and reported that, Raman shifts of the vibrational modes of oxygen O_4 and of the couple O_2-O_3 are affected sharply by an internal pressure effect resulted from yttrium substitution.

The aim of the present work is to optimize the influence of Pr-doping ratio $x=0.15$ mole on yttrium sites on the different structural parameters affected on lattice stability. The selected optimum Pr-doped sample was quoted from the work already done by the author himself and the selection was based on superconducting properties (best $T_{c-offset} = 92.3$ K at $x= 0.15$ mole).

EXPERIMENTAL

Samples Preparation

The pure YBCO ($YBa_2Cu_3O_7$) and the optimally Pr-doped YBCO superconductor with general formula; $Y_{0.85}Pr_{0.15}Ba_2Cu_3O_7$ were prepared by solution route and sintering procedure using two different precursors.

(a) First precursor was formed from the appropriate amounts of oxides ($Pr_2O_3 + Y_2O_3$) which were dissolved in few drops of concentrated nitric acid with formation of praseodymium and yttrium nitrates that finally diluted to 100 ml by distilled water and pH-adjusted to be neutral by ammonia solution.

(b) Second precursor was prepared from the appropriate amounts of $BaCO_3$ and CuO , each of chemical grade purity with dissolution in a few drops of concentrated nitric acid, diluting the net solution to 100 ml by using distilled water and pH-adjusted to be neutral by ammonia solution.

The mixtures (a + b) were shifted to 1 L a round flask while 0.5 M urea/ NH_3 solution was added carefully dropwise with continuous stirring with formation of a heavy gelatinous precipitate. The precipitate were filtered off and dried, then calcinated at 850 °C under a compressed O_2 atmosphere for 30 hrs, then grounded and pressed into pellets (thickness 0.2 cm and diameter 1.2 cm) under 8 Ton cm^{-2} . Sintering was carried out under oxygen stream at 940 °C for 100 h. The samples were slowly cooled down

(20 °C h⁻¹) till 500 °C and annealed there for 25 hrs under oxygen stream. The furnace is shut off and cooled down slowly to room temperature. Finally the materials are kept in vacuum desiccator over silica gel dryer. A levitation preliminary superconductivity test was thoroughly applied for the achievement of superconductive phase and hence superconductivity.

Phase Identification

The X-ray diffraction (XRD) measurements were carried out at room temperature on the fine ground samples using Cu-K_α radiation source, Ni-filter and a computerized STOE diffractometer/Germany with two θ step scan technique .

Scanning Electron Microscopy (SEM) measurements were carried out using a small pieces of the prepared samples by using a computerized SEM camera with elemental analyzer unit (PHILIPS-XL 30 ESEM /USA).

Raman Spectroscopy Measurements

The measurements of Raman spectra were carried out on the finally ground powders with laser wavelength = 632.8 nm (He-Ne laser with power = 1mW) and laser power applied to the site of the sample = 0.4 mW with microscope objective = x20, accumulation time = 1000 - 4000s, up to more than an hour.

Visualized Investigations

To visualize the praseodymium doped 123-YBCO crystal structure DIAMOND-IMPACT CRYSTAL version 3.2 GERMANY program was used depending up on the lattice coordinates given in Table.2. The visualized studies included 12 atomic parameters, 8 symmetry operation and the constructed unit cell has 14 atoms . The lattice contains (created bonds ~ 136 bonds , 8 cell corners and 12 cell edges and created atoms in it ~ 101 atoms).

A visualized studies made is concerned by matching and comparison of experimental and theoretical data of atomic positions, bond distances, oxidation states and bond torsion on the crystal structure formed. Some of these data can be obtained free of charge from ICSD-Fiz-Karlsruhe-Germany.

RESULTS AND DISCUSSION

Phase Identification

Fig. 1.a and b displays the X-ray powder diffractometry patterns of pure 123-YBCO ($YBa_2Cu_3O_7$) and optimally Pr-doped superconductor which prepared via solution route technique respectively. Analysis of the corresponding 2θ values and the inter-planar spacings d (Å) were carried out and indicated that the X-ray crystalline structure mainly belongs to a single superconductive orthorhombic phase 123-YBCO in major besides few peaks of Pr_2O_3 as secondary phase in minor as clear (black squares) in Fig.1b. The unit cell dimensions were calculated using the most intense X-ray reflection peak and found to be $a=3.8234$ Å,

$b=3.8662$ Å and $c=11.7941$ Å for the pure 123-YBCO phase and $a=3.8124$ Å, $b=3.8532$ Å and $c=11.8303$ Å for Pr-doped-123-YBCO. These lattice parameter values are in complete agreement with the mentioned ones in the literature.⁶⁻⁸

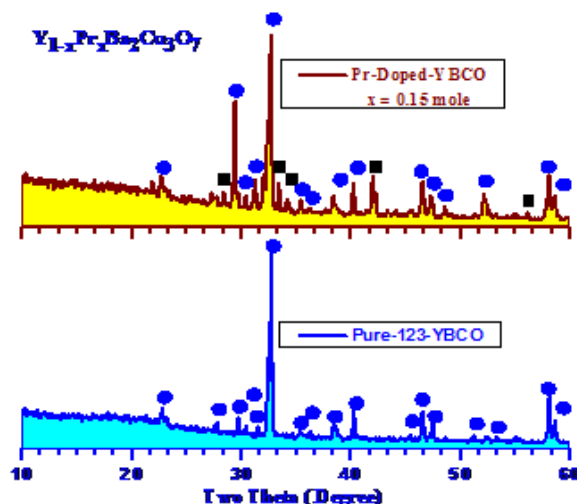


Figure 1a and b. X-ray diffraction patterns for pure YBCO and optimally doped-Pr-123-YBCO superconductors

It is obvious that, the doping with Pr-ions have a negligible effect on the main crystalline structure of the 123-YBCO regime as shown in Fig. 1a and b.

One can indicate that c -axis increases in case of optimally Pr(III) dopant concentration $x = 0.15$ mole than the pure 123-YBCO .This is an indication for (Pr^{3+}) ions substitute successfully by high extent in the superconductive lattice structure and cause elongation in c -axis on the basis of atomic radius since praseodymium ion is larger than that of yttrium ($Pr^{3+} = 113$ while Y^{3+} is 90 pm).

SEM measurements

Fig. 2a and b show the SEM-micrographs for pure and optimally Pr-doped YBCO with $x=0.15$ mole applied on the ground powders that prepared by solution route.

The average particle size was calculated and found in the range of 0.43 and 0.74 μ m. The EDX examinations for random spots in the same sample confirmed and are consistent with our XRD analysis for polycrystalline doped-YBCO composites, such that the differences in the molar ratios EDX estimated for the same sample is emphasized and an evidence for the existence of 123-YBCO superconductive phase with good approximation in contrast with real molar ratios.

From Fig.2a and b it is so difficult to observe inhomogeneity within the micrograph due to that the powders used are very fine and the particle size estimated is too small.

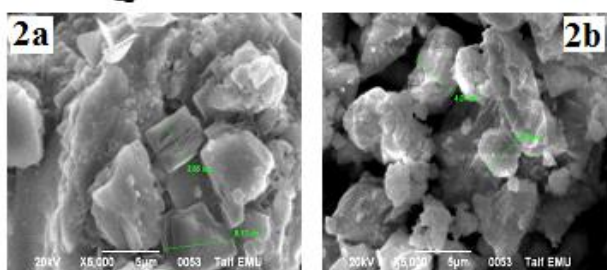


Figure 2a and b. SEM-micrographs recorded for pure YBCO and optimally doped-Pr-123-YBCO superconductors.

The grain size for 123-YBCO-phase was calculated according to Scherrer's formula¹⁸

$$B = 0.87 \frac{\lambda}{D \cos \theta} \quad (1)$$

where D is the crystalline grain size in nm, θ is the half of the diffraction angle in degree, λ is the wavelength of X-ray source (Cu-K α) in nm, and B , degree of widening of diffraction peak which is equal to the difference of full width at half maximum (FWHM) of the peak at the same diffraction angle between the measured sample and standard one. From SEM-mapping, the estimated average grain size was found to be (2.43-3.91 μ m) which is relatively large in comparison with that calculated applying Scherrer's formula for pure 123-phase ($D \sim 1.69 \mu$ m). This indicates that, the actual grain size in the material bulk is smaller than that detected on the surface morphology. Furthermore, in our EDX (energy disperse X-ray) analysis, Pr³⁺ was detected qualitatively with good approximate to the actual molar ratio but not observed at 123-YBCO grain boundaries which confirms that, Pr (III) has diffused regularly into material bulk of superconducting 123-YBCO-phase and Pr³⁺-ion induces in the crystalline structure through solid state reaction by high extent specially at optimum concentration $x = 0.15$ mole.

Table 1. Mode Frequencies of Raman spectra recorded for Pr-doped-123 YBCO in the present work in contrast with some references.

References		YBCO Doping	
Ref. ¹⁷	Ref. ^{19,20}	$x = 0$ mole	$x = 0.15$ mole
229	229	224.6s	223s
336	336	314m	318m
500	575	337.8m	330m
575	592	386.28b	-
440	633	438w	481m
		495.37s	580b
		571.2b	631s

s = strong, m = moderate, b = broad and w = weak.

Raman Spectroscopy

Fig. 3a and b show the Raman spectrograms recorded for pure and optimally Pr-doped -YBCO superconductors. From the modes frequencies which are listed and compared with the work already done.¹⁸⁻²⁰ Table 1, one can indicate that 123-YBCO phase is the dominating phase present in

polycrystalline YBCO superconductors beside small traces of impurity phases such as unreacted praseodymium oxide in very minor traces.

From Raman spectrograms it is clear that, the fundamental vibrational modes of composites with Pr-content $x = 0.15$ mole and pure 123-YBCO sample (Fig.3a and b) were nearly identical with those reported earlier^{18,19} while sample with Pr-content $x=0.15$ mole exhibited strong peak at (631 cm^{-1}) which is attributable to the impurity phase BaCuO₂¹⁸ besides very broad line lies at $\sim 480 \text{ cm}^{-1}$ that appears also in pure sample but shifting by $\pm 10 \text{ cm}^{-1}$ may be attributable to praseodymium(III) ions interactions make as raman scattering materials with other different M-O vibrational modes.

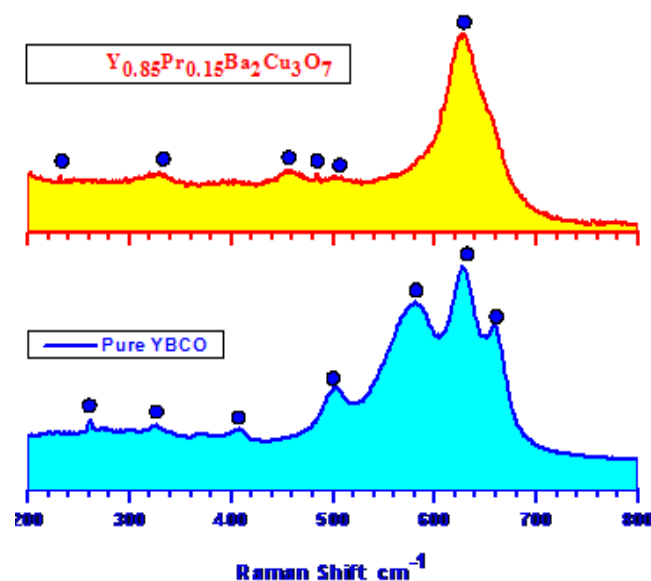


Figure 3a and b. Raman spectrograph recorded for pure YBCO and optimally doped-Pr-123-YBCO superconductors.

The vibrational Raman active-phonon mode lies at $\sim 480 \pm 10 \text{ cm}^{-1}$ originally is due to the apical oxygen O4 (A_{1g})¹⁸. This vibrating mode became flat and very broad to be noticeable in the YBCO-composites with $x = 0.15$ mole. This flattening is attributed to disturbances and changes occurred in the inter-atomic distances of apical oxygen O4 to the two copper layers (Cu2) whereas Pr³⁺ substitutes Y-sites by high extent at low concentration optimum doping ratio ($x = 0.15$ mole) and as a result O4-Cu2 interatomic distances became more closer. In addition to a disorder is occurred on the Cu-O chain which is due to oxygen deficiency on the 123-YBCO lattice structure. Further more Pr₂O₃ which appears as impurity phase as confirmed in our X-ray measurements Fig.1b can play as strong raman scattering material¹⁹.

It is known that the vibrational mode lies at $330 \pm 10 \text{ cm}^{-1}$ is the out-of-phase B_{1g} of the couple O₂-O₃ which in our results strongly shifted down due to Pr-ions substitutions.

According to results reported by Thomsen et al.²² the two lines lie at 224 and $570 \pm 10 \text{ cm}^{-1}$ (which in our results shifted down $\sim 10\text{-}20 \text{ cm}^{-1}$) have been identified as the

Table 2: Lattice coordinates data of Pr-doped-YBCO.

Atomic parameters								
Atom	Ox.	Wyck.	Site	S.O.F.	x/a	y/b	z/c	
Ba1		2t	mm2	0.99	1/2	1/2	0.18200	
Y1		2t	mm2	0.005	1/2	1/2	0.18200	
Pr1		2t	mm2	0.005	1/2	1/2	0.18200	
Y2		1h	mmm	0.850	1/2	1/2	1/2	
Pr2		1h	mmm	0.150	1/2	1/2	1/2	
Cu1		1a	mmm	1.00	0	0	0	
Cu2		2q	mm2	1.00	0	0	0.35000	
O1		1b	mmm	0.03	1/2	0	0	
O2		1e	mmm	0.97	0	1/2	0	
O3		2r	mm2	1.00	0	1/2	0.19500	
O4		2r	mm2	1.00	0	1/2	0.37200	
O5		2s	mm2	1.00	1/2	0	0.39400	

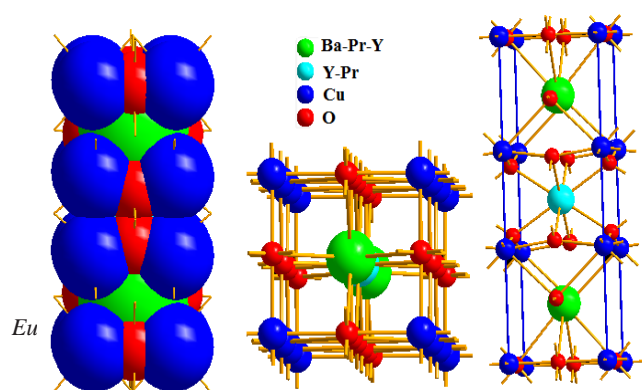
forbidden vibration modes of copper and oxygen in the Cu-O chain layer respectively. Based on the selection rules generally these modes are forbidden in case of samples having sufficient oxygen content.

Duong et al.¹⁸ confirmed that when the number of oxygen atoms in the unit cell is < 7 , the CuO chain could start to become disordered and its inversion center of symmetry is broken and then the mentioned two lines (at 229 and 567 cm^{-1}) can appear.

Regarding these informations reported^{22,18} present results are partially agreement and consistent with them since the optimally Pr-doped sample displays two lines with different intensities as per the oxygen content inside lattice. From Fig.3a and b one can notice that there is no monotonic behaviour on the recorded Raman spectrograph due to high sensitivity of both 123-YBCO systems and Raman spectra favour applicable variables, such as structure quality which depends upon oxygen content and impurity phases. All of these variables can make a change on the Raman phonon modes as mentioned in literature before. Figure 4a. Orthorhombic crystal structure of Pr-optimally doped-123-YBCO superconductor.

Structural Visualization

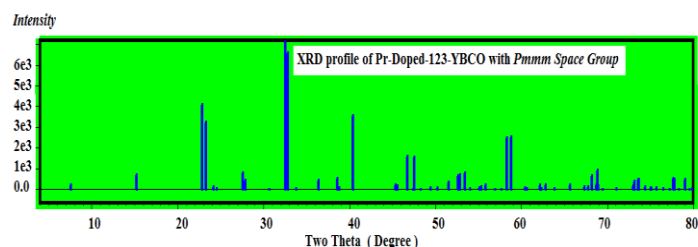
The pure crystal and praseodymium doped crystal were built up depending upon the atomic parameters and lattice coordinates in Table 2 with the help of DIAMOND visualizer and can be seen at Figs. 4a-c. The comparison between fingerprint peaks in Fig.1a and b and theoretical XRD-pattern Fig.4b indicated that there are good fitting between both the patterns which reflect the success of



praseodymium doping ($x=0.15$ mole) to substitutes without distorting the original orthorhombic structure. It is well known fact that superconduction mechanisms inside these cuprates layered structures are mainly depend upon Cu-O chains and planes as shown in Fig.4c. Furthermore any kind of shortening or lengthening in these (chains and planes) could damage superconductivity nature inside these superconductors^{2,3,4}.

Figure 4a. Orthorhombic crystal structure of Pr-optimally doped-123-YBCO superconductor.

So a visualized studies made is concerned by matching and comparing of experimental and theoretical data of atomic positions, bond distances, oxidation states and bond torsion on the crystal structure formed.

**Figure 4b.** Visualized XRD-profile recorded for Pr-optimally doped-123-YBCO.

The analysis of tables (3, 4 and 5) indicated that there is no violation in bond lengths especially for praseodymium-oxygen since praseodymium found in two types symbolized as Pr1 and Pr2 respectively.

It was noticed that Pr1 linked with five types of oxygen atoms namely O1, O2, O3, O4 and O5 recording the following bond lengths 2.8763, 2.8551, 1.9165, 2.9251 and 3.1432 Å respectively.

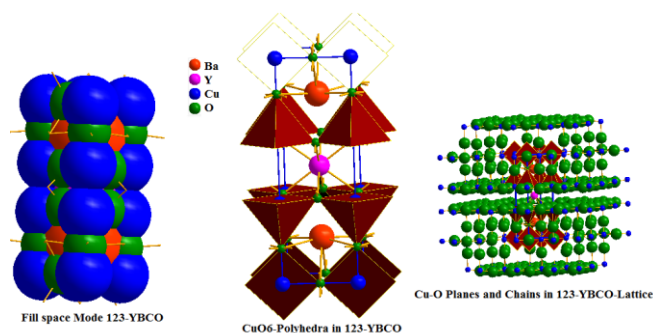


Figure 4c. Copper–oxygen planes and chains and CuO_6 -poly octahedrons.

These recorded data for type one are slightly different from those of type two (Pr2) which linked with O_5 and O_4 and recording 2.3018 and 2.4242 Å respectively. The differences in bond lengths could be interpreted on the basis that Pr-ions have more than one oxidation state inside crystal lattice. With respect to stability of CuO_6 polyhedrons inside the optimally-Pr-doped YBCO crystal lattice, it was observed that bond distances between copper and oxygen atoms environment are within the limits and no violation was recorded except only in $Cu1-O5$ is longer than others due to axial positioning of $O5$. Furthermore, no abnormal torsions observed on the angles of copper which support and increase stability of lattice.

Table 3. Some selected structural data inside crystal lattice of Pr-doped-YBCO.

Atom1	Atom2	d_{1-2} Å	Atom3	d_{1-3} Å	$\wedge 213^\circ$
Ba1 Pr1 Y1	O3	1.9165	O3	1.9165	170.929
	O3	1.9165	O2	2.8551	136.537
	O3	1.9165	O2	2.8551	52.535
	O3	1.9165	O1	2.8763	93.344
	O3	1.9165	Ba1 Pr1 Y1	3.8840	90.000
	O3	1.9165	Ba1 Pr1 Y1	3.8840	90.000
	O3	1.9165	O2	2.8551	52.535
	O3	1.9165	Cu1	3.4530	59.804
	O3	1.9165	Y2 Pr2	3.7072	85.464
	O3	1.9165	Ba1 Pr1 Y1	3.8210	4.536
	O3	1.9165	Ba1 Pr1 Y1	3.8210	175.464
	O3	1.9165	Ba1 Pr1 Y1	3.8840	90.000
	O2	2.8551	Cu1	3.4530	85.043
	O2	2.8551	Cu1	3.4530	34.223
	O2	2.8551	Y2 Pr2	3.7072	137.999
	O2	2.8551	Ba1 Pr1 Y1	3.8210	47.999
	O2	2.8551	Ba1 Pr1 Y1	3.8210	132.001
	O2	2.8551	Ba1 Pr1 Y1	3.8840	90.000
	O2	2.8551	Ba1 Pr1 Y1	3.8840	90.000
	O2	2.8551	Ba1 Pr1 Y1	3.8840	90.000
	O1	2.8763	O1	2.8763	84.934
	O1	2.8763	O4	2.9251	123.958
	O1	2.8763	O4	2.9251	123.958
	O1	2.8763	O5	3.1432	175.692
	O1	2.8763	O5	3.1432	99.374
	O1	2.8763	Cu2	3.3552	145.224
	O1	2.8763	Cu2	3.3552	145.224
	O1	2.8763	Cu2	3.3552	92.282
	O4	2.9251	Cu2	3.3552	35.518
	O4	2.9251	Cu2	3.3552	35.518
	O4	2.9251	Cu2	3.3552	85.979
	O4	2.9251	Cu1	3.4530	145.758
	O4	2.9251	Cu1	3.4530	95.965
	O4	2.9251	Cu1	3.4530	145.758
	O4	2.9251	Cu1	3.4530	95.965
	O5	3.1432	Cu1	3.4530	146.164
	O5	3.1432	Cu1	3.4530	97.798
	O5	3.1432	Y2 Pr2	3.7072	38.159
	O5	3.1432	Ba1 Pr1 Y1	3.8210	90.000
	O5	3.1432	Ba1 Pr1 Y1	3.8210	90.000
	O5	3.1432	Ba1 Pr1 Y1	3.8840	128.159
	O5	3.1432	Ba1 Pr1 Y1	3.8840	51.841
	O5	3.1432	Cu2	3.3552	84.181
	O5	3.1432	Cu2	3.3552	84.181

Table 4. Selected structural data inside crystal lattice of Pr-doped-YBCO.

Atom1	Atom2	d_{1-2} Å	Atom3	d_{1-3} Å	$\angle 213^\circ$
Y2 Pr2	O5	2.3018	O5	2.3018	180.000
	O5	2.3018	O5	2.3018	64.939
	O5	2.3018	O5	2.3018	115.061
	O5	2.3018	Cu2	3.2372	102.481
	O5	2.3018	Cu2	3.2372	102.481
	O5	2.3018	Cu2	3.2372	37.238
	O5	2.3018	Cu2	3.2372	37.238
	O5	2.3018	Ba1 Pr1 Y1	3.7072	57.530
	O5	2.3018	Ba1 Pr1 Y1	3.7072	122.470
	O5	2.3018	Y2 Pr2	3.8210	90.000
	O5	2.3018	Y2 Pr2	3.8210	90.000
	O4	2.4242	Cu2	3.2372	37.096
	O4	2.4242	Ba1 Pr1 Y1	3.7072	127.992
	O4	2.4242	Ba1 Pr1 Y1	3.7072	52.008
	O4	2.4242	Y2 Pr2	3.8210	37.992
	O4	2.4242	Y2 Pr2	3.8210	142.008
	O4	2.4242	Ba1 Pr1 Y1	3.7072	52.008
	O4	2.4242	Ba1 Pr1 Y1	3.7072	127.992
	O4	2.4242	Y2 Pr2	3.8210	142.008
	O4	2.4242	Y2 Pr2	3.8210	37.992
	O4	2.4242	Y2 Pr2	3.8840	90.000
	O4	2.4242	Y2 Pr2	3.8840	90.000
	O4	2.4242	Y2 Pr2	3.8840	90.000
	O4	2.4242	Y2 Pr2	3.8840	90.000
	O4	2.4242	Y2 Pr2	3.8840	90.000
	Cu2	3.2372	Cu2	3.2372	72.339
	Cu2	3.2372	Cu2	3.2372	114.607
	Cu2	3.2372	Cu2	3.2372	73.726
	Cu2	3.2372	Cu2	3.2372	106.274
	Cu2	3.2372	Y2 Pr2	3.8210	126.169
	Cu2	3.2372	Y2 Pr2	3.8840	53.137
	Cu2	3.2372	Y2 Pr2	3.8840	126.863
	Ba1 Pr1 Y1	3.7072	Ba1 Pr1 Y1	3.7072	180.000
	Ba1 Pr1 Y1	3.7072	Y2 Pr2	3.8210	90.000
	Ba1 Pr1 Y1	3.7072	Y2 Pr2	3.8210	90.000
	Ba1 Pr1 Y1	3.7072	Y2 Pr2	3.8840	90.000
	Y2 Pr2	3.8210	Y2 Pr2	3.8210	180.000
	Y2 Pr2	3.8210	Y2 Pr2	3.8840	90.000
	Y2 Pr2	3.8210	Y2 Pr2	3.8840	90.000

Table 5. Selected structural data inside crystal lattice of Pr-doped-YBCO.

Atom1	Atom2	d_{1-2} Å	Atom3	d_{1-3} Å	$\angle 213^\circ$
Cu1	O1	1.9105	O1	1.9105	180.000
	O1	1.9105	O2	1.9420	90.000
	O1	1.9105	O2	1.9420	90.000
	O1	1.9105	O3	2.9899	90.000
	O1	1.9105	Ba1 Pr1 Y1	3.4530	56.407
	O1	1.9105	O2	1.9420	90.000
	O1	1.9105	O3	2.9899	90.000
	O1	1.9105	Cu1	3.8840	90.000
	O2	1.9420	Ba1 Pr1 Y1	3.4530	124.223
	O2	1.9420	Cu1	3.8210	90.000
	O2	1.9420	Cu1	3.8210	90.000
	O2	1.9420	Cu1	3.8840	0.000
	O2	1.9420	Cu1	3.8840	180.000
	O2	1.9420	O3	2.9899	130.506
	O2	1.9420	Ba1 Pr1 Y1	3.4530	124.223
	O3	2.9899	O3	2.9899	81.012
	O3	2.9899	O3	2.9899	98.988
	O3	2.9899	O3	2.9899	180.000

Table 5 (cont.). Selected structural data inside crystal lattice of Pr-doped-YBCO.

Atom1	Atom2	d ₁₋₂ Å	Atom3	d ₁₋₃ Å	∠213°
Cu1	O3	2.9899	Ba1 Pr1 Y1	3.4530	146.357
	O3	2.9899	Cu1	3.8840	49.494
	O3	2.9899	Cu1	3.8840	130.506
	O3	2.9899	Ba1 Pr1 Y1	3.4530	33.643
	O3	2.9899	Ba1 Pr1 Y1	3.4530	84.151
	Ba1 Pr1 Y1	3.4530	Ba1 Pr1 Y1	3.4530	75.826
	Ba1 Pr1 Y1	3.4530	Ba1 Pr1 Y1	3.4530	180.000
	Ba1 Pr1 Y1	3.4530	Ba1 Pr1 Y1	3.4530	67.186
	Ba1 Pr1 Y1	3.4530	Cu1	3.8840	124.223
	Ba1 Pr1 Y1	3.4530	Cu1	3.8840	55.777
	Cu1	3.8210	Cu1	3.8210	180.000
	Cu1	3.8210	Cu1	3.8840	90.000
	Cu1	3.8210	Cu1	3.8840	90.000
	Cu1	3.8210	Cu1	3.8840	90.000
	Cu1	3.8210	Cu1	3.8840	90.000

Conclusions

The conclusive remarks regarding this article can be summarized in the following points;

Doping with Pr-ions at optimal ratio have a negligible effect on the main crystalline structure of the 123-YBCO regime ($x = 0.15$ mole).

The average particle size was calculated and found in the range of 0.43 and 0.74 μm .

The vibrational mode lies at $330 \pm 10 \text{ cm}^{-1}$ is the out-of-phase B_{1g} of the couple O2-O3 which in present investigations strongly shifted down with Pr- doping $x=0.15$ mole.

Structural visualization studies confirmed that Pr-doping with optimal ratio $x=0.15$ mole reinforces the stability of 123-YBCO lattice structure .

Acknowledgement

The authors would like to thank deeply JANSEN Department represented by Prof. M.Jansen (Max Planck Institute for Solid State Research-1-D-Heissenberg Str. - Stuttgart-Germany) for their technical support of some measurements inside this article.

References

- Xiao, G., Streitz, F. H., Gavrini, A., Du, Y. W., Chien, C. L., *Phys. Rev. B*, **1987**, 35, 8782.
- Maeno, Y., Tomita, T., Kyogoku, M., Aoki, Y., Hoshino, K., Minami, A., Fujita, T., *Nature*, **1987**, 328, 512 .
- Tarascon, J. M., Barbour, P., Maceli, P. F., Greene, L. H., Hull G. W., *Phys.Rev. B*, **1988**, 37, 7458.
- Renevier, H., Hodeau, J. L., Marezio, M., Santoro, A., *Physica C*, **1994**, 220, 143 .
- Kulkarni, R. G., Kuberkar, D. G., Baldaha, G. J., Bichile, G. K., *Physica C*, **1993**, 217, 175.
- Bringley, J. F., Chen, T. M., Averill, B. A., Wong K. M., Poon, S. J., *Phys. Rev.B* , **1988**, 38, 2432.
- Shimak, Y. A., Kubo Y., Utsumi, K., Takeda, Y., Takano, M., *Jpn. J. Appl. Phys.*, **1988**, 27, 1071 .
- Hiroi, Z. , Takano, M., Takeda, Y., Kanno, R., Bando, Y., *Jpn. J. Appl. Phys.*, **1988**, 27, 580 .
- Delamare, M. P., Hervieu M., Monot Land Tendeloo G., *Physica C*, **1996**, 262, 220.
- Peters, P. N., Sisk, R. C., Ubran, E., Huang, C. Y., Wu M. K., *Appl. Phys. Lett.*, **1988**, 52, 2066 .
- Huang, C. Y., Shapiro, Y., McNiff, E. J., Peters, P. N., Shwartz B. B., Wu, M. K., Shull, R. D., Chiang, C. K., *Mod. Phys.Lett.*, **1988**, 2, 869.
- Singh J. P., Leu, H. L., Poeppel, R. B., Voorhees, E., Goudery, G. T., Winsley, K., Shi, D., *J. Appl. Phys.*, **1989**, 66, 3154.
- Dwir, B., Affronte, M. and Pavuna, D., *Appl. Phys. Lett.*, **1989**, 55, 399.
- Jung, J., Mohammed, M. A., Cheng, S. C., Frank, J. P., *Phys. Rev. B*, **1990**, 42, 6181.
- Singh, J. Joo, J. P., Gangopadhyay, A. K., Mason, T. O., *J. Appl. Phys.*, **1992**, 71, 2351.
- Khan, H. R., Fancavilla, T. L., Hein, R. A., Pande, C. S., Quadri S. B., Soulen, R. J., Wolf, S. A., *J. Supercond.*, **1990**, 3, 189.
- Tomita, M. and Murakami M., *Supercond.Sci. Technol.*, **2000**, 13, 722 .
- Duong, C. H. , Vu, L. D. and Hong, L.V., *J. Raman Spectrosc.*, **2001**, 32, 827.
- Zhang, L. D. , Mu, J. M., Nano-materials Science, *Liaoning Science & Technology Press*, Shengyan, China, **1994**, p. 92.
- Kaihana, M., Borjesson, L., Eriksson, S., *Physica C*, **1989**, 162, 1253.
- Chang, H., Ren, Y., Sun, Y., Wang, Q., Xue, Y., Chu C. W., *Physica C*, **1994**, 228, 383 .
- Thomsen, C., Cardona, M., Gegenheimer, B., Lui, R., Simon, A., *Phys. Rev. B*, **1988**, 37, 284.

²³Sekkina M. M. A., Elsabawy, K. M., *Mater. Sci. Eng.*, **2003**, B103, 71-76.

²⁴Elsabawy, K. M., Elsayed, K. E., *Mater. Res. Bull.*, **2007**, 42, 1051-1060.

Received: 20.10.2012.

Accepted: 13.11.2012.



ALTERATIONS IN ADULT MOUSE TESTIS AFTER SUBACUTE INTOXICATION WITH CADMIUM AND MONENSIN DETOXICATION

Ekaterina Pavlova^[a], Juliana Ivanova^[b], Donika Dimova^[a],
Yordanka Gluhcheva^[a], Nina Atanassova^[a]

Paper was presented at the 4th International Symposium on Trace Elements in the Food Chain, Friends or Foes, 15-17
November, 2012, Visegrád, Hungary

Keywords: cadmium intoxication, monensin, *in vivo* model, testis morphology

Cadmium (Cd) is a heavy metal and a major environmental pollutant. The general population is exposed to Cd mainly via drinking water and food products. We have developed a mouse experimental model to investigate the *in vivo* effects of Cd and the chelating agent monensin on testis and sperm count during adulthood. Animals were divided into three groups: normal control (receiving distilled water and food): Cd group, exposed to 20 mg kg⁻¹ b.w. Cd(II) acetate for the first 2 weeks of the experimental period and Cd+monensin group, receiving monensin (18 mg kg⁻¹) after Cd-intoxication (from 15th to 28th day). Histological observations of the testis demonstrated that Cd induced desquamation of germ cell and their assembly in the luminal region of the tubules. Areas in the testis without spermatides in latest steps of differentiation were also observed in this group. Monensin administration to Cd-treated animals restored histology of the testis to normal to a great extent (despite some Sertoli-cell-only tubules). Statistically significant changes in sperm count were not established for any of the experimental groups. Monensin can reduce injury of the testis and normalize its morphology after subacute exposure to Cd. The results of the present study demonstrated that monensin is a good compound in chelating therapy of some heavy metal intoxications.

Corresponding Author: Ekaterina Pavlova

Fax: +359 2 871 01 07

E-Mail: e_bankova@yahoo.com

- [a] Institute of Experimental Morphology, Pathology and Anthropology with Museum, Bulgarian Academy of Sciences, Acad. Georgi Bonchev Str., bl. 25 Acad. Georgi Bonchev Str., bl. 25, 1113 Sofia, Bulgaria
- [b] Faculty of Medicine, Sofia University "St. Kliment Ohridski", Kozjak 1 Kozjak 1, 1407 Sofia, Bulgaria

for treatment of Cd intoxication. Recent studies have been demonstrated that polyether ionophore antibiotic, monensin is much more effective than the traditional chelators as EDTA (ethylenediaminetetraacetic acid) and DMSA (meso-dimercapto-succinic acid) in reducing lead (Pb) concentrations. Tetraethylammonium salt of monensic acid forms complexes with other toxic metal ions as Li⁺, Na⁺, Cd(II) and Hg(II), suggesting that could be applied for treatment of intoxications with these metals.^{7,8}

Introduction

Cadmium (Cd) is a heavy metal and an environmental contaminant mostly found in tobacco smoke and industrial pollution, but also in water and food chain.¹ Cd is also bio-accumulative due to its long biological half-life and depending on its dose, route and duration of exposure it can affect target organs such as kidney, liver, lung, testis, adrenals, adipose tissue and hemopoietic system.^{2,3} Cd induces apoptosis and affects cell proliferation, differentiation and other cellular activities (gene expression, signal transduction, DNA repair and DNA methylation). Co interferes with enzymes of the cellular antioxidant system and generates of reactive oxygen species (ROS).⁴ In fact, the International Agency for Cancer Research classified cadmium as the 7th toxicant in the priority list of Hazardous Substances⁵.

Chelation therapy is the preferred medical treatment of reducing the toxic effects of metals. Chelating agents are capable of binding to toxic metal ions to form complex structures which are easily excreted out from the body removing them from intracellular or extracellular spaces⁶. Different compounds have been tested as chelating agents

The aim of our study was to investigate the *in vivo* effects of Cd and the chelating agent monensin on the testis and sperm count in adulthood.

Materials and Methods

60-day old adult male ICR mice were fed a standard diet and had access to food *ad libitum*. Mice were maintained in the institute's animal house at 23°C ± 2 °C and 12:12 h light - dark cycle in individual standard hard bottom polypropylene cages. The animals were left to acclimatize for one week prior to dosing.

Mice were divided into three groups: The first group was a control and had free access to distilled water and food during the experimental period. The second group was subjected to subacute Cd(CH₃COO)₂·2H₂O intoxication with daily dose of 20 mg kg⁻¹ b.w. for two weeks. The compound was dissolved and prepared with distilled water. In the next 14 days of the experiment the animals from this group obtained distilled water and food *ad libitum*. The third group was exposed to Cd intoxication as that of the second group followed by treatment with tetraethylammonium salt of monensic acid at daily dose of 18 mg kg⁻¹ b.w. from day 15 to day 28 of the experimental process.

On day 29 the experimental mice were sacrificed. Testes and epididymides were sampled, weighed and embedded in paraffin using routine histological practice. Spermatozoa were isolated from both vasa deferentia and counted using Buerker's chamber. Data were statistically processed using Student's t-test.

Results

On day 90 spermatogenesis in mouse is completed, and all the stages of the spermatogenic cycle can be seen. Germ cells are organized in twelve stages according to the classification of Clermont and Perey⁹ arranged in 5-6 layers in seminiferous epithelium. Mature spermatozoa are released into the tubular lumen in stages VII-VIII of the cycle (Figure 1). Histological observation of testes after subacute Cd intoxication demonstrated disorganization of seminiferous epithelium. Germ cells were sloughed off from the seminiferous epithelium and were located in the luminal region of the tubules. Seminiferous tubules devoid of spermatides in latest steps of differentiation were frequently observed in this group (Figure 2). After monensin administration of Cd intoxicated animals we established restoration of normal morphology of the testis to a great extent (Figure 3) despite Sertoli-cell-only tubules at some places. In contrast to our expectations at this stage of the experiment we did not establish significant negative alterations of Cd acetate on gonado-somatic index (calculated as a ratio of testis weight to body weight) or sperm count in adult mice (data not shown).

Discussion

After subacute Cd intoxication of adult mice we observed pathological changes of testis morphology. Our data regarding the germ cell loss is supported by the findings of Siu et al.⁹. Cd exerts its effect in the testis by perturbing blood-testis barrier function, affecting germ cell adhesion in the seminiferous epithelium that probably explains germ cell loss and disorganization of the epithelium. In male rodents, it is well established that Cd works as endocrine disruptor by affecting the synthesis and regulation of several hormones (testosterone, LH, FSH)¹⁰. For instance, a significant decrease in serum and testicular testosterone level was reported in mice exposed to acute doses of Cd compounds illustrating that Cd can disrupt the hypothalamic-pituitary-testicular axis by creating a hormonal disbalance and affecting male fertility.¹¹ Manipulation of androgen (or of the androgen receptor in Sertoli cells) can be a potential target candidate to manage Cd-induced testicular toxicity³. Moreover, Cd-induced toxicity has been associated with generations of reactive oxygen species (ROS)¹². Spermatogenesis is a sensitive process and changes in hormonal levels or elevation of ROS would influence the normal proceeding of spermatogenesis and the structure of seminiferous epithelium.

The work already done by our group¹² demonstrated significant increase in Cd accumulation in all investigated organs (liver, kidney, spleen, lung, heart and testes) in Cd-intoxicated animals. The administration of tetraethylammonium salt of monensic acid to Cd-treated animals depleted Cd concentrations to a great extent in all

organs as compared to Cd-intoxicated mice. In the testis Cd content was reduced with 55% as compared to Cd-treated group. These results are in agreement with the good chelating effects of monensin on testis histology.

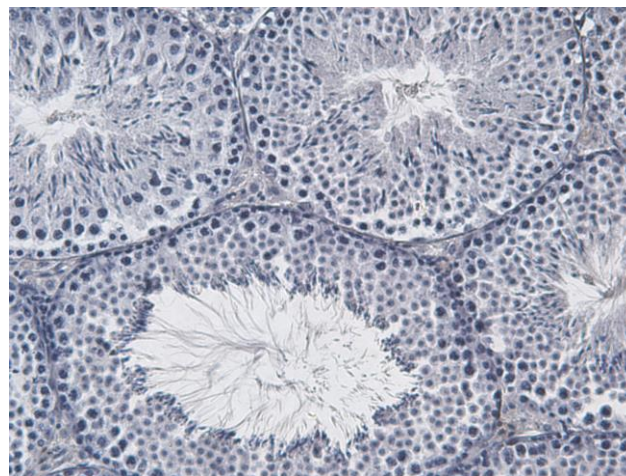


Figure 1. Morphology of the seminiferous tubules on control testis cross sections of adult mice. HE, x 400.

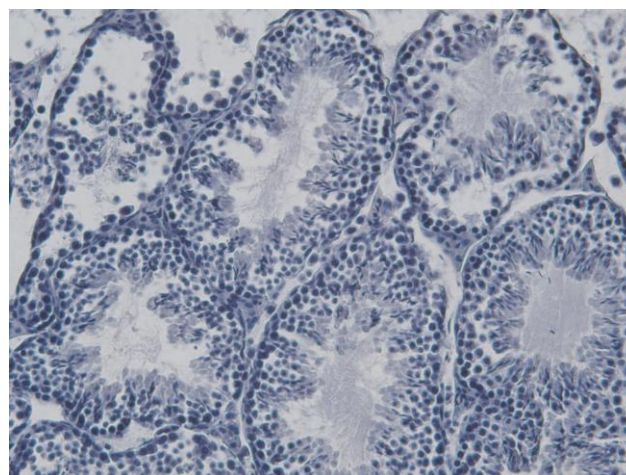


Figure 2. Morphology of the seminiferous tubules on testis cross sections of adult mice after subacute Cd intoxication ($20 \text{ mg kg}^{-1} \text{ b.w.}$) Disorganization of seminiferous epithelium was observed. HE, x 400.

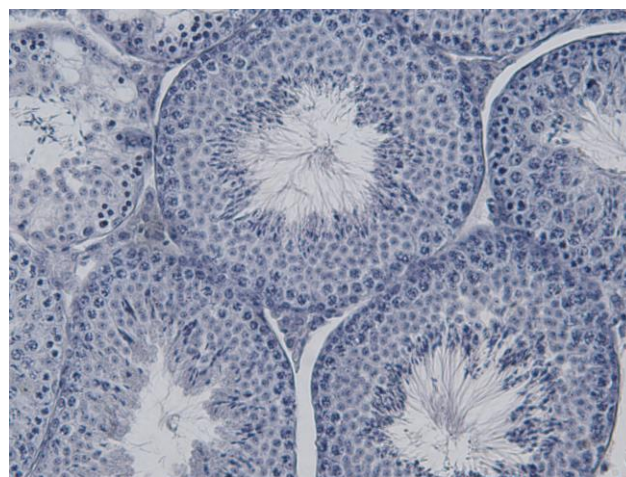


Figure 3. Restoration of normal morphology of the testis to a great extent after chelating therapy with monensin ($18 \text{ mg kg}^{-1} \text{ b.w.}$) of Cd intoxicated mice ($20 \text{ mg kg}^{-1} \text{ b.w.}$). HE, x 400.

We found that Cd accumulation in the testis had no effect on testicular weight. The data by Teiichiro et al.¹³ and Haouem et al.¹⁴ support our results while El-Demardash et al.¹⁵ observed that Cd decreased this parameter. Blanco et al.¹⁶ reported that Cd caused a decrease in testicular weight at concentration in the testis of about 1 $\mu\text{g g}^{-1}$. This value is much higher than the concentration of Cd observed in the testes of our experimental animals¹² which could be a possible explanation for the lack of effect on gonado-somatic index. Usually, impaired spermatogenesis is associated with reduced testis weight and low sperm count. Haouem et al.¹⁴ established that sperm concentration was comparable between control and Cd-contaminated rats after 4th and 8th weeks of treatment, while after 12 weeks of exposure this parameter was significantly decreased in Cd-treated animals compared to corresponding control. Probably the effect of Cd on sperm production depends on the duration of the treatment and therefore prolonged treatment would induce changes not only on histological level but also on quantitative parameters of mice spermatogenesis.

Conclusion

Our investigations demonstrated that subacute Cd intoxication induced severe changes in testis morphology but not in the gonado-somatic index and epididymal sperm count. Monensin reduced testis injury and recovered its morphology to a great extent that can suggest monensin as a favorable compound in chelating therapy of some heavy metal intoxications.

Acknowledgements: The financial support of this work by the University of Sofia "St. Kliment Ohridski" Fund for Scientific Research (grant 72/2012, project leader: Juliana Ivanova) is acknowledged.

References

- ¹IARC Monographs. International Agency for Research on Cancer, 1993, Lyon, France.
- ²Waalkers, M.P., *Mutat. Res.*, **2003**, 533, 107.
- ³Siu, E. R. Mruk, D. D., Porto, C. S., Yan Cheng, C. *Toxicol. Appl. Pharm.*, **2009**, 238, 240.
- ⁴Waisberg, M., Joseph, P., Hale, B., Bayersmann, D. *Toxicology*, **2003**, 192, 95.
- ⁵Thompson, J., Bannigan, J. *Reprod. Toxicol.*, **2008**, 25, 304.
- ⁶Swaran, J. S., Pachauri, F., Pachauri, V. *Int. J. Environ. Res. Pub. Health* **2010**, 7(7), 2745.
- ⁷Hamidinia, S.A., Shimelis, O.I. Tan, B., Erdahl, W.L., Chapman, C. J., Renkes, G. D., Taylor, R. W., Pfeiffer, D. R. *J. Biol. Chem.* **2002**, 277(41), 38111.
- ⁸Singh, M., Kalla, N. R., Sanyal, S. N. *Pharmacol. Reports*, **2007**, 59, 456.
- ⁹Clermont, Y., Perey, B. *Am. J. Anatomy*. **1957**, 100 (2), 241.
- ¹⁰Lafuente, A., Gonzalez-Carracedo, A., Romero, A., Cano, P., Esquifino, A. I., *Toxicol. Lett.* **2004**, 146, 175.
- ¹¹Mruk, D. D., Yan Cheng, C. *Landes Biosci.*, **2011**, 1(4), 283.
- ¹²Ivanova, J., Gluhcheva, Y.G., Kamenova, K., Arpadjan, S., Mitewa, M. *J. Trace Elem. Med. Biol.* **2012**, in press.
- ¹³Teiichiro, A., Hirmichi, I., Keisuke, M., Kunihiro, H., Makoto, H. *Reprod. Med. Biol.* **2002**, 1, 59.
- ¹⁴Haouem, S., Najjar, M.F., El Hani, A., Sakly, R. *Exp. Toxicol. Pathol.* **2008**, 59, 3007.
- ¹⁵El-Demardash, F. M., Yousef, M. I., Kedwany, F. S., Bagdadi, H. *H. Food Chem. Toxicol.* **2004**, 42, 563.
- ¹⁶Blanco, A., Moyano, R., Vivi, J., Frores-Acuna, R. Molina, A., Blanco, C. et al. *Environ. Toxicol. Pharmacol.* **2007**, 23, 96.

Received: 15.10.2012.
Accepted: 13.11.2012.



SURVIVAL TO EARLY TOXIC COPPER EXCESS: BIOCHEMICAL AND ANATOMICAL CHANGES DURING GERMINATION OF INDIAN MUSTARD

Réka Szöllősi^{[a]*}, Erika Kálmán^[a], Anna Medvegy^[a], Ilona Sz. Varga^[b]

Paper was presented at the 4th International Symposium on Trace Elements in the Food Chain, Friends or Foes, 15-17 November, 2012, Visegrád, Hungary

Keywords: copper stress, *Brassica juncea* L., germination, oxidative stress, callose, lignin.

It is well-known that essential heavy metals like copper (Cu), mainly at higher concentrations usually cause overproduction of reactive oxygen species (ROS) resulting in oxidative stress in plants. Till date many experiments were carried out to evaluate how Cu toxicity influences in adult plants but only a few reports are available about the effects during germination. Since this is a very sensitive period and the effects of heavy metal stress are more serious. The aims of our study were to investigate potential oxidative stress and antioxidative defense mechanisms beside potential morphological and/or anatomical alterations in germinating seeds of Indian mustard (*Brassica juncea* L.) exposed to excess Cu. The following parameters were evaluated to describe oxidative stress: FRAP (ferric reducing ability of plasma), lipid peroxidation (LP), reduced glutathione content (GSH), total protein content and the activity of glutathione-S-transferase (GST), superoxide dismutase (SOD), catalase (CAT), guaiacol peroxidase (GPOX) and glutathione reductase (GR). We also made an assessment of histochemically LP and the loss of plasma membrane integrity in the root tips, the production of callose and the lignification of cell walls. Our results showed that Cu treatments were followed by notable GSH-depletion. We could detect LP histochemically in the root tips. The application of Cu increased the activity of SOD in time and dose-dependent manner. The activity of CAT and GPOX increased after 48-96h Cu excess. Morphological symptoms of metal toxicity occurred such as stunted, hooked-formed and brownish root tips. Production of callose and lignification of cell walls could be visualized, too.

* Corresponding Authors

Fax: +36 62 54 4307

E-Mail: szoszo@bio.u-szeged.hu

[a] Department of Plant Biology, University of Szeged, H-6726 Szeged, P.O. Box 654, Hungary

[b] Department of Biochemistry and Molecular Biology, University of Szeged, H-6726 Szeged, Közép fasor 52., Hungary

metals at levels even 100-fold higher than nonaccumulator plants.⁸ Indian mustard (*Brassica juncea* L., Brassicaceae, Mustard family) is known as Cd-hyperaccumulator but it can tolerate Cu. Because of its fast growth and relatively small size it can be a good model.

Most of the earlier studies reported oxidative stress only in adult plants (including Indian mustard). After heavy metal stress there are not many reports on the effects in the early stages of ontogenesis in *Brassica juncea* L., which was exposed to heavy metal stress, since germination, which is a very sensitive period of development and the effects of heavy metal stress are more expressed and visual than later.^{4,9, 10}

Aims

The aims of our study were to investigate potential oxidative stress and antioxidative defense mechanisms in germinating seeds of Indian mustard exposed to copper excess. We wanted to know whether copper as an essential heavy metal can cause changes similar to cadmium, which is basically toxic for the plants. We intended to answer the following questions:

-Does heavy metal treatment cause oxidative stress during the germinative stage ?

-Which biochemical parameters are the most appropriate to describe this oxidative stress ?

-How can the duration and heavy metal concentration influence oxidative stress ?

Introduction

It is well-known fact that heavy metals due to their common presence in soil-water-plant- animal- human system may affect development, growth, basic metabolisms etc. in living organisms. Essential heavy metals like copper (Cu) which are often co-factors of various enzymes such as oxidases or components of the photosynthetic system, also might act as pollutants at higher concentrations in the environment due to industrial, municipal or agricultural activities.^{1, 2, 3, 4} Similarly to toxic heavy metals (e.g. Pb, Cd), essential heavy metals at higher levels may also provoke overproduction of reactive oxygen species (ROS) resulting in oxidative stress in plants, and consequently lipid peroxidation in the membranes, disorders in various metabolic processes and visible morphological and/or histological changes.^{4, 5, 6} Though Cu is an important biometal and its average amount concentration in natural soils is 2-40 mg kg⁻¹ DM (dry matter), it can accumulate in agricultural soils 10-15-fold higher than the recommended levels due to emission of sewage sludge and fertilizers, and may trigger remarkable changes in the photosynthetic activity.^{1, 2, 3, 7}

Numerous plants can survive with the excess of Cu, taken up and allocate it to different plant parts, generally to root or shoot. These tolerant plants can also accumulate this metal, hence are called 'hyperaccumulators' because of amassing

-How can oxidative stress be proved and visualized histochemically ?

-What morphological and/or histological alterations occur in the root tips after heavy metal exposure ?

Experimental

Plant material and germination conditions

Seeds of Indian mustard (*Brassica juncea* L.) derived from Research Institute of the Hungarian Academy of Sciences, Budakalász, Hungary, were germinated in sterilized Petri dishes at 0, 50, 100 and 200 mg L⁻¹ Cu concentrations (indicated as Control, Cu50, Cu100, Cu200, Table 1).

Table 1. Parameters of Cu concentrations applied

Salt form	Concentration, mg L ⁻¹	Concentration, mM	pH at the beginning
	0	0.00	7.07
CuSO ₄	50	0.78	4.93
	100	1.57	4.72
	200	3.15	4.57

The effect of each concentration of copper was investigated on 0.5-0.5 g seeds with 8 repetitions. The seeds were sown on Petri dishes with four-layered filter paper wetted with 10 mL of metal solutions. Then the Petri dishes were closed and were kept in dark for 12, 24, 48 and 96 h, at 24±1°C. The control group of seeds was germinated in the same way by the addition of distilled water only.

Determination of Cu content in seeds

In order to detect the heavy metal content in the germinating seeds, about 0.5-0.5 g fresh plant material from each treatment was separated for drying at room temperature until at least 5 days. The real copper content in Indian mustard seeds was determined by atomic absorption spectrophotometry (AAS) (Hitachi, Z-8200, Japan). Values of Cu concentration in seeds are given in mM g⁻¹ dry weight (DW).

Preparation of the samples

At each metal concentration 8 replicates of 0.3 g fresh material (germinated seeds) were homogenised with 1.2 ml cool phosphate buffer using quartz sand in a cold mortar and centrifuged for 10 min at 12.000. x g, then the supernatant layer was used for all assays. In the assays for the spectrophotometric measurements, Thermo Spectronic Biomate 5 was used.

Determination of total antioxidant capacity

To evaluate the antioxidant power of the homogenates a simple and quick method was used called ferric reducing ability of plasma (FRAP).¹¹ The procedure described in the

literature was modified and applied for plant material.¹² The total antioxidant capacity was expressed in units of µmol g⁻¹ fresh weight (FW).

Determination of lipid peroxidation

Since malonyldialdehyde (MDA) is one of the end products of lipid peroxidation, the assay of MDA was applied to estimate lipid peroxidation (LP; modified method).¹³ MDA content was determined and is expressed in units nmol g⁻¹ fresh weight (FW).

Glutathione (GSH) evaluation

Glutathione content was measured using the method of Sedlak and Lindsay¹⁴. Data are expressed in µmol GSH g⁻¹ fresh weight (FW).

Estimation of total protein content

Protein content of plant homogenate was measured spectrophotometrically at 675 nm using the method of Lowry et al.¹⁵ These data were used to calculate the enzyme activities.

Activities of enzymes

The activity of glutathione-S-transferase (GST, EC 2.5.1.18.) was determined according to Mannervik and Guthenberg.¹⁶ Guaiacol peroxidase (GPOX, EC 1.11.1.7) activity was evaluated by the modified method of Singh et al., while for catalase (CAT, EC 1.11.1.6) we applied the assay of Beers and Sizer.^{17, 18} Total superoxide dismutase (SOD, EC 1.15.1.1) activity assayed as described by Misra and Fridovich.¹⁹ Glutathione reductase (GR, EC 1.6.4.2) activity was measured applying the method of Pinto and Bartley.²⁰ The values were calculated as the production of 1 mM conjugate per min and expressed as unit mg⁻¹ protein.

Histochemical detection of oxidative stress and its consequences

We assessed the loss of plasma membrane integrity in the root tips *in vivo* using Trypan blue, Aniline blue was applied for callose staining, Schiff's reagent was used for the detection of LP, and phloroglucinol-HCl for visualization of the lignification of cell walls as described by Yamamoto et al., Arduini et al. and Lequeux et al.^{21, 22, 23}

Statistics

Statistical analysis of the results was carried out using STATISTICA 9.0 software. We used Kruskal-Wallis ANOVA to test the differences between the mean values. In order to determine the relationship between the metal concentration and the four biochemical parameters, Spearman's Rank Order Correlation was used. Data are given in mean values ± standard deviation (SD) and calculated for fresh homogenate. The level of significance was generally p<0.05.

Results and discussion

Parameters of oxidative stress

Oxidative stress occurred in the seeds due to heavy metal treatments and all parameters were significantly affected by time duration and metal concentration used. Increase of time duration and/or metal concentration resulted in higher metal uptake in germinating seeds of *Brassica juncea* L. (Table 2A, B) similar to the results of Mihoub et al.²⁴ The data of the Tables show that the changes of all parameters depended either on the Cu concentration or the time of exposure, or both.

FRAP showed to be a good and quick semi-quantitative parameter to prove that oxidative stress caused by heavy metals is followed by the rapid activation of antioxidant defence system including e.g. ascorbic acid and phenolic components.²⁵ Cu-treatment was also followed by GSH-depletion which was probably due to the increased activity of GST and the enzymes of Halliwell-Asada cycle and the elevated synthesis of phytochelatins, as well (Fig. 1).^{25, 26}

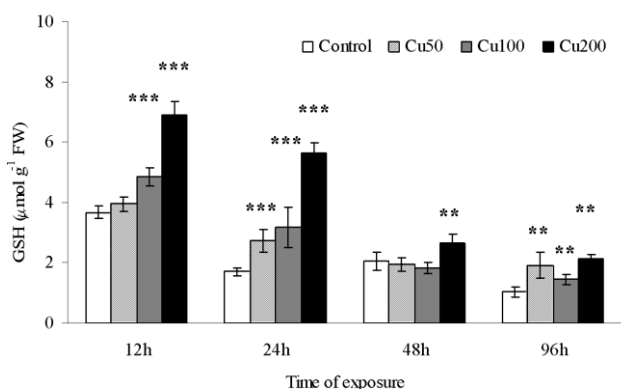


Figure 1. Time and dose-dependent changes of GSH-level in Cu-treated *B. juncea* seeds. Asterisks indicate significant differences between control and treated plants at * $p < 0.05$, ** $p < 0.01$ and *** $p < 0.001$.

The level of lipid peroxidation (LP) determined as malondialdehyde (MDA) content showed time- and dose-dependence, too. Generally, lipid peroxidation was higher in

the beginning of germination at all concentrations, and then attenuated. Significant differences were observed between the control and the treated seeds after each period. The reduction of LP in the second period of the germination was probably due to the activation of antioxidants and the elimination of lipid peroxides.²⁵

The application of excess Cu increased the activity of SOD in time-dependent manner in good agreement with the results of Wang et al.¹⁰ The activity of CAT and GPOX increased after 48-96h Cu treatment and was in significantly positive correlation with the changes of SOD activity (Spearman's $r = 0.63$ and $r = 0.44$; $p < 0.001$).^{10, 27}

Histochemical detection of oxidative stress and morphological changes

LP as one the markers of oxidative stress was detected after staining with Schiff's reagent in root tips (Fig. 2). Typical morphological symptoms of metal toxicity occurred in Cu-stressed plants (stunted, hook-formed and brownish root tips).^{23, 24}



Figure 2. Histochemical detection of LP in the root apices of germinating *B. juncea* seeds after 96 h Cu treatment. Bars indicate 1 mm.

Table 2A. The effect of Cu concentration and duration on the parameters (AAS, FRAP, GSH and GR) testing by two-way ANOVA. The level of significance: * $p < 0.05$, ** $p < 0.01$ and *** $p < 0.001$.

Effect	AAS	FRAP	GSH	GR
Cu concentration	$F_{3, 89} = 109.44^{***}$	$F_{3, 110} = 92.96^{***}$	$F_{3, 111} = 616.51^{***}$	$F_{3, 80} = 104.89^{***}$
Time	$F_{3, 89} = 297.97^{***}$	$F_{3, 110} = 13.63^{***}$	$F_{3, 111} = 270.67^{***}$	$F_{3, 80} = 71.45^{***}$
Conc. x time	$F_{9, 89} = 28.14^{***}$	$F_{9, 110} = 11.17^{***}$	$F_{9, 111} = 42.37^{**}$	$F_{9, 80} = 26.46^{***}$

Table 2B. The effect of Cu concentration and duration on the parameters (GST, GPOX, CAT and SOD) testing by two-way ANOVA. The level of significance: * $p < 0.05$, ** $p < 0.01$ and *** $p < 0.001$

Effect	GST	GPOX	CAT	SOD
Cu conc.	$F_{3, 93} = 66.37^{***}$	$F_{3, 90} = 124.40^{***}$	$F_{3, 88} = 127.85^{***}$	$F_{3, 76} = 242.80^{***}$
Time	$F_{3, 93} = 27.57^{***}$	$F_{3, 90} = 10.63^{***}$	$F_{3, 88} = 15.25^{***}$	$F_{3, 76} = 19.73^{***}$
Conc. x time	$F_{9, 93} = 27.91^{***}$	$F_{9, 90} = 13.74^{***}$	$F_{9, 88} = 10.91^{***}$	$F_{9, 76} = 24.60^{***}$

After 96 h using Trypan blue we found remarkable disruption of the rhizodermal and the cortical cells mainly the elongation zone due to increased level of LP.^{21, 23}

Decreased root elongation and induced production of callose could be visualized using Anilin blue as a fast reaction of the cells to avoid Cu toxicity, while lignification of cell walls was detected by phloroglucinol-HCl which refers to the long-term adaptation of the root tips.^{5, 21, 23, 27}

Acknowledgments

I thank Dr. Gábor Laskay for correcting the English of the manuscript.

References

- ¹Prasad, M. N. V., Strzałka, K., *Physiology and biochemistry of metal toxicity and tolerance in plants*. Kluwer Academic Publishers, Netherlands, **2002**, 235.
- ²Hirt, H. and Shinozaki, K., *Topics on Current Genetics*. Vol. 4. Springer-Verlag, Berlin Heidelberg, **2004**, 188-189.
- ³Prasad, M. N. V., *Heavy metal stress in plants: from biomolecules to ecosystems*. Springer-Verlag, Berlin Heidelberg, **2004**, 147.
- ⁴Janas, K. M., Zielinska-Tomaszewska, J., Rybaczek, D., Maszewski, J., Posmyk, M.M., Amarowicz, R., Kosinska, A., *J. Plant Phys.*, **2010**, *167*, 270–276.
- ⁵Chen X-Y. and Kim J-Y., *Plant Sign. Behav.*, **2009**, *4*(6), 489-49.
- ⁶Szöllösi, R., Varga, I. Sz., Erdei, L., Mihalik, E., *Ecotox. Environ. Safe.*, **2009**, *72*(5), 1337-1342.
- ⁷Prasad, M. N. V., Sajwan, K. S., Naidu, R., *Trace elements in the environment: biogeochemistry, biotechnology, and bioremediation*. CRC Press, Taylor & Francis Group, **2006**, 634-641.
- ⁸Kranner, I., Colville, L., *Env. Exp. Bot.*, **2011**, *72*, 93-105.
- ⁹Panou-Filotheou, H., Bosabalidis, A. M., Karataglis, S., *Ann. Botany*, **2001**, *88*, 207-214.
- ¹⁰Wang, S-H., Yang, Z-M., Yang, H., Lu, B., Li, S-Q., Lu, Y-P., *Bot. Bull. Acad. Sin.*, **2004**, *45*, 203-212.
- ¹¹Benzie, I. F. F., Strain, J. J., *Anal. Biochem.* **1996**, *239*, 70-76.
- ¹²Varga, I. Sz., Szöllösi, R., Bagyánszki, M., *Curr. Topics Biophys.*, **2000**, *24*(2), 219-225.
- ¹³Placer, Z. A., Cushman, L. L., Johnson, B. C., *Anal. Biochem.*, **1966**, *16*, 359-364.
- ¹⁴Sedlak, I., Lindsay, R. H., *Anal. Biochem.*, **1968**, *25*, 192-205.
- ¹⁵Lowry, O. H., Rosebrough, N. J., Farr, A. L., Randall, R. J., *J. Biol. Chem.*, **1951**, *193*, 265-275.
- ¹⁶Mannervik, B., Guthenberg, C., *Methods Enzymol.* **1981**, *77*, 231-235.
- ¹⁷Singh S., Melo J. S., Eapen S., D' Souza S.F., *J. Biotech.* **2006**, *123*, 43-49.
- ¹⁸Beers, R. F., Sizer, I. W. Jr., *J. Biol. Chem.*, **1952**, *195*, 133-140.
- ¹⁹Misra, H. P., Fridovich, I. *J. Biol. Chem.*, **1972**, *47*(10), 3170-3175.
- ²⁰Pinto, R. E., Bartley, W., *J. Biochem.*, **1969**, *112*, 109-115.
- ²¹Yamamoto, Y., Kobayashi, Y., Matsumoto, H., *Plant Physiol.*, **2001**, *125*, 199–208.
- ²²Arduini, I., Godbold, D. L., Onnis, A., *Tree Phys.*, **1995**, *15*, 411-415.
- ²³Lequeux, H., Hermans, C., Lutts, S., Verbruggen, N., *Plant Phys. Biochem.*, **2010**, *48*(8), 673-682.
- ²⁴Mihoub, A., Chaoui, A. El Ferjani, E., *Compt. Rend. Biologies*, **2005**, *328*, 33-41.
- ²⁵Blokhina, O., Virolainen, E., Fagerstedt, K. V., *Ann. Botany*, **2003**, *91*, 179-194.
- ²⁶Yruela, I., *Braz. J. Plant Phys.*, **2005**, *17*(1), 145-156.
- ²⁷Maksymiec, W., *Acta Physiol. Plant.*, **2007**, *29*, 177-187.

Received: 16.10.2012.

Accepted: 08.11.2012



CORROSION INHIBITION BY AMINO ACIDS - AN OVER REVIEW

S. GOWRI^{[a],*}, J. SATHIYABAMA^[a], S. RAJENDRAN^{[a],[b]}

Keywords: corrosion inhibition, amino acids, polarization, metals and alloys.

Amino acids have the ability to control corrosion of various metals such as carbon steel, zinc, tin and copper. It behaves as an inhibitor in acid medium, neutral medium and in deaerated carbonate solution. Various techniques like weight loss method, polarization study and AC impedance spectra have been used to evaluate the corrosion inhibition efficiency of amino acids. The protective film has been analyzed by IR spectroscopy, atomic force microscopy, scanning electron microscopy and auger electron spectroscopy. Adsorption of amino acid on metal surface obeys Langmuir, Flory-Huggins or Temkin isotherm, depending on nature of metal and corrosive environment. Polarization study reveals that amino acids can function as anodic or cathodic or mixed type of inhibitor depending on nature of metal and corrosive environment.

* Corresponding Author

E-Mail: divisrigowri@yahoo.in, sakthigowri@gmail.com

[a] PG and Research Department of Chemistry, Corrosion Research Centre, GTN Arts College, Dindigul-624 005, India.

[b] Department of Chemistry, RVS School of Engineering and Technology, Dindigul, India.

1. Introduction

Generally amino acids have two polar groups, namely, one amino group and one carboxyl group. It can coordinate with metals through the nitrogen atom and oxygen atom of the carboxyl group. So it has been widely used as corrosion inhibitor¹⁻⁵⁸. It has the ability to control the corrosion of a wide variety of metals such pure iron, carbon steel, zinc aluminum and tin. It behaves as corrosion inhibitor in acid medium, neutral medium and in deaerated carbonate solution. Various techniques have been used to evaluate the corrosion inhibition efficiency of amino acids and to analyze the nature of protective film formed on the metal surface. Depending on the nature of metal and nature of corrosive environment amino acids obeys different types of isotherms and behaves as different type of inhibitor, namely, anodic, cathodic or mixed type.

2. DISCUSSION

2.1. Metals

Amino acids and derivatives of amino acids have been used to prevent the corrosion of a wide variety of metals. Amino acids and its derivatives have the ability to prevent the corrosion of carbon steel (mild steel)^{1,5,6,9,11,17,19,20,22,23,27,29,31,32,37,50,53,54,56,58,66,69}, Cu-Ni alloys^{8,26,35}, aluminum^{38,39,51,52}, aluminum 7075 alloy^{10,48}, aluminum silicon carbide composite³⁰, pure iron^{16,40}, stainless steel¹³, copper^{3,14,18,21,25,36,43,61,64,67,68}, aluminum and zinc pigments⁴⁴, nickel^{2,65}, tin⁴¹, NST-44 carbon steel^{15,27,34,44}, Pb-Ca-Sn

alloy²⁴, Pb-Sb-Se-As alloy^{28,33}, reinforcing steel⁴², sulfur on the corrosion of mild steel⁴⁶, aluminum and magnesium alloys⁴⁷, Armco iron⁴⁹, copper electrode⁵⁵, cobalt³⁴, brass⁷, and bronze¹².

2.2. Medium

Amino acids and its derivatives have been used as inhibitor to prevent corrosion of metals in various environments- acidic neutral and deaerated carbonate solutions. The mainly used acid is hydrochloric acid^{1,6,9,11,16-18,25,30-32,36,55} and rarely used acids are sulphuric acid^{8,13,24,28,33,57,58}, citric acid⁴⁰, acetic acid²⁶, sodium chloride^{7,10}, sulfamic acid¹⁹, lime fluid (citrus aurantifolia)^{27,34}, and nitric acid^{3,21}.

2.3. Techniques

Even though several modern techniques are on the anvil, the mainly used methods in evaluation of inhibition efficiency of amino acids in preventing corrosion of metals are weight loss method^{3,5,11,13,15,21,24,28,31,33,34,36,38,40,49}, electrochemical studies such as polarization and AC impedance spectra^{1,3,4,6-8,11,13,20,21,23-26,28,29,31-33,35-38,40,42,43,45,46,49,51,52,54,55,61-69} and cyclic voltammetry⁵¹. XPS has been used to analyze the film formed on carbon steel surface²⁹. SEM technique has been used to study the morphology of the corroded surface of zinc in acidic medium in the presence of luecine and methionine^{22,24}. Infrared spectroscopy has been used to analyse the protective film formed on the metal surface⁵⁰.

2.4. Adsorption

The protective nature of amino acids is attributed to its adsorption on the metal surface. Various adsorption isotherms have been proposed. The adsorption isotherms include Langmuir isotherms^{11,16,18,19,24,28,33,38,39,46,69}, Flory-Huggins isotherm^{19,29,52}, Freundlich isotherm²³ and Temkin isotherm^{13,19,30,61,62}.

Table 1: Use of Amino acids as Corrosion Inhibitors

S. no	Metal	Medium	Inhibitors	Additive	Method	Findings	Ref.
1	Mild steel	1 M HCl	cysteine, serine amino butyric acid threonine, alanine valine aromatic amino acids, phenylalanine, tryptophan and tyrosine	-	Tafel polarization and electrochemical impedance spectroscopy methods and computationally by the quantum chemical calculation and molecular dynamics simulation	-	1
2	Nickel	Acid medium	12 amino acids	-	Density functional theory (DFT)	-	2
3	Copper	HNO ₃	L-methionine (MIT), L-methionine sulfoxide (MITO) and L-methionine sulfone (MITO ₂)	-	Weight loss, dc polarization and ac impedance techniques	Fukui functions	3
4	-	Acid media	cysteine	-	Electro chemical method	-	4
5	Carbon steel	Acid medium	Potassium salts of glycine and taurine.	CO ₂ loading, and piperazine	Weight loss method	-	5
6	Mild steel	1.0 M HCl	Alanine (Ala), cysteine (Cys) and S-methyl cysteine (S-MCys)	-	Tafel polarization and impedance measurements. Electrochemical frequency modulation (EFM) technique and inductively coupled plasma atomic emission spectrometry (ICP-AES)	Cathodic inhibitor, mixed-type inhibitor	6
7	Brass metal	0.6 M aqueous sodium chloride	Glycine, L(-) aspartic acid and L(-) glutamic acid	-	Potentiodynamic polarization and electrochemical impedance spectroscopy	-	7
8	Cu-30Ni alloy	0.5 M H ₂ SO ₄	Cysteine	nickel	Potentiodynamic polarization and impedance spectroscopy (EIS) at open circuit potential	Cathodic process	8
9	Mild steel	HCl	Glutamine, asparagines, aspartic acid, glutamic acid	-	Quantum chemical parameters, namely energy of the highest occupied molecular orbital, energy of the lowest unoccupied molecular orbital, energy gap, dipole moment, total energy, total electronic energy, core-core repulsion, ionisation potential, cosmo area, cosmo volume and other quantum descriptors [calculated from PM6, PM3, AM1, RM1 and modified neglect of diatomic overlap (MNDO) Hamiltonians]	-	9
10	Aluminum alloy Al7075	3.5% NaCl solution	L-glutamine	-	Higher corrosion current density, while the charge transfer resistance decreases and corrosion potential shifts toward more positive values	-	10
11	Carbon steel	1 M HCl	L-tryptophane	-	Weight loss experiment and Tafel polarization curve in the used temperature range (298-328 K) Langmuir adsorption isotherm	-	11
12	Bronze	0.2 g/L NaHCO ₃ +0.2 g/L Na ₂ SO ₄ aqueous solution (pH 5)	Two innocuous amino acids derivatives DL alanine and DL cysteine	-	X-ray fluorescence spectrometry	-	12
13	Stainless steel	Sulphuric acid (0.5 M H ₂ SO ₄ on AISI 316)	Enaminone compounds ethyl-3-[(2-aminoethyl) amino]-2-butenate (compound I) and ethyl-3-(2-amino-anilino)-2-butenate (compound II)	-	Weight loss and potentiostatic polarization techniques, Temkin isotherm in acid media	Mixed anodic-cathodic nature	13
14	Copper	aqueous solution	Glycine, alanine, methionine and glutamic acid	-	Thermodynamic studies by EMF measurement	-	14
15	NST-44 carbon steel	Cassava fluid	Leucine, alanine, methionine and glutamic acid	-	Weight loss immersion method, optical microscopic techniques	Alanine showed the highest inhibitive potential	15
16	Iron	HCl solution	Methionine and tyrosine	-	Electrochemical, FTIR, and quantum-chemical study, Langmuir isotherm, chronoamperometric measures	-	16

Table 1 (cont.): Use of Amino acids as Corrosion Inhibitors

S. no	Metal	Medium	Inhibitors	Additive	Method	Findings	Ref.
17	Carbon steel	HCl	Non ionic amino acid Schiff bases	-	Gravimetric technique, spectroscopic technique	-	17
18	Copper	0.5 M HCl solution	Amino acids are aspartic acid (Asp), glutamic acid (Glu), asparagine (Asn), glutamine (Gln)		Potentiodynamic and EIS measurements, Langmuir isotherm		18
19	Mild steel	5% sulfamic acid solution at 40 °C	N-acetylcysteine (ACC), cysteine (RSH), S-benzylcysteine (BzC) cysteine (RSSR), methionine (CH3SR)		Langmuir model while the Temkin isotherm, Flory-Huggins isotherm	Anodic sites	19
20	Mild steel	Acidic environment	α -amino acids alkylamides		Electrochemical testing was carried out using polarization scans and weight loss measurements.		20
21	Copper	Molar nitric solution	Valine (Val) and Glycine (Gly) accelerate the corrosion process; but Arginine (Arg), Lysine (Lys) and Cysteine (Cys)		Weight loss and electrochemical polarization measurements, quantum chemical calculations and inhibition efficiency was discussed using semi-empirical methods		21
22	Mild steel	Acidic medium	L-Leucine	Zinc	Scanning electron microscopy (SEM) and infrared studies (IR)	Cathodic and anodic sites to same extent, passivating type of inhibitors	22
23	Mild steel	Acid solution	Vanadium in aqueous solutions of amino acids(, glycine, alanine, valine, histidine, glutamic and cysteine)	-	Open-circuit potential measurements, polarization techniques and electrochemical impedance spectroscopy (EIS), Freundlich isotherm	-	23
24	Pb-Ca-Sn alloy	Sulfuric acid solution	cysteine (Cys), methionine (Met) and alanine (Ala)	-	Potentiodynamic polarization, electrochemical impedance spectroscopy (EIS), weight loss measurement and scanning electron microscopy (SEM) methods, Langmuir isotherm	--	24
25	Copper	0.5 mol/L HCl solution	Octanoyl glutamic acid, DL-threonine, DL-serine	-	Potentiodynamic polarization and electrochemical impedance spectroscopy	-	25
26	Cu-Ni alloys	Aqueous chloride solutions	Glycine	-	Polarization and impedance techniques	-	26
27	NST-44 mild steel	Lime fluid (citrus aurantifolia)	Leucine, alanine, methionine and glutamic acid.		Optical microscopic techniques		27
28	Pb-Sb-Se-As alloy	1.28 s.g. H ₂ SO ₄ solution	Tryptophane, proline and methionine	-	Linear polarization and weight loss measurements methods, Langmuir isotherm		28
29	Carbon steel	Decylamides of α -amino acids	Tyrosine and glycine derivatives, alanine and valine	-	Gravimetric and electrochemical techniques, Flory-Huggins adsorption isotherms, X-ray photoelectron spectroscopy	Cathodic type	29
30	Al-SiC(p) composite in	0.01, 0.1 and 1.0 N HCl (GG)	Glycyl Glycine		Chemisorbed following Temkin's model	Anodic inhibitor	30
31	Mild steel	in 1.0 M HCl medium	Leucine		Weight loss and Polarization studies Electrochemical impedance spectroscopic (EIS) data.	Cathodic control	31
32	Carbon steel	Hydrochloric acid	α -amino acids derivatives (tyrosine and glycine alanine and valine)		Gravimetric and electrochemical techniques X-ray photoelectron spectroscopy	Cathodic type	32
33	Pb-Sb-Se-As alloy	H ₂ SO ₄ solution	Tryptophane, proline and methionine		Linear polarization and weight loss measurements methods Langmuir isotherm		33

Table 1 (cont.): Use of Amino acids as Corrosion Inhibitors

S. no	Metal	Medium	Inhibitors	Additive	Method	Findings	Ref.
34	NST-44 mild steel	Lime fluid (citrus aurantifolia)	Leucine, alanine, methionine and glutamic acid.		Weight loss immersion method		34
35	Cu-Ni alloys	Aqueous chloride solutions	Amino acid like glycine cysteine		Polarization and impedance techniques.		35
36	Copper	0.5 mol/l-1 HCl solution	dl-alanine and dl-cysteine,	-	Weight-loss measurements, potentiodynamic polarisation curves, and electrochemical impedance spectroscopy	Anodic current densities	36
37	Mild steel	40% H ₃ PO ₄ solution	Cysteine (RSH), methionine (CH ₃ SR), cysteine (RSSR) and N-acetyl/cysteine (ACC)	-	Potentiostatic and electrochemical impedance (EIS) techniques under anodic and cathodic polarization conditions.	Mixed inhibitors	37
38	Aluminum	1 M HCl + 1 M H ₂ SO ₄ solution	Alanine, leucine, valine, proline, methionine, and tryptophan		Weight loss measurement, linear polarization and SEM techniques, Langmuir and Frumkin isotherms		38
39	Aluminum	1.0 N NaOH ₂	Arginine		Langmuir adsorption isotherm. Polarisation	Mixed type	39
40	Iron	Citric acid solution at pH = 5	glycine, leucine, D-L aspartic, arginine and methionine		Weight-loss, polarisation and EIS measurements	Cathodic inhibitors	40
41	Tin	Deaerated solution of citric-chloride solution (pH = 5)	Arginine		Potential-current curves Frumkin adsorption isotherm model.	Cathodic inhibitor	41
42	Reinfor-cing steel	Chloride ions, using extract solutions	Amino alcohol	-	Electrochemical measurements	-	42
43	Copper	sulfuric acid medium	Cysteine	-	Electrochemical methods	Cnodic dissolution	43
44	Aluminum and zinc pigments	Aqueous alkaline media	Amino and polyamino acids	-	-		44
45	Aluminum 2024	Luria Bertani medium	20 amino acid polyaspartate peptide		Electrochemical impedance spectroscopy		45
46	Sulfur on the corrosion of mild steel		cysteine and N-acetylcystein methionine and cysteine. Adsorption of methionine	-	Corrosion potential (Ecorr) using both the polarization resistance method and electrochemical impedance spectroscopy (EIS) Frumkin adsorption isotherm Langmuir adsorption isotherm.		46
47	Aluminum and magnesium alloys		N-acyl glutamates	-	Spectroscopic techniques		47
48	Aluminum alloy 7075	0.05 M NaCl solution	Amino acids	-	Potentiostatic method		48
49	Armco iron	Acid chloride solution	Tryptophane	-	Weight-loss measurement and various electrochemical AC and DC corrosion monitoring techniques.	Cathodic inhibitor Langmuir adsorption isotherm	49
50	Mild steel	Neutral aqueous environment containing 60 ppm Cl ⁻	Amino acids	Amino (trimethylene phosphoric acid), (ATMP), mono-lybdate and Zn ²⁺	X-ray diffraction technique FTIR and luminescence spectra. It seems that the protective film		50

Table 1 (cont.): Use of Amino acids as Corrosion Inhibitors

S. no	Metal	Medium	Inhibitors	Additive	Method	Findings	Ref.
51	Al	0.1 M NaCl solution	Arginine histidine glutamine asparagine alanine glycine.	-	Potentiodynamic technique cyclic voltammetry using a flow cell technique		51
52	Aluminum	in acidic chloride solutions	aspartic acid.	-	Polarization technique Flory-Huggins adsorption isotherm	Mixed-type inhibitors	52
53	Mild steel		Aqueous solutions of glycyl-tryptophan (GT) was studied	-	Kinetics of UV-induced chemiluminescence (CL)		53
54	Mild steel	pH, temperature, and hydrodynamic conditions	Polyaspartic acid,	-	Impedance spectroscopy (EIS), the rotating cylinder electrode (RCE), and coupon immersion.		54
55	Copper electrode	1 M HCl solution	amino acids	-	Polarization technique	Cathodic Tafel line	55
56	Mild steel	pH 9.5 to 10 (measured at 25 °C) in H ₂ SO ₄	Aspartic acid (C ₄ H ₇ NO ₄),	-	pH diagram for iron		56
57	Cobalt		Nineteen amino acids	-	Linear polarisation method	cathodic Tafel regions	57
58	Mild steel	hot sulphuric acid.	Aromatic amino acid tyrosine	-	Adsorption of the additive on the metal surface,		58
59	Brass	0.6 M aqueous sodium chloride	glycine (I), L(-) aspartic acid (II) and L(-) glutamic acid (III), benzenesulphonyl derivatives	-	Potentiodynamic polarization and electrochemical impedance spectroscopy		59
60	Nickel	acidic medium	12 amino acids	-	Density functional theory (DFT) study was carried out using the B3LYP/LANL2DZ method.		60
61	Copper	8 M phosphoric acid	proline, cysteine, phenyl alanine, alanine, histidine and glycine	-	Potentiodynamic polarization and rotation techniques, Temkin adsorption isotherm		61
62	Low chromium alloy steel (ASTM A213 grade T22)	7 wt percent sulfamic acid solutions	Tyrosine	-	Electrochemical impedance spectroscopy (EIS) and the new technique electrochemical frequency modulation (EFM), Temkin's adsorption isotherm.		62
63	Iron	0.1 M H ₂ SO ₄ solution	Glutamic acid	-	Electrochemical impedance spectroscopy (EIS) and polarization techniques	Self-Assembled films	63
64	Copper	0.5 M HCl	L-phenylalanine (L-Phe) and Ce(SO ₄) ₂	-	Weight-loss, electrochemical methods and surface analysis		64
65	Ni	1 M H ₂ SO ₄ solution	Alanine	-	Potentiodynamic polarization, electrochemical impedance spectroscopy (EIS) and the new electrochemical frequency modulation (EFM) methods	anodic-type inhibitor	65
66	Mild steel	0.1 M H ₂ SO ₄	L-Histidine (LHS)	-	weight loss measurements, and potentiodynamic polarization measurements, scanning electron microscopy (SEM) and atomic force microscopy	cathodic inhibitor	66
67	Copper	3% NaCl	Phenylalanine (Phe) and tryptophan (Trp)	-	Poten- tiodynamic polarization and electrochemical impedance spectroscopy.		67
68	Copper	0.5 M hydrochloric acid	Glutamic acid, cysteine, glycine	-	Electrochemical impedance spectroscopy and cyclic voltammetry		68
69	Mild steel in	0.1 M HCl solution	L-Tryptophan	-	Weight loss and potentiodynamic polarization measurements, Langmuir's adsorption isotherm	cathodic inhibitor	69

2.5. Langmuir adsorption isotherm

This type of isotherm is observed when iron immersed in HCl, in the presence of methionine and tyrosine¹⁶. Similar observation has been made when mild steel was immersed in HCl, in the presence of cysteine and N-acetylcystein, methionine and cysteine⁴⁶.

2.6. Flory-Huggins isotherm

This type of isotherm is obeyed when carbon steel is immersed in HCl, in the presence of decylamides of α -amino acid derivatives²⁹. Morad observed that Flory-Huggins isotherm is obeyed when mild steel was immersed in sulfamic acid in the presence of N-acetylcysteine (ACC), cysteine (RSH), S-benzylcysteine (BzC) cystine (RSSR) methionine (CH₃SR)¹⁹.

2.7. Temkin isotherm

This type of isotherm is obeyed when is Al-SiC(p) composite in immersed in HCl in the presence of amino acid glycyl glycine³⁰. The type of adsorption very much depends on the nature of metal, environment and amino acids used.

2.7.1. Mechanism of corrosion inhibition

Amino acids H₂NCH₂COOH, has two polar groups, namely, one amino group and one carboxyl group. It can coordinate with metals through nitrogen atom and oxygen atom.

Inhibition of corrosion of metals by amino acids is attributed to the adsorption of amino acids on the metal surface. The adsorption obeys Langmuir isotherm or Flory-Huggins isotherm or Temkin isotherm depending on the nature of metal and corrosive environment. Adsorption may be physisorption or chemisorption; film formation is also attributed^{3, 9, 27, and 38}. The degree of inhibition efficiency depends on molecular structure of amino acids and its solubility rather than difference in molecular weights alone¹. Strength of the inhibitor-metal bond also plays a major role in deciding the degree of inhibition by amino acids². Polarization study reveals that amino acids functions as anodic inhibitor or cathodic inhibitor or mixed type of inhibitor depending on the nature of environment and nature of metal.

2.7.2. Anodic inhibitor

dl-alanine and dl-cysteine, function as anodic inhibitor in controlling corrosion of copper in HCl medium³⁶.

2.7.3. Cathodic inhibitor

Glycine, valine, alanine, and tyrosine behaved as cathodic inhibitors in controlling corrosion of carbon steel in hydrochloric acid³².

2.7.4. Mixed type inhibitor

cysteine (RSH), methionine (CH₃SR), cystine (RSSR) and N-acetylcysteine (ACC) system retarded both the anodic and cathodic partial reactions of mild steel in phosphoric acids solutions³⁷.

References

- Eddy N.O., *Journal of Advanced Research*, **2011**, 2(1), 35-47.
- Gece G., Bilgiç S., *Corrosion Science*, **2010**, 52(10), 3435-3443,
- Khaled K.F., *Corrosion Science*, **2010**, 52(10), 3225-3234.
- Tkalenko D.A., Venkatesvaran G., Vishevskaya Yu.P., Keny S.J., Byk M.V., Muthe K., *Protection of Metals and Physical Chemistry of Surfaces*, **2010**, 46(5), 609-614.
- Ahn S, Song H.-J, Park J.-W., Lee J.H, Lee I.Y, Jang K.-R., *Korean Journal of Chemical Engineering*, **2010**, 27(5), 1576-1580;
- Amin M.A, Khaled K.F., Mohsen Q., Arida H.A., *Corrosion Science*, **2010**, 52(5), 1684-1695.
- Ranjana Banerjee R., Nandi M.M., *Indian Journal of Chemical Technology*, **2010**, 7(3), 176-180.
- Saifi H., Bernard M.C., Joiret S., Rahmouni K., Takenouti H., Talhi B., *Materials Chemistry and Physics*, **2010**, 120(2-3), 661-669.
- Eddy. N.O, *Journal of Advanced Research*, **2010**, 36(5), 354-363.
- Ashassi-Sorkhabi H., Asghari E., *Journal of Applied Electrochemistry*, **2010**, 40(3), 631-637.
- Fu J.-J., Li S.-N., Cao L.-H., Wang Y., Yan L.-H., Lu L.-D., *Journal of Materials Science*, **2010**, 45(4), 979-986.
- Varvara S., Popa M., Rustoiu G., Bostan R., Mureşan L., *Studia Universitatis Babeş-Bolyai Chemia*, **2009**, 2, 73-85.
- Hosseini S.M.A., Salari M., Ghasemi M., Abaszadeh M., *Zeitschrift für Physikalische Chemie*, **2009**, 223(7), 769-779.
- Spah M., Spah D.C., Deshwal B., Lee S., Chae Y.-K., Park J.W., *Corrosion Science*, **2009**, 51(6), 1293-1298.
- Alagbe M., Umoru L.E., Afonja A.A., Olorunniwo O.E., *Anti-Corrosion Methods and Materials*, **2009**, 56(1), 43-50.
- Zor S., Kandemirli F., Bingul M., *Protection of Metals and Physical Chemistry of Surfaces*, **2009**, 45(1), 46-53.
- Negm N.A., Zaki M.F., *Journal of Dispersion Science and Technology*, **2009**, 30(5), 649-655.
- Zhang D.-Q., Cai Q.-R., He X.-M., Gao L.-X., Zhou G.-D., *Materials Chemistry and Physics*, **2008**, 112 (2), 353-358.
- Morad M.S., *Journal of Applied Electrochemistry*, **2008**, 38(11), 1509-1518.
- Olivares-Xometl O., Likhanova N.V., Domínguez-Aguilar M.A., Arce E., Dorantes H., Arellanes-Lozada P., *Materials Chemistry and Physics*, **2008**, 110(2-3), 344-351.
- Barouni K., Bazzi L., Salghi R., Mihit M., Hammouti B., Albourine A., El Issami S., *Materials Letters*, **2008**, 62(19), 3325-3327.
- Singh P., Bhrara K., Singh G., *Applied Surface Science*, **2008**, 254(18), 5927-5935.
- El-Rabee M.M., Helal N.H., El-Hafez Gh.M.A., Badawy W.A., *Journal of Alloys and Compounds*, **2008**, 459(1-2), 466-471.
- Kiani M.A., Mousavi M.F., Ghasemi S., Shamsipur M., Kazemi S.H., *Corrosion Science*, **2008**, 50(4), 1035-1045.

- ²⁵ Zheng H.-A., Zhang D.-Q., Xing J., *Corrosion and Protection*, **2007**, 28(12), 607-609.
- ²⁶ Badawy W.A., Ismail K.M., Fathi A.M., *Electrochimica Acta*, **2006**, 51(20), 4182-4189.
- ²⁷ Alagbe M., Umoru L.E., Afonja A.A., Olorunniwo O.E., *Journal of Applied Sciences*, **2006**, 6(5), 1142-1147.
- ²⁸ Ghasemi Z., Tizpar A., *Applied Surface Science*, **2006**, 252(10), 3667-3672.
- ²⁹ Olivares O., Likhanova N.V., Gómez B., Navarrete J., Llanos-Serrano M.E., Arce E., Hallen J.M., *Applied Surface Science*, **2006**, 252(8), 2894-2909.
- ³⁰ Rao S.A., Padmalatha, Nayak J., Shetty A.N., *Transactions of the SAEST (Society for Advancement of Electrochemical Science and Technology)*, **2006**, 41(1), 01-04.
- ³¹ Dhayabaran V.V., Rajendran A., Selvaraj V., Suganya P., *Transactions of the SAEST (Society for Advancement of Electrochemical Science and Technology)*, **2006**, 41(1), 8-11.
- ³² Olivares O., Likhanova N.V., Gómez B., Navarrete J., Llanos-Serrano M.E., Arce E., Halle J.M., *Applied Surface Science*, **2006**, 252(8), 2894-2909.
- ³³ Ghasemi Z., Tizpar A., *Applied Surface Science*, 2006, 252(10), 3667-3672.
- ³⁴ Alagbe M., Umoru L.E., Afonja A.A., Olorunniwo O.E., *Journal of Applied Sciences*, 2006, 6(5), 1142-1147.
- ³⁵ Badawy W.A., Ismail K.M., Fathi A.M., *Electrochimica Acta*, **2006**, 51(20), 4182-4189.
- ³⁶ Zhang D.-Q., Gao L.-X., Zhou G.-D., *Journal of Applied Electrochemistry*, **2005**, 35(11), 1081-1085.
- ³⁷ Morad M.S., *Journal of Applied Electrochemistry*, **2005**, 35(9), 889-895.
- ³⁸ Ashassi-Sorkhabi H., Ghasemi Z., Seifzadeh D., *Applied Surface Science*, **2005**, 249(1-4), 408-418.
- ³⁹ Jeyaraj T., Paramasivam M., Raja C., Jayaprakash S., Mariarajan R., *Transactions of the SAEST (Society for Advancement of Electrochemical Science and Technology)*, **2005**, 40(4), 113-117.
- ⁴⁰ Zerfaoui M., Oudda H., Hammouti B., Kertit S., Benkaddour M., *Progress in Organic Coatings*, **2004**, 51(2), 134-138.
- ⁴¹ Zerfaoui M., Hammouti B., Oudda H., Benkaddour M., Kertit S., *Bulletin of Electrochemistry*, **2004**, 20(10), 433-437.
- ⁴² Jamil H.E., Shriiri, A., Boulif R., Bastos C., Montemor M.F., Ferreira M.G.S., *Electrochimica Acta*, **2004**, 49(17-18), 2753-2760.
- ⁴³ Matos J.B., Pereira L.P., Agostinho S.M.L., Barcia O.E., Cordeiro G.G.O., D'Elia E., *Journal of Electroanalytical Chemistry*, **2003**, 570(1), 91-94.
- ⁴⁴ Müller, B., *Pigment and Resin Technology*, **2002**, 31(2), 84-87.
- ⁴⁵ Örnek D., Jayaraman A., Syrett B., Hsu C.-H., Mansfeld, F., Wood T., *Applied Microbiology and Biotechnology*, **2002**, 58(5), 651-657.
- ⁴⁶ Morad M.S.S., Hermas A.E.-H.A., Aal M.S.A., *Journal of Chemical Technology and Biotechnology*, **2002**, 77(4), 486-494.
- ⁴⁷ Silverman D.C., Hirzel T.K., *Corrosion*, **2002**, 58(2), 99-102.
- ⁴⁸ Bereket G., Yurt A., *Corrosion Science*, **2001**, 43(6), 1179-1195.
- ⁴⁹ Aouniti A., Hammouti B., Abed Y., Kertit S., *Bulletin of Electrochemistry*, **2001**, 17(1), 13-17.
- ⁵⁰ Gomma G.K., *Bulletin of Electrochemistry*, **1998**, 14(12), 456-461.
- ⁵¹ El-Shafei A.A., Moussa M.N.H., El-Far A.A., *Journal of Applied Electrochemistry*, **1997**, 27(9), 1075-1078.
- ⁵² Al-Mayouf A.M., *Corrosion Prevention and Control*, **1996**, 43(3), 68-74.
- ⁵³ Lozovskaya E.L., Makareeva E.N., Bol'shakova I.V., Sapezhinskij I.I., *Radiatsionnaya Biologiya, Radioekologiya*, **1996**, 36(3), 405-410.
- ⁵⁴ Silverman D.C., Kalota, D.J., Stover, F.S., *Corrosion*, **1995**, 51(11), 818-825.
- ⁵⁵ Gomma G.K., Wahdan M.H., *Materials Chemistry and Physics*, **1994**, 39(2), 142-148.
- ⁵⁶ Kalota D.J., Silverman D.C., *Corrosion*, **1994**, 50(2), 138-145.
- ⁵⁷ Bilgiç S., Aksut A.A., *British Corrosion Journal*, **1993**, 28(1), 59-62.
- ⁵⁸ Oni A., *Corrosion Prevention and Control*, **1992**, 39(5), 128-130.
- ⁵⁹ Ranjana Banerjee R., Nandi M., *Indian Journal of Chemical Technology*, **2010**, 17(3), 176-180.
- ⁶⁰ Gece G., Bilgiç S., *Corrosion Science*, **2010**, 52(10), 3435-3443.
- ⁶¹ Abdel Rahman H.H., Moustafa A.H.E., Awad M.K., *International Journal of Electrochemical Science*, **2012**, 7(2), 1266-1287.
- ⁶² Abdel-Fatah H.T.M., *Anti-Corrosion Methods and Materials*, **2012**, 59(1), 23-31.
- ⁶³ Zhang Z., Yan G., Ruan L., *Advanced Materials Research*, **2012**, 415-417, 964-967.
- ⁶⁴ Zhang D.-Q., Wu H.B., Gao L.-X., *Materials Chemistry and Physics*, **2012**, 133(2-3), 981-986.
- ⁶⁵ Hamed E., Abd El-Rehim S.S., El-Shahat M.F., Shaltot A.M., *Materials Science and Engineering B: Solid-State Materials for Advanced Technology*, **2012**, 177(5), 441-448.
- ⁶⁶ Mobin M., Parveen M., Rafiquee M.Z.A., *Journal of Materials Engineering and Performance*, **2012**, 1-9, Article in Press.
- ⁶⁷ Liu P., Gao L., Zhang D., *Journal of the Chinese Society of Corrosion and Protection*, **2012**, 32(2), 163-167.
- ⁶⁸ Zhang D.-Q., Xie B., Gao L.-X., Cai Q.-R., Joo H.G., Lee K.Y., *Thin Solid Films*, **2011**, 520(1), 356-361.
- ⁶⁹ Mobin M., Parveen M., Alam Khan M., *Portugaliae Electrochimica Acta*, **2011**, 29(6), 391-403.

Received: 31.10.2012.
Accepted: 15.11.2012.



AN OVERVIEW OF WAX HYDROFINING CATALYSTS IN CHINA

Liu Shu^{[a]*} and You Hongjun^[b]

Keywords: China; wax; overview; hydrofining; catalysts

Catalytic properties of FV series and RFW-3 wax hydrofining catalysts have been introduced and compared. Effects of different catalysts such as FV-10, FV-30, RJW-2 and RJW-3 on the quality of wax at a pilot plant have been also discussed. FV-30's life has been also tested at a large-scale plant. The experimental results show that RJW-3 have high catalytic performance and wax products obtained meet the requirement of Chinese wax standard.

* Corresponding Author

Fax: 86-24-56860869

E-Mail: liushu-2012@hotmail.com

[a] Liaoning Shihua University, Fushun, Liaoning, P.R. China.

[b] SAIT Polytechnic, Calgary, Alberta, Canada.

Introduction

Wax during the oil refinery process is one of the important chemical products.¹ Wax plays an important role in *Chinese* industries such as lighting, packaging, farming, chemicals, rubber, medicine and homecare products, etc. *China* is No. 1 in production and consumption of wax in the world. The production and consumption of wax in *China* has reached to a tune of 16 and 7.81 million tons respectively in 2011.² Although *China* has a lot of wax, it still imports special wax products from other countries due to the high quality performance. Sinopec *Fushun* Research Institute of Petroleum and Petrochemicals have developed new hydrofining catalysts for petroleum wax such as FV series wax hydrofining catalysts such as FV-1, FV-10, FV-20 and FV-30 have large pore volume, high specific surface area and concentrated pore structure which are suitable to wax hydrofining. They have good activity, selectivity and stability, high mechanical strength, especially highly condensed aromatics saturation activity. Catalysts have good repetition characteristics. Successful commercial application of FV series catalysts is used under medium pressure, low temperature and low H₂-to-wax ratio conditions. Wax hydrofining process can produce petroleum wax products which meet requirements for the national standard of wax (food grade) (GB7189-94).³ RJW-3 wax hydrofining catalysts have been applied on a 100,000 t/y Wax Hydrofining Plant of Jingmen Petrochemical Company. It is a tri-lobe shape for wax hydrofining catalysts with Ni-W as its active component. RJW-3 wax hydrofining catalysts have high activity for aromatic hydrogenation, anti-cracking ability, proper pore structure, small diffusion resistance and improving mass transfer in gas-liquid dispersions of a reactor.⁴

In the present paper, catalytic properties of FV series and RFW-3 wax hydrofining catalysts have been reviewed. Effects of different catalysts such as FV-10, FV-30, RJW-2 and RJW-3 on the quality of wax at a pilot plant have been also introduced, in comparison to product quality and performance of FV and RJW series wax hydrofining catalysts. FV-30's life has been also studied at a large-scale plant.

Discussion

Comparing catalytic properties between FV series and RJW-3 wax hydrofining catalysts

Table 1 shows catalytic properties of FV series and RFW-3 wax hydrofining catalysts.^{4,5} FV series and RFW-3 wax hydrofining catalysts consisted of Ni element. Furthermore, FV-20, FV-30 and RJW-3 had the same components (Mo-Ni). On the other hand, FV-1 and FV-10 only included W element. The catalysts had different shapes except FV-20 and FV-30. FV-10 and FV-20 almost have the same performance such as diameter, pore volume, surface area, porosity and mechanical strength. In addition, FV-1 and FV-30 have the similar properties such as diameter, pore volume, surface area and mechanical strength.

Effects of different catalysts such as FV-10, FV-30, RJW-2 and RJW-3 on the quality of wax at a pilot plant

Zhang Yanxia³ introduced a new catalyst (FV-30). She described how to produce FV-30 and studied effects of different catalysts (FV-10 and FV-30) on the quality of wax in Table 2. The experimental results showed that FV-10 and FV-30 had the same performance except easy absorbance, however easy absorbance of FV-30 is very close to that of FV-10.

On the other hand, wax products met the requirement of *Chinese* wax standard except needle penetration when FV-10 and FV-30 as catalysts were used. FV-30 had good catalytic performance, high strength, small particular and more adaptable to wax feedstock. Its shape was five tooth balls.

Liu Yuqing⁴ studies on catalytic properties of RJW-2 and RJW-3. Table 3 showed effects of different catalysts (RJW-2 and RJW-3) on the quality of wax at a pilot plant. The experimental results showed that RJW-2 and RJW-3 had the same performance except readily carbonizable substances and UV absorbance of condensed-nuclei aromatics. When RJW-2 was used as a catalyst, readily carbonizable substances of wax products did not meet *Chinese* food grade wax standard. RJW-3 had the high catalytic activity, high performance for aromatics saturation, anti-cracking ability and high compressive strength.

Table 1. Properties of FV series wax hydrofining catalysts and RFW-3 hydrofining catalysts.

Quality parameters	Catalysts				
	FV-1	FV-10	FV-20	FV-30	RJW-3
Active metal components	W-Ni	W-Mo-Ni	Mo-Ni	Mo-Ni	Mo-Ni
Catalysts' shape	Five tooth balls /sphere	Sphere	Cloverleaf pattern	Cloverleaf pattern	Butterfly
Diameter (mm)	2.2-2.6	1.1-1.5	1.1-1.2	2.0-2.4	1.6
Pore volume, (mL·g ⁻¹)	≥0.40	≥0.35	≥0.34	≥0.42	≥0.22
Surface area, (m ² ·g ⁻¹)	≥150	≥150	≥150	≥160	≥110
Bulk density, (g·cm ⁻³)	0.90-0.95	0.82-0.88	0.74-0.81	0.70-0.76	0.97
Porosity (%)	35	44	42	45	-
Mechanical strength (N·mm ⁻¹)	≥30 (N/grain)	≥18	≥16	≥30 (N/grain)	≥18

Table 2. Effects of different catalysts (FV-10 and FV-30) on the quality of wax at a pilot plant

Quality parameters	FV-10	FV-30	#58 semi-refined wax standard	FV-10	FV-30	#64 fully refined wax standard
Feedstock	No.1	No.1		No.2	No.2	
Temperature (°C)	260	260		260	260	
Pressure (MPa)	6.0	6.0		6.0	6.0	
Volume hour space velocity (h ⁻¹)	1.1	1.1		1.0	1.0	
H ₂ -to-wax ratio	300	300		500	500	
Saybolt colour (number)	+30	+30	≥+17	+30	+30	≥+25
Light stability (number)	5-6	5-6	≤7	3	3	≤5
Thermal stability (number)	+15	+15		+25	+25	
Melting point (°C)	58.90	58.90	58-60	65.8	65.8	64-66
Weight of oil (%)	1.10	1.10	≤1.80	0.30	0.30	≤0.50
Needle penetration, 25°C (0.1mm)	28	28	≤20	17	17	≤16
Easy absorbance (cm ⁻¹)						
280 nm	0.466	0.473		0.102	0.106	
290 nm	0.242	0.244		0.510	0.502	

Table 3. Effects of different catalysts (RJW-2 and RJW-3) on the quality of wax at a pilot plant

Quality parameters	RJW-2		RJW-3		Food grade wax standard
	Feedstock	Product	Feedstock	Product	
Temperature (°C)	243		235		
Hydrogen pressure (Mpa)	6.50		5.70		
Weight hour space velocity (h ⁻¹)	14		16		
Colorimetry colour (number)			7		
Saybolt colour (number)	+16	+30		+30	≥25
Melting point (°C)	63.6	63.6	60.7	60.8	
Mechanical impurities	No	No	Yes	No	No
Water	No	No	No	No	No
Light stability (number)	6	3	6	3	≤5
Weight of oil (%)	0.36	0.38	0.45	0.48	≤0.50
Readily carbonizable substances	Fail	Fail	Fail	Pass	Pass
UV absorbance of condensed-nuclei aromatics (cm ⁻¹)					
280-289nm	0.09	0.011	0.20	0.11	≤0.15
290-299nm	0.16	0.006	0.24	0.076	≤0.12
300-359nm	0.19	0.001	0.31	0.052	≤0.08
360-400nm	0.01	0.001	0.03	0.004	≤0.02

FV-30's life tests at a large scale plant

Wang Shixin⁵ explained more details about FV-30's life tests at a large scale plant. Table 4 showed results of FV-30's life tests at a large scale plant. The experimental results showed that FV-

30 kept the same catalytic performance such as light stability, thermal stability, Saybolt colour and readily carbonizable substances after 2505 hours. However, products' easy absorbance and UV absorbance of condensed-nuclei aromatics did not follow any rules.

Table 4. Results of catalyst life tests at a large-scale plant

Quality parameters	201 h	449 h	1217 h	1593 h	2025 h	2505 h
Light stability (number)	3	3	3	3	3	3
Thermal stability (number)	+29	+29	+28	+28	+28	+28
Saybolt colour (number)	+30	+30	+30	+30	+30	+30
Readily carbonizable substances	Pass	Pass	Pass	Pass	Pass	Pass
Easy absorbance (cm ⁻¹)						
280nm	0.024	0.013	0.022	0.026	0.023	0.013
290nm	0.015	0.006	0.011	0.016	0.012	0.007
UV absorbance of condensed-nuclei aromatics (cm ⁻¹)	Pass	-	Pass	-	Pass	Pass
280-289nm	0.013		0.013		0.048	0.009
290-299nm	0.009		0.009		0.036	0.007
300-359nm	0.004		0.003		0.012	0.005
360-400nm	0.001		0		0.001	0

Conclusion

Based on the above review and discussion, RJW-3 used to refine wax products is better than that of FV-30. RJW-3 has the high catalytic activity, high performance for aromatics saturation, anti-cracking ability and high compressive strength. Wax products obtained meet Chinese food grade wax standard. On the other hand, although FV-30 has a lot of advantages such as it has good catalytic performance, high strength, small particular and more adaptable to wax feedstock, wax products' needle penetration does not meet the requirement of Chinese wax standard, so RJW is one of the best catalysts for refining wax products.

References

- ¹ Zhang, X. L. *Eur. Chem. Bull.*, 2012, 1(6), 210.
- ² Huang, W. *Eur. Chem. Bull.*, 2012, 1(7), 266.
- ³ Zhang, Y. X., Yuan, S. H., Yuan, P. F., Zhang, H., Gao, P. and Fu, Q. H. *Journal of Petrochemical and Universities*, 2012, 25(1), 41.
- ⁴ Liu, Y. Q. *Petroleum Processing and Petrochemicals*, 2011, 41(5), 24.
- ⁵ Wang, S. X. *Contemporary Chemical Industry*, 2012, 41(7), 695.

Received: 05.11.2012.
Accepted: 15.11.2012.



TOXIC ELEMENTS IN THE SEWAGE SLUDGE – SOIL – PLANT CHAIN

Attila Tomócsik^{[a]*}, Viktória Orosz^[a], Tibor Aranyos^[a], Marianna Makádi^[a] and György Füleky^[b]

Paper was presented at the 4th International Symposium on Trace Elements in the Food Chain, Friends or Foes, 15-17 November, 2012, Visegrád, Hungary

Keywords: sewage sludge compost, agriculture, toxic element, sandy soil

According to statistical data the amount of sewage sludge does not increase as it was prognosed some years ago. Although this is a positive effect, we have to solve the problem of recycling of the sewage sludge. The appropriate chemical composition of municipal sewage sludge compost is suitable for nutrient supply in the agriculture. The small-plot experiment with sewage sludge compost was started in the spring of 2003. Three doses of compost (9, 18, 27 t ha⁻¹) and a control treatment were used in the experiment. The small-plot experiment was re-treated in the fall of 2006 and 2009. In the composting process bentonite, rhyolite and wheat straw were used as additives for improving the quality of the compost. Our purpose was to stabilize or increase the fertility of sandy soil and contribute to the reduction of environmental pollution. In the plot experiment there were three test plants: triticale, maize and pea. These three plants were sown in crop rotation. We examined the concentration of nickel (Ni) and zinc (Zn) in two soil layers, 0-30 and 30-60 cm in 2008-2009 years. We could not observe toxic effects on the test plants. The aim of the experiment was to investigate whether the application of sewage sludge compost cause hazardous accumulation of toxic elements in the soil and plants.

* Corresponding Authors

Fax: (+36)-42-496-009

E-Mail: tomocsik@agr.unideb.hu

[a] Research Institutes of University of Debrecen, H-4400 Nyíregyháza, Westsik Vilmos u. 4-6.

[b] Szent István University, Department of Soil Science and Agricultural Chemistry, H-2103 Gödöllő, Páter Károly u. 1.

Introduction

Sewage sludge is an organic waste which usually contains high levels of nitrogen and phosphorous as well as significant concentrations of micronutrients^{1,2}. The use of sewage sludge in soil has very beneficial effects on the quantity and availability of nutrients, on the restoration of structural stability of the soil and on resistance against soil erosion^{3,4}.

Composting offers an effective method for treating sewage sludge by stabilizing organic matter, reducing odour, and killing human pathogens and weed seeds by the heat generated^{5,6}. The products can be used as soil conditioner to improve soil physical properties by increasing soil organic matter content. In this way the water holding capacity and aggregate stability are increased, but soil bulk density is reduced⁷. Sewage sludge compost also represents a source of nitrogen (N), phosphorus (P), potassium (K) and trace elements such as zinc (Zn), copper (Cu) and molybdenum (Mn) for plant growth⁸.

However, the presence of toxic elements in composts is the main cause of adverse effects on animal and human health, transmitted through the food chain from soil, groundwater and plants⁹.

The sewage sludge contains toxic elements within an organic matrix. This may lead to the increased solubility of some of the metals (due to the formation of soluble organic complexes) or to their immobilization and subsequent reduced possibility of being assimilated by the plant¹⁰. Consequently, exact analyzing the contents of toxic elements in composts is very important for the routine monitoring and risk assessment and regulation of environmental protection.

In the present study, we aimed to measure toxic element, such as nickel (Ni) and potential toxic element, like zinc (Zn). During the experiment we would like to follow the movement of toxic elements in the food chain.

Experiments

Experimental design

The small-plot experiment was established in spring, 2003 at the Research Institute of CAAES of University of Debrecen, at the town of Nyíregyháza, located in the NE part of Hungary. It was re-treated in 2006, when the field experiment was re-arranged and the size of plots was enlarged.

The size of small-plots was 19 x 36 meters. The experiment was done in five replications on sandy soil. Our compost fills the requirements of the Agricultural Ministry Order of 36/2006 (V.18.). The compost includes 40% sewage sludge, 25% straw, 30% rhyolite and 5% bentonite. These materials have good effects on light textured sandy soils especially when they are mixed with organic material

(e.g. sewage sludge). The compost was applied at 9, 18, 27 t ha⁻¹ doses, ploughed into the 0-30 cm soil layer before sowing. The effect of the applied compost on triticale (*Triticosecale Wittmack*), maize (*Zea mays*) and pea (*Pisum sativum L.*) was studied.

Toxic elements of plant samples were measured after harvesting. In the case of triticale and maize the toxic elements content of grain was measured. The toxic element content of pea plants were measured in its three parts (root, straw + pods and grain). Composite soil samples were mixed from 5 subsamples in each plot from 0-30 and 30-60 cm soil layers after harvesting of all test plants.

The applied compost

In the Table 1 can be seen the important parameters of the applied compost

Table 1. Main characteristics of the applied compost

Parameter	Value
pH (H ₂ O 1:10)	7.2
Dry matter content [m/m% raw matter]	54
Organic matter content [m/m % dry matter]	26
Total N-content [m/m% dry matter]	1.68
Total P ₂ O ₅ -content [m/m% dry matter]	0.7
Total K ₂ O-content [m/m% dry matter]	0.4
As (mg kg ⁻¹)	5.26
Cd (mg kg ⁻¹)	0
Co (mg kg ⁻¹)	0
Cr (mg kg ⁻¹)	21.96
Cu (mg kg ⁻¹)	149.7
Hg (mg kg ⁻¹)	1.42
Ni (mg kg ⁻¹)	12.09
Pb (mg kg ⁻¹)	23.33
Se (mg kg ⁻¹)	2.51

In the composted sewage sludge there were nitrogen (N), phosphorus (P) and potassium (K), which are useful for enhancing the available nutrients content of soil. The toxic elements content of compost was low therefore it is good for agricultural utilization. In the applied compost amount of nickel was under the limit value determined by the Agricultural Ministry Order of 36/2006 (V.18.).

Chemical and statistical analysis

The Zn and Ni content of soil and plant samples were measured according to the MSZ –08-0012/16-87. Briefly, the samples were digested with cc. HNO₃ : H₂O₂ and after filtering, the heavy metal contents of solutions were measured by using an ICP-OES emission spectrometer.

Statistical significance (P<0.05) of the differences was determined by one-way ANOVA and Tukey's multiple range test. Statistical analysis was performed with SPSS 13.0., with five replications.

Results and Discussion

Toxic elements in the soil

The utilization of sewage sludge in agriculture may cause to get a certain amount of toxic elements into the soil. This could result in the contamination of soil and plants by toxic elements. In our data reveal the fate of Zn and Ni in the sewage sludge-soil-plant chain.

The heavy metal content in soils comes from two sources: first, from the natural heavy metal content of soil and on the other hand, as a result of soil pollution. The measurable concentration of the micronutrients in the soil usually increases when the amount of heavy metals entering into the soil is higher than their leached or utilized quantity¹¹.

In the Table 2 the Ni and Zn concentrations of soil of the three test plants measured in 2008 are shown. The Ni and Zn content of the soil were below the 40 and 200 mg kg⁻¹ limit in all treatments in this year. Concentration of Zn was increased after the treatments in the upper 0-30 cm soil layer, but this increase was not statistically significant. The measured Zn concentrations were around 30 mg kg⁻¹. In Canada¹² various crop responses were measured to a mixed municipal solid waste compost and the fate of certain metals associated with compost were examined. Plant and soil samples were collected after the compost application to analyse for content of Arsenic (As), Copper (Cu), Zn, Mercury (Hg) and Lead (Pb). The research results showed that the compost slightly increased the heavy metal concentrations of the soil. The amount of Ni did not increase in the top soil under triticale.

Similar results were found when sea weeds compost was applied (leaves of beached *Posidonia oceanica* were used), which had high concentrations of heavy metals. Except of Ni, they measured higher heavy metal concentrations in soil samples amended with compost than in the control ones. The low concentration of Ni in soluble and exchangeable form explains its low mobility and biological activity¹³.

Toxic elements content of soil samples measured in 2009 can be seen in Table 3. Ni concentrations of soil samples were similar in both soil layers (7.35 – 10.09 mg kg⁻¹) in 2009 and neither was above the 40 mg kg⁻¹ threshold limit. The compost treatment did not increase its concentration. Low increase of Zn concentration in all treatments was found in the top soil samples collected from green pea's plots. On the contrary a researcher¹⁴ observed significantly higher levels of Zn, manganese (Mn) and Cu in soil amended with compost at a rate of 19 t ha⁻¹ but their applied compost had high heavy metal content (Zn: 566 mg kg⁻¹, Mn: 176 mg kg⁻¹ and Cu: 226 mg kg⁻¹).

Concentrations of measured elements were under the limit value (Ni: 40 and Zn: 200 mg kg⁻¹).

Toxic elements in the test plants

Pea (*Pisum sativum L.*)

In Table 4 presents the ratio of toxic elements content in different parts of pea in the sewage sludge compost treatment. The amount of Ni measured in the pea grain yield was slightly higher than the plants growing in unpolluted sites but among the treatments the differences are not

significant. The amount of Zn was higher in the grain yield compared to other two parts of the plants in the year 2008 and 2009. Due to the 18 and the 27 t ha⁻¹ treatment the Zn concentration increased in different parts of the plants. In

2009 the amount of Zn increased only in the 9 and 27 t ha⁻¹ treatments compared to the control plots, while the Zn concentrations measured in the 18 t ha⁻¹ treatments were similar to the control ones.

Table 2. Nickel and zinc content in two layers of soil under test plants in the sewage sludge compost experiment in 2008

Plant	Dose of compost (t ha ⁻¹)	Ni (mg kg ⁻¹)				Zn (mg kg ⁻¹)			
		0-30 cm		30-60 cm		0-30 cm		30-60 cm	
		Mean	S.D.	Mean	S.D.	Mean	S.D.	Mean	S.D.
Triticale	control	4.724	6.364	9.116	1.648	33.84	2.64	29.22	1.13
	9	4.230	5.649	9.274	1.494	35.26	1.79	28.40	1.54
	18	4.280	5.588	8.295	0.246	36.76	4.29	28.45	1.39
	27	4.058	5.065	10.768	3.353	35.48	4.97	29.36	1.81
Maize	control	0.065	0.055	9.860	1.120	32.53	2.29	28.46	1.11
	9	3.878	5.236	9.380	1.176	33.04	2.17	29.17	0.32
	18	4.118	5.110	9.393	0.405	34.98	2.33	29.42	2.51
	27	3.908	4.917	9.394	0.973	35.96	1.35	29.24	1.81
Green pea	control	0.123	0.037	10.478	1.100	32.15	7.48	26.88	1.28
	9	3.828	4.808	10.010	1.174	36.46	10.37	31.64	6.85
	18	3.746	4.974	9.862	2.059	33.94	3.57	27.84	2.85
	27	4.894	6.488	9.584	1.741	33.40	1.78	27.80	1.98
approved limit ¹ (mg kg ⁻¹)		40				200			

¹ (50/2001. Government regulation). There was not significant difference among treatments, according to the Tukey's test (p>0.05)

Table 3. Nickel and zinc content in two layers of soil under test plants in the sewage sludge compost experiment in 2009

Plant	Dose of compost (t ha ⁻¹)	Ni (mg kg ⁻¹)				Zn (mg kg ⁻¹)			
		0-30 cm		30-60 cm		0-30 cm		30-60 cm	
		Mean	S.D.	Mean	S.D.	Mean	S.D.	Mean	S.D.
Triticale	control	8.256	1.177	8.294	0.275	21.857	2.547	21.971	2.703
	9	7.924	0.734	8.992	0.816	22.201	2.172	21.989	1.370
	18	7.761	1.130	8.616	1.576	22.137	1.726	19.755	4.213
	27	8.058	0.377	7.994	1.623	22.580	2.325	20.258	5.766
Maize	control	8.510	1.528	10.099	1.228	20.082	1.423	20.270	5.449
	9	9.625	3.265	9.411	2.593	23.016	4.989	22.221	9.451
	18	8.322	1.680	8.381	2.760	20.941	1.057	17.681	3.592
	27	7.703	1.617	8.390	1.729	20.673	0.989	17.249	3.363
Green pea	control	8.203	1.297	8.346	2.680	22.677	2.779	20.359	3.167
	9	8.503	1.454	8.509	0.426	23.665	3.686	22.375	1.463
	18	8.034	1.308	7.356	2.572	24.137	2.708	21.104	4.664
	27	8.161	1.511	7.845	3.304	27.806	3.471	19.502	4.702
approved limit ¹ (mg kg ⁻¹)		40				200			

¹ (50/2001. Government regulation) There was not significant difference among treatments, according to the Tukey's test (p>0.05)

Table 4. Nickel and zinc concentrations in different parts of pea in the sewage sludge compost experiment

	Dose of compost (t ha ⁻¹)	Ni, mg kg ⁻¹				Zn, mg kg ⁻¹			
		2008		2009		2008		2009	
		Mean	S.D.	Mean	S.D.	Mean	S.D.	Mean	S.D.
Root	control	33.58	23.25	15.08	5.25	20.52	8.24	26.33	6.23
	9	32.87	23.47	14.25	7.64	15.26	11.77	29.16	6.72
	18	36.39	30.23	5.77	2.69	22.24	12.18	22.87	9.07
	27	52.40	51.23	3.64	1.47	23.88	8.10	32.59	5.66
Straw + Pods	control	1.75	1.03	12.48	7.33	13.04	5.14	25.29	3.66
	9	2.59	2.75	20.88	15.83	15.04	2.70	21.45	3.81
	18	1.61	1.24	33.30	30.31	13.60	2.57	24.27	4.99
	27	1.71	0.71	25.52	18.45	19.10	8.11	24.78	6.93
Grain	control	12.36	8.87	7.92	3.48	48.27	11.13	46.91	5.27
	9	7.61	5.34	5.55	2.52	43.99	20.87	44.72	7.73
	18	8.69	3.22	2.38	0.94	51.08	4.20	45.15	4.11
	27	9.02	2.95	2.39	1.40	51.82	5.95	49.13	2.80
in unpolluted plants, mg kg ⁻¹		0.1 - 5.0				25 - 150			

There was not significant difference among treatments, according to the Tukey's test ($p > 0.05$)

Maize (*Zea mays*)

In Figure 1 presents Zn content in maize in the sewage sludge compost experiment. Zn concentration was under 30 mg kg⁻¹ in the test plant. The quantity of Zn measured in maize was higher in the 9 t ha⁻¹ dose of compost treated plots in 2008.

In 2008 we did not find significant differences between the three treatments, as it is showed in Figure 2. Other researchers found significantly increased Ni concentration in the roots of the lettuce plants after compost application. The Ni concentration was particularly higher in the leaves of the control sample¹³. Quantity of Ni in the maize crop was lower than detection limit in 2009.

Triticale (*x Triticosecale Wittmack*)

Figure 3 shows Zn content of triticale crop in the sewage sludge compost experiment in 2008 and 2009. We can see that amount of Zn was increased in the treatments in 2008. Measurements by Chaney¹⁵ demonstrated that in plant tissue, the concentration of Zn was the highest in the compost treatment which reflect the high Zn concentrations in the compost material.

In the year 2009 the amount of Zn increased only in the 9 t ha⁻¹ treatment in comparison with the control plot, while the measured Zn concentrations of the other two treatments were similar to the concentrations of control samples. Figure 4 presents the Ni concentration in triticale in the sewage sludge compost treatment. Effect of compost treatment did not increase the amount of Ni in 2008.

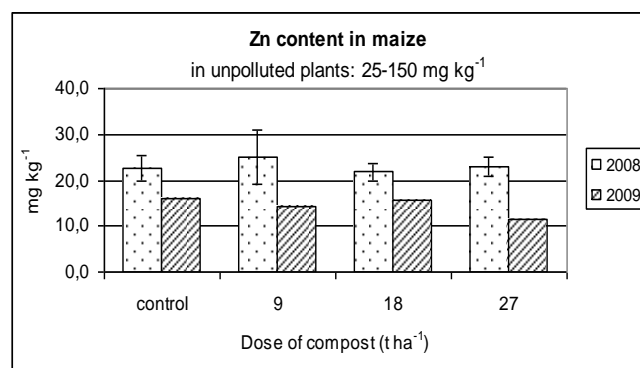


Figure 1. Zinc (Zn) content of maize in the sewage sludge compost experiment

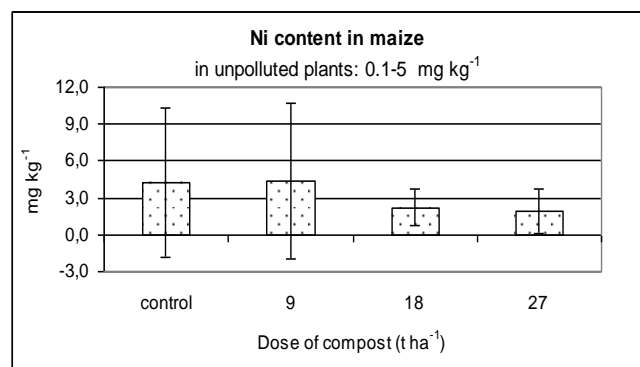


Figure 2. Nickel (Ni) content of maize in the sewage sludge compost experiment in 2008

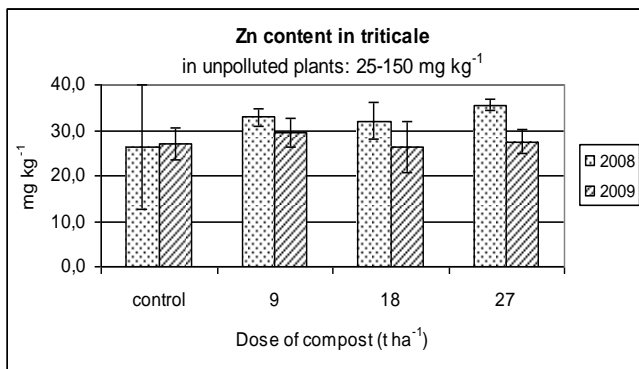


Figure 3. Zinc (Zn) content of triticale seed in the sewage sludge compost experiment

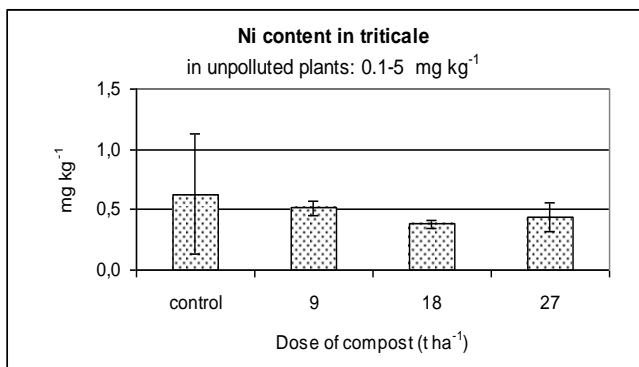


Figure 4. Nickel (Ni) content in triticale seed in the sewage sludge compost treatment in 2008

Similar to the Ni content of the corn, Ni content of triticale samples could not be measured in 2009.

Conclusion

Our results proved that the repeated use of composted sewage sludge for crop production did not cause any danger for agriculture and feed/food safety. We have not found toxic elements accumulation in the measured layers of the soil. The green pea accumulated Ni primarily in its root, which is important from food safety aspect, because it is not edible part of the plant. The other two test plants (triticale and maize) contain similar quantity of Zn in the grain while green pea concentrated this element in its grain with a higher quantity. The content of Zn and Ni were the lowest in the grain of maize.

Both measured elements were in the soil and plants, but these Zn and Ni did not accumulate hazardous in soil-plant chain. In conclusion it can be stated that the good quality and the circumspect application of the sewage sludge compost could guarantee its safe utilization.

References

- ¹Epstein, E., Taylor, J.M., Chaney, R.L., *J. Environ. Qual.* **1976**, 5 (4), 422–426.
- ²Sopper, W.E., *Municipal Sludge Use in Land Reclamation*. Lewis Publishers, Boca Raton. **1993**.
- ³Sort, X., Alcaniz, J.M. *Land Degrad. Dev.* **1996**, 7, 69–76.
- ⁴Debosz, K., Petersen, S.O., Kure, L.K., Ambus, P. *Appl. Soil Ecol.* **2002**, 19, 237–248.
- ⁵Riffaldi, R., Minzi, R. L., Pera, A. & de Bertoldi, M. *Waste Mgmt Res.* **1986**, 4, 387-396.
- ⁶Bevacqua, R. F., Mellano, V. J. *California Agric.* **1993**, 47(3), 22-24.
- ⁷Smith, S. R. *Journal of Horticultural. Sci.* **1992**, 67, 703-716.
- ⁸Tester, C. F. *Soil Sci.* **1990**, 148, 452-458.
- ⁹Senesi, G.S., Baldassarre, G., Senesi, N., Radina, B., *Chemosphere.* **1999**, 39, 343–377.
- ¹⁰Garcia, C., Hern~andez, T. & Costa, F. *Environmental Management.* **1991**, 15, 433-439.
- ¹¹Simon L. *Talajszennyeződés, talajtisztítás.* **1999**, 3-27.
- ¹²Zhang, M.; Heaney, D.; Solberg, E.; Heriquez, B. *Compost Science & Utilization.* **2000**, 8, 3, 224-235.
- ¹³Paola Castaldi; Giovanni Garau; Pietro Melis. *Fresenius Environmental Bulletin.* **2004**, 13, 11b, 1322-1328.
- ¹⁴Mylavarapu, R. S. and Zinati, G. M. *Scientia Horticulture.* **2009**, 120, 426-430.
- ¹⁵Chaney, R.L. *Land Treatment of Hazardous Wastes. Noyes Data Corp.* **1983**, 152–240.

Received: 31.10.2012.
Accepted: 20.11.2012.



MICROELEMENT CONTENT OF HERB VARIETIES ON A FLOODPLAIN PASTURE OF UPPER TISZA RIVER

Zoltán Győri^{[a]*}, Péter Sipos^[a], Diána Ungai^[a] and Norbert Boros^[b]

Paper was presented at the 4th International Symposium on Trace Elements in the Food Chain, Friends or Foes, 15-17 November, 2012, Visegrád, Hungary

Keywords: microelement content, pasture, herb

In order to produce good quality products it is necessary to find out about the quality of pastures to be grazed. It is also important to know the element composition of grazed herbs and the demands of animals bred on pastures, especially where the environment may influence the feed safety conditions of plants – as in the case of floodplains. Our objective was to determine that what the element composition (Cu, Zn, Mn and Fe contents) of herbs grown on a floodplain which was subsided by a heavy metal contaminated sediment. Our results call an attention to the differences in the accumulation of herbs. *Bidens tripartitus*, *Lotus corniculatus* and *Vicia cracca* grown in the floodplain showed the higher amounts of Fe and Zn, but the effect of heavy metal contamination on the element contents of other examined plants cannot be proved.

* Corresponding Authors

Tel: +36 (30) 983 2880

E-Mail: z.gyori@hotmail.com

- [a] Institute of Food Science, Quality Assurance and Microbiology, Faculty of Agricultural, Food Science and Environmental Management, University of Debrecen
 [b] Environmental and Chemical Engineering Department, Faculty of Engineering, University of Debrecen

Introduction

At the beginning of year 2000, dams broke at two Romanian mining companies (at Baia Mare first and Baia Borsa second). The first one releasing 100 000 m³ of contaminated water with cyanide to the river Tisza via its tributary Szamos. The heavy metal content of the polluted water was several times higher than the limits for heavily contaminated surface water (Ministry for Environment, 2000).¹ While the cyanide caused severe damage to organisms in the river, other heavy metals present in the water may also have been deposited in the sediments.

The second disaster sent about 20 000 tons of mud containing heavy metals into the river Tisza along with a simultaneous flood settling, forming a layer of approximately 5-10 cm in depth on the pre-existing soil (Fig. 1 and Fig. 2). As most of the affected areas were under agricultural use, and the economy of the region depends heavily on their continued productivity, it is important to study the heavy metal concentration within herbaceous plants in the floodplain.

The composition of herb varieties of a pasture is very important considering animal husbandry.² Mineral element composition is one of its most important quality parameters.³ However, pastures are often that kinds of fields that are close to rivers and its alluvial deposits cover them yearly. The heavy metal contamination of the flood of Tisza river in the year 2001 caused considerable injuries for the

ecosystem⁴, and the long-term effects of the metals settled in the floodplain are not known.

Our objective was to determine the element composition (Cu, Zn, Mn and Fe contents) of herbs grown on this exhaustively examined (to 300 cm depth) soil. The results of in-depth soil analysis were presented by Győri et al.⁵

We present the sediment analysis data on the Fig. 1 and Fig. 2. The samples came from the banks of the river and the terraces of the holiday houses, at the altitudes of 112.750 mB.a.; 114.670 mB.a.; 108.940 mB.a. and 105.450 mB.a. in samples 1 to 4 respectively. For comparison this data with a chernozem soil data we can see on Fig. 3. We have to underline that in the most fertile soil Zn and Cu content was twofold lower than in floodplain soil.

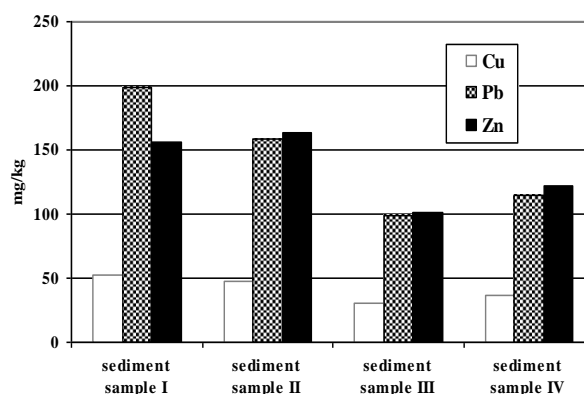


Figure 1 Total Cu, Pb and Zn content of sediment samples (Tivadar, 2001)

Considering that this 300 cm depth sediment of the floodplain subsided in the last 150 years, a control plot selection was almost impossible. This is the reason we used the results of Tölgyesi⁶ and also Hungarian measurement⁷ results by Leányvár for comparison.

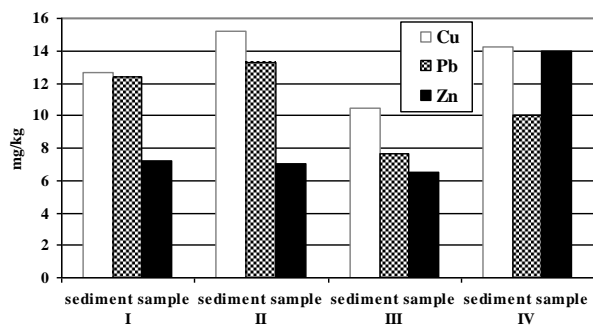


Figure 2. Lakanen-Erviö soluble Cu, Pb and Zn content of sediment samples (Tivadar, 2001)

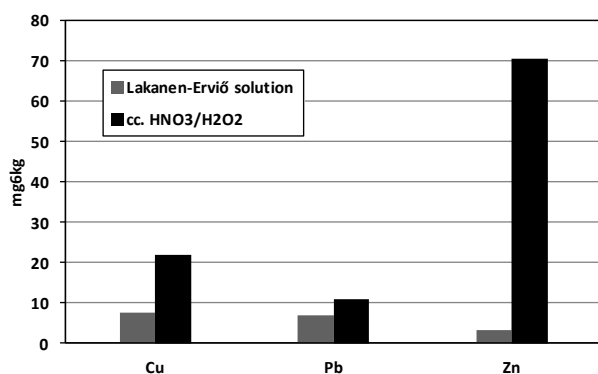


Figure 3. Lakanen-Erviö soluble and total Cu, Pb and Zn content of chernozem soil (Látókép, 1998)⁸

Materials and methods

Samples were taken in a floodplain meadow of upper the Tisza River near Tivadar and Gergelyugornya in 2001-2003. Samples of 42 herb varieties from natural flora were collected from 1x1 m plots (ten times) near the boreholes in the floodplain.



Figure 4. Sampling sites on the river Tisza, Hungary

Plant samples were dried at 60°C and grounded by Retsch SK-1 hammer mill with 1 mm sieve. The chemical analysis was carried out with analytical grade HNO₃-H₂O₂ (E. Merck, Darmstadt, Germany) digestion by the method of Kovács et al.^{9,10} by PERKIN-ELMER OPTIMA 3300 DV type ICP-OES (Inductively Coupled Plasma - Optical Emission

Spectrometry). Ultrapure water was used to prepare the solutions (Millipore, Paris, France). The easily available element contents extracted according to the Lakanen-Erviö method.¹¹

Table 1. Geographical data of sampling sites

Sampling site	Geographical coordinates	River kilometers
Tivadar	N 48° 04' 00.6" E 22° 31' 04.8"	708.7
Gergelyugornya	N 48° 07' 46.5" E 22° 19' 39.5"	683.0

We determined the following elements: Al, B, Ba, Ca, Cd, Co, Cr, Cu, Fe, K, La, Li, Mg, Mn, Mo, Na, Ni, P, S, and Zn. Out of the 20 elements examined, Cu, Fe, Mn, and Zn are discussed in detail in the present study. We used the SPSS 17.0 for Windows and Microsoft Excel 2007 programs for statistical analysis of data. Results are mean values of two replications.

Results and discussion

Previously Tölgyesi⁵ analyzed seventeen varieties in 1969, so this was the base of our comparison. We found that the newly measured Mn values representing the herb samples collected at Tivadar were lower than the previous findings at Leányvár exception of *Salvia nemorosa*, while the Zn content of new samples were higher in the case of most of the examined herbs.

These systematic differences are taken into account for the differences in the basic of soil properties or analytical methods. The differences in Cu and Fe content were varied by herb to herb (Table 1).

Comparing our results to the previous findings, we found significant differences in several cases. Tölgyesi⁵ found that *Solanum dulcamara*, *Symphytum officinale* and *Taraxacum officinale* accumulate Cu in high degree.

We confirmed these results and recommend that the list of Cu accumulating herbs can be complemented by *Salvia nemorosa* and *Bidens tripartitus*. We found high Fe content in the case of *Salvia nemorosa*, *Althea officinalis*, *Rumex acetosa* and *Solanum dulcamara* (above 500 mg kg⁻¹). The highest Mn contents were measured in the case of *Salvia nemorosa*, *Althea officinalis* and *Equisetum arvense* (in descending order). *Lotus corniculatus*, *Salvia nemorosa* and *Bidens tripartitus* contained the highest concentrations of Zn.

As we mentioned above we analyzed more than forty herb varieties from the floodplain of upper Tisza. The microelement contents of additional 21 herb varieties are summarized in Table 2.

The copper content in case of *Convolvulus arvensis* and *Ranunculus repens* were more than 25 mg kg⁻¹. These values were the maximum among the studied herb varieties. Two high iron contents (more than 600 mg kg⁻¹) were determined in case of *Cephalaria transsilvanica* and *Xanthium strumarium*.

Table 1 Mineral element content of different herbs Legend: L = Leányvár, 1963., T = Tivadar, 2001.

Herbs	Mineral elements mg kg ⁻¹ in dry matter							
	Cu		Fe		Mn		Zn	
	L	T	L	T	L	T	L	T
<i>Althea officinalis</i>	6.9	8.4	494	732	98	41.5	28	32.5
<i>Bidens tripartitus</i>	24.2	18.7	278	86.8	118	24.4	31	59.0
<i>Cichorium intybus</i>	12.1	11.3	209	296	35	18.5	35	44.4
<i>Equisetum arvense</i>	7.7	6.0	253	177	117	41	27	37.9
<i>Galium verum</i>	6.6	11.4	200	63.5	40	33.6	21	45.0
<i>Lotus corniculatus</i>	7.0	10.2	83	226	-	38.8	22	66.1
<i>Lathyrus tuberosus</i>	9.0	4.8	170	121	46	14.5	19	39.5
<i>Poa pratensis</i>	6.1	8.0	143	74	43	29.8	22	15.8
<i>Potentilla argentea</i>	5.4	7.12	362	171	96	38.9	22	29.6
<i>Ranunculus acris</i>	8.3	7.8	138	163	65	37.6	25	26
<i>Rumex acetosa</i>	4.7	8.7	145	572	37	26.3	25	23.1
<i>Salvia nemorosa</i>	9.2	17.5	369	869	56	67.1	44	61.8
<i>Solanum dulcamara</i>	15.4	14.8	315	509	91	33.1	20	31.7
<i>Sonchus arvensis</i>	15.7	10.2	754	154	49	25.6	63	55.4
<i>Symphytum officinale</i>	14.8	15.7	405	301	55	19.4	34	26.9
<i>Taraxacum officinale</i>	14.6	12.4	286	401	44	33.9	40	33.6
<i>Vicia cracca</i>	12.5	11.8	412	136	59	36.7	33	52.4

The manganese content of these varieties group was higher than in the recorded in previous table. Compare with the *Salvia nemorosa*'s manganese content we found that *Plantago major*, *Potentilla reptans*, *Trifolium repens*, and *Glechoma hederacum* are near 60 mg kg⁻¹ manganese.

Table 2 Microelement content of other herbs

Herbs	Mineral content [mg kg ⁻¹]			
	Cu	Fe	Mn	Zn
<i>Agrostis alba</i>	8.6	137	36.1	49.5
<i>Ambrosia elatior</i>	15.1	369	33.5	86.4
<i>Bromus arvensis</i>	4.9	74.6	44.8	7.6
<i>Cephalaria transsilvanica</i>	9.0	670	35.3	50.8
<i>Convolvulus arvensis</i>	29.6	249	48.5	385
<i>Glechoma hederacum</i>	9.8	330	59.6	93.5
<i>Lathyrus vernus</i>	8.3	151	28.4	49.4
<i>Lolium perenne</i>	5.5	208	33	42.6
<i>Matricaria maritima ssp. inodora</i>	11.6	217	35.6	48.5
<i>Plantago lanceolata</i>	9.9	159	25	71
<i>Plantago major</i>	7.3	317	61.5	18.2
<i>Potentilla anserina</i>	5.0	134	41.4	39.8
<i>Potentilla reptans</i>	7.6	180	62.3	54.9
<i>Ranunculus repens</i>	26.8	284	81.6	55.4
<i>Rorippa austriaca</i>	6.3	246	31.2	52.8
<i>Trifolium pratense</i>	12.1	130	32.1	29.4
<i>Trifolium repens</i>	9.7	446	62.2	24.3
<i>Vicia angustifolia</i>	8.3	173	30.6	31.1
<i>Vicia grandiflora</i>	8.9	381	37.9	38.7
<i>Vicia sepium</i>	8.6	421	50.7	32.7
<i>Xanthium strumarium</i>	12.0	638	38.7	32.2

It seems the *Ambrosia elatior*, *Glechoma hederacum*, and *Plantago lanceolata* varieties accumulate the zinc (more than 70 mg kg⁻¹).

We also investigated the mineral content of *Rorippa austriaca*. This variety was the first to grow from the drying up mud layer. Four places were the origin of samples out of which two came from the floodplain and two from arable fields. The iron, sulfur and the zinc content were higher in the floodplain samples (see Table 3). The zinc content of *Rorippa austriaca* was higher (50 mg/kg) with twenty percent in the floodplain samples.

Table 3. Mineral content of *Rorippa austriaca* samples from different sampling sites (2000)

Elements content, mg kg ⁻¹	Sampling sites			
	Csaroda	Beregsurány	Tivadar	Gergely-ugornya
B	25.2	28.5	33.5	27.6
Cd	<0.05	0.1	<0.05	<0.05
Cr	0.4	0.7	0.6	1.6
Cu	5.7	7.7	6.6	10.0
Fe	75.4	128	183	222
Li	0.7	0.9	0.9	0.8
Mg	1295	1837	1537	1138
Mn	20.8	28.5	22.7	23.9
Na	298	331	371	376
Ni	1.5	4.0	2.2	1.6
P	2243	2016	1834	2253
Pb	<0.02	<0.02	<0.02	<0.02
S	6957	7001	8515	8638
Zn	31.8	44.3	44.2+	55.1

This result demonstrates the high sulfur content of the new sediment contains sulfide and sulfate chemical form of zinc.

We analyzed the *Trifolium pratense* samples (Table 4) collected in different time to get information about the changing of mineral content time to time.

Table 4. The changing of mineral content during the vegetation period (*Trifolium pratense*)

Mineral content, mg kg ⁻¹	Sampling time		
	May	June	July
Al	97.6	108.5	34.7
Ba	14.4	19.8	15.1
Ca	10971	18025	9549
Cd	0.03	0.04	0.04
Co	0.07	0.1	<005
Cr	0.5	0.9	0.4
Cu	11.2	10.1	12.1
Fe	142	263	130
K	27446	19668	23888
La	0.4	0.4	0.1
Li	0.3	0.5	0.4
Mg	2828	3074	2398
Mn	30.9	38.4	32.1
Mo	0.6	1.0	0.5
Na	276	275	195
Ni	1.3	1.5	1.2
P	2401	2652	2872
S	1685	2254	1997
Zn	22.7	54.8	29.4

The copper content was very stabile during the sampling period. On the other hand the iron, calcium, manganese, and zinc content were higher in June than in May or July.

Conclusions

Comparing the plant varieties element by element we found that as regards several elements it was *Althea officinalis*, *Salvia nemorosa*, *Bidens tripartitus*, *Lotus corniculatus*, *Symphytum officinale*, *Taraxacum officinale* and *Vicia cracca* that accumulated high amount of studied elements.

In terms of micro-element contents we found these plants are the most valuable ones of the plant community we analyzed.

The heavy metal contamination on the studied varieties cannot be proved.

References

- ¹Ministry for Environment of the Republic of Hungary. *Preliminary evaluation of the cyanide pollution in the rivers Szamos and Tisza*. Directorate for Environmental Protection. 2000.
- ²Kádár, I. *Gyepgazdálkodási Közlet.*, **2004**, 2, 57-65.
- ³Brekken, A., Steinnes, E., *Sci. Total Environ.*, **2004**, 326(1-3), 181-195.
- ⁴Győri, Z., Alapi, K., Szilágyi, Sz. In: *Natural Attenuation of metals along the Tisza River-Floodplain-Wetlands Continuum*. Eds: Adriano, D. C., Németh, T., Győri, Z. Debrecen: University of Georgia - MTA TAKI - DE ATC, **2003**, 146-161.
- ⁵Győri Z., Alapi K., Prokisch, J., Németh, T., Adriano, D., Sipos, P. *Agrochem. Soil Sci.*, **2010**, 59(1), 117-124.
- ⁶Tölgyesi, Gy., *A növények mikroelem-tartalma és ennek mezőgazdasági vonatkozásai*. Mezőgazdasági Kiadó Budapest, **1969**, 198.
- ⁷Tölgyesi, Gy., Haraszti, E., *Agrochem. Soil Sci.*, **1970**, 19(4), 521-530.
- ⁸Győri Z. *D.Sc. Thesis*, MTA, **1999**, 197.
- ⁹Kovács, B., Dániel, P., Győri Z., Loch, J., Prokisch, J. *Commun. Soil Sci. Plant Anal.*, **1998**, 29, 2035-2054.
- ¹⁰Kovács, B., Győri, Z., Prokisch, J., Loch, J., Dániel, P. *Commun. Soil Sci. Plant Anal.*, **1996**, 27, 1177-1198.
- ¹¹Lakanen, E., Erviö, R. *FAO Soils Bulletin*, **1982**, 10.

Received: 16.10.2012.

Accepted: 14.11.2011.

:



BIOAVAILABILITY OF TRACE METALS IN TERRESTRIAL ENVIRONMENT: METHODOLOGICAL ISSUES

Marija Romić^[a]

Paper was presented at the 4th International Symposium on Trace Elements in the Food Chain, Friends or Foes, 15-17 November, 2012, Visegrád, Hungary

Keywords: Soil contamination, Metal speciation, Chemical extraction; Fractionation, Potential mobility.

Beside anthropogenic sources, trace metals can be found in the parent material from which the soils develop. Whether these inputs will become toxic and to what extent mobility depends upon a number of factors: specific chemical and physical trace metal characteristics, soil type, land use, geomorphological characteristics within the soil type and exposure to emission sources. Processes that control the mobility, transformation and toxicity of metals in soil are of special importance in the soil root developing zone – the rhizosphere. For this reason, there is a considerable interest in understanding trace metals behaviour in soil, with special emphasis on the way they enter the soil and on processes by which plants take them up. Full understanding and prediction of chemical behaviour of an element in the environment is possible only by identification of all forms in which that element can be found under different environmental conditions. Various chemical methods, geochemical models and biotests are used for assessment of the bioavailable metal fraction in soil. However, these methods are not universally applicable for all elements and different soil characteristics. Chemical methods for assessment of metal bioavailability are commonly grouped within methods for identification of total metal content in soil, methods for assessment of currently available and potentially available fractions, methods for prediction of metal speciation in soil solution. This article offers a critical review of methodologies available for assessing metal speciation in solid and liquid phases in soils taking into consideration the array of parameters that might influence uptake and effects upon the plant.

Corresponding Author

Fax: +38512394099

E-Mail: mromic@agr.hr

University of Zagreb Faculty of Agriculture, Dept. of Amelioration, Svetosimunska 25, 10000 Zagreb, Croatia

Introduction

Two thirds of all elements found in nature are metals. According to their chemical definition, metals are elements and as such cannot be synthesized or degraded by biological or chemical processes, though these processes can change chemical forms of metals. Metals are contained in the Earth's crust and in parent rocks. By weathering of rocks soils are formed, so their presence differs in different geographic regions. Terms like heavy metals, metalloids and microelements are the most commonly encountered in ecological studies. Among the 96 known metals, 17 are semimetals or metalloids (e.g., B, Si, Ge, As, Sn, Te, Po ...). The term heavy metal refers to a group of 53 metals with density higher than 5 g/cm³. From the geochemical point of view, trace elements are metals whose percentage in rock composition does not exceed 0.1% (e.g., Cu, Cr, F, Fe, Mo, Ni, Se, Zn, As, Cd, Hg, Pb). In very small amounts, some of these elements are essential for normal growth and development of living organisms and they are, from the physiological aspect, called micronutrients or microelements (e.g., Fe, Mn, Zn, Cu, Mo, Ni, Se), while others are toxic even in small concentrations¹. The issue of toxicity is usually simply a matter of quantity, with the range varying for each element. The concentration of metals in uncontaminated soil primarily depends upon the chemical composition of the parent material from which the soil was formed.

Metals are chemically very reactive in the environment, which results in their mobility and bioavailability to living organisms. Metals can be present in all environmental compartments as different species, with the parent element associating with different ligands, but never being irreversibly transformed or metabolized, and in those terms metals are different from organic compounds. People can be exposed to high levels of toxic metals by inhaling air, drinking water, or eating food products that contains them. As a consequence, metals get into the human body by different routes - by inhaling, over skin, and ingestion of contaminated food via food chain. The issue of toxicity is usually simply a matter of quantity, with the range varying for each element.

Trace metals occur naturally in rocks and soils, but increasingly higher quantities of them are being released into the environment by anthropogenic activities. There are environments (or areas) in which anthropogenic loading of trace metals puts ecosystems and their inhabitants at a health risk. Repeated use of metal-rich chemicals, fertilizers, and organic amendments such as sewage sludge and wastewater may cause contamination at a larger scale. So far, it is believed that most soils in Europe², have not been significantly rich in trace metals by anthropogenic activity. This is changing as livestock production expands, fertilizer application increases, and bio-solids and effluent applications to agricultural soils become more common. Increased concentration of Cu and Zn in soils under long-term production of grapevine, citrus and other fruit crops have been recorded in various studies^{3,4,5,6}. Phosphate and micronutrient fertilizers contain potentially harmful trace elements, such as arsenic (As), cadmium (Cd), and lead (Pb). Chen et al.⁷ observed significant correlations between Cd and Pb and soil phosphorus in California vegetable

croplands, indicating the application of P-fertilizers contributes significantly to the accumulation of Cd and Pb in soils. Romić et al.⁸ pointed out that the application of P-fertilizers also contributes significantly to the accumulation of Cd in horticultural soils of fluvial terraces in the Croatian coastal region.

The focus of this overview is methodologies available for assessing metal speciation in solid and liquid phases in soils to study the origin and fate of these metals in terrestrial environments.

Metal bioavailability approach

The concepts of «Bio-availability» and «Bio-accessibility» were introduced to express whether the actual concentration of a toxic element would have effects on organisms⁹. The main challenge that comes out from the assessment of loads of trace and toxic metals is the methodology of determination or prediction of the trace element content in a soil that results in toxicity.

Metal-soil interaction is such that when metals are introduced at the soil surface, their mobilisation does not occur to any great extent unless the metal retention capacity of the soil is overloaded, or metal interaction with the associated waste matrix enhances mobility¹⁰. The impact of trace metals on soil and the surrounding environment mostly cannot be predicted simply by measuring the total concentration. This is because only the soluble and mobile fractions have the potential to leach or to be taken up by plants and enter the food chain.

Metal bioavailability is a complex issue that depends on a series of properties pertaining to the soil matrix, plant properties and environmental conditions. Different definitions and uses of the term metal bioavailability can be found in scientific literature, but most of them refer to the proportion of total metals that are available for incorporation into biota. The issue of bioavailability and bio-accessibility often determines whether or not the concentration at which a chemical is present will have effects on organisms. Peijnenburg and Jager¹¹ define «bio-available fraction» as the fraction of the total amount of a chemical present in a specific environmental compartment that, within a given span of time, is either available or can be made available for uptake by micro-organisms or plants, from either the direct surrounding of the organisms or the plant, or by intake in food.

Distribution, mobility, bioavailability and toxicity of metals depend not only on metal species and concentration but also on the form in which metals exist in soil. Full understanding and prediction of chemical behaviour of an element in the terrestrial environment is possible only by identification of all forms in which that element can be found in soil under different environmental conditions.

Metal speciation is one of the most important properties that determine the behaviour and toxicity of metals in the environment. Chemical speciation of an element refers to its specific form characterized by a different isotopic composition, molecular structure, and electronic or oxidation state¹². Speciation is the process of identification and determination of different chemical and physical forms

of elements present in a sample¹³. Metals that occur in cationic forms have a higher ability of binding to negatively charged soil colloids, and are thus less bioavailable, but more easily accumulate in soil, unlike the anionic forms that are mainly present in soil solution and are more bioavailable, but are more readily leached from the soil.

Soil extraction methods

Soil properties, speciation of trace metals and transfer mechanisms between trophic levels (like human intake of Cd from plant seeds that is limited by nutritional factors) have to be characterized to assess the bioavailability of metals and to get the respective data gaps filled in. Major soil properties that affect changes in metal speciation, and thereby also their fractionation, are soil pH^{14,15}, redox-potential¹⁶, soil mineralogy^{17, 18} and existence of different organic and inorganic reactants – ligands^{19,20}.

Metals that occur in cationic forms have a higher ability of binding to negatively charged soil colloids, and are thus less bioavailable, but more easily accumulate in soil, unlike the anionic forms that are mainly present in soil solution and are more bioavailable, but are more readily leached from the soil. Various metals distribute them differently among fractions of soil solid and liquid phases. Several forms of trace metals in soils can be emphasised:

- *Soil solution forms* (ionic, molecular, chelated and colloidal forms), characterized by high metal mobility.
- *Ions at the exchange interface*, non-selectively sorbed, readily exchangeable ions in inorganic or organic fractions;
- *Ions specifically sorbed by inorganic colloids*, more firmly bound ions, medium mobility;
- *Ions complexed or chelated by organic colloids*, as well as elements present in decomposing organic materials and the soil biomass, medium to high mobility because of the decomposition of organic matter with time;
- *Ions occluded by, or structural components of, secondary minerals and other inorganic compounds*; strongly dependant on environmental conditions, medium metal mobility
- *Elements incorporated in precipitated sesquioxides and insoluble salts*, or fixed in crystal lattices of clay minerals, or present in the structure of primary minerals; low metal mobility, available after weathering or decomposition.

Single chemical extractions

All fractions of metals are in dynamic equilibrium, and only metals in aqueous soil solution are directly available to biota. Soil solution is in direct contact with the soil solid phase and transformations going on in it are a consequence of mineral equilibrium, exchange processes and sorption processes in the soil mineral phase and organic matter, as well as complex formation with organic matter in the solid phase and in solution²¹. The concentration of metals in the soil solution, at any given time, is governed by a number of interrelated processes, including inorganic and organic complex formation, oxidation-reduction, precipitation

/dissolution and adsorption / desorption reactions respectively. McLean and Bledsoe²² emphasize the importance of the accuracy with which the multiphase equilibria can be determined or calculated for the prediction of the concentration of a given metal in the soil solution.

Most assessments of metal availability have involved single chemical extractants (e.g. EDTA, DTPA, acetic acid, diluted inorganic acids) intended to remove the entire reservoir of reactive metal and have been used primarily in soil fertility assessment. Single chemical extractions provide inexpensive and rapid assessment methods, and they are generally used to assess available amounts of soil metals and usually aim to extract the water-soluble, easily exchangeable and some of organically bound metals. For example, dilute salt solutions of replacing cations, such as $MgCl_2$, $CaCl_2$, $NaNO_3$, are commonly used to extract the soluble and easily replacing cations.

Dilute HCl is one of the most widely used reagents, in techniques which employ acid solutions to isolate the non-residual phase, in a variety of solid environmental media, and it is assumed to extract metals on exchange sites, due to its acidic properties²³. Several studies suggest that HCl extraction might lead to overestimation of soil available metals²⁴ or that its correlation with metal plant uptake is generally low²⁵.

Single chemical extractability of trace metals by using 0.43 M HNO_3 appeared strongly related to the estimated anthropogenic enrichment and therefore used to assess the hazard of human-induced enrichment of Cd, Cu, Pb and Zn²⁶. The procedure recommended for estimation of “mobile fraction” indicating the “potential availability” has been standardized within the framework of harmonization of leaching procedures for risk assessment of trace metals in soils²⁷.

Diethylenetriaminepentaacetic acid (DTPA) is a potent synthetic chelating agent, and the method of extraction with DTPA was developed for the purpose of determining zinc, iron, manganese or copper deficiency in neutral and carbonate soils²⁸. Haq and Miller²⁹ reported negative results of the DTPA test, which they explained by their failure to determine important significant relations between concentrations of metals (copper and manganese) extracted from soil and those found in the tested plants. O'Connor³⁰ gave a number of comments on the DTPA test, based also on non-significant correlation between DTPA-extractable metals in soil and their concentrations in plants. Regardless of the above considerations, DTPA is the most widely used agent for extraction of “available” cadmium, copper, nickel and zinc, and thereby also the most standardized one^{31,32,33}. Starting from the fact that the data on total copper content reveals very little about its bio-availability, such strong correlation between copper extracted with *aqua regia* and DTPA actually indicates that neither the latter extraction method is suitable for assessing copper availability to plants.

Romic et al.³⁴ applied multiple linear regression analysis to establish the relation between copper fractions after particular single extractions (*aqua regia*, DTPA and $CaCl_2$) and soil properties that may affect their behavior in soil and availability to plants. Most of the colloidal particles in soil strongly adsorb copper, which forms stronger organic

complexes than other bivalent transition metals and therefore soils rich in organic matter can retain it more, without causing plant toxicity. As shown in Table 1, DTPA-extractable copper was largely explained by the total copper contents, but it was also found that the DTPA-extractable copper decreased with increasing cation exchange capacity of soil.

Table 1. Linear regression of DTPA-extractable (Cu_{DTPA}) as a function of $CaCl_2$ -extractable (Cu_{CaCl_2}) and soil organic matter (Org.C)³⁵.

Source of variation	Degree of freedom	Sum of squares	F	Pr > F
Cu_{CaCl_2}	1	685.7	240.0	0.0000
Org.C	1	44.54	15.59	0.0002
Total	63	1224		

In the same study, two parameters were included into the regression model of $CaCl_2$ -extractible copper: organic matter content (Org-C) and pH, and the model explains 62% of total variance (Table 2). Concentrations of $CaCl_2$ -extractible copper mainly depend on pH, which relation was also confirmed by this investigation. However, since these are predominantly alkaline soils, this relation is not as strong as in the case of soils with a more varying pH³⁶.

Soil extraction 0.01 M $CaCl_2$ is the method that was increasingly used in the last decades for soil testing to determine soil fertility and the behaviour of nutrients and contaminants in it^{37,38}. Due to the availability of advance instrumental techniques it has become possible to determine very low concentrations of nutrients and pollutants in soil extracts. The advantage of this method for determining metal concentrations in soil is that the concentration of electrolytes stays practically constant and metal concentrations reflect the difference in binding strength or solubility between soils. The extractant is an un-buffered solution and therefore the measured metals reflect their availability at the pH of the soil. The best criterion of the efficiency of the method for determining the soil bio-available fraction is the high correlation between the Cu content observed in plants grown in situ, at least for neutral to acid soils³⁹.

Peijnenburg et al.⁴⁰ gave the comprehensive overview of empirical methods for extraction of metals from soils and noted that, depending on the purpose of the study, information on general soil properties is needed to properly interpret the results of any extraction.

Sequential extraction procedures

Changes in soil conditions may cause trace metal mobilization and favour the contamination of surrounding environmental compartments. Major soil properties that affect changes in metal speciation, and thereby also their fractionation, are soil pH, redox-potential, and existence of different organic and inorganic reactants – ligands. Therefore, identification of the main binding sites and phase associations of soil trace metals is needed to evaluate their remobilisation potential and the risks induced⁴¹.

The sequences of different chemical extractions, usually starting with the weakest, least aggressive and ending with

the strongest and most aggressive, are commonly used to quantify the different fractions of metal retention in soils. Despite the fact that the procedures have been widely used since early 1970s⁴², many questions regarding the uniformity in procedures, problems of poor selectivity, redistribution during extraction, and the dependency of results on operating conditions have been still frequently raised^{43,44,45}. The principal advantage claimed for sequential extraction over the use of single extractants is that phase specificity is improved. One of the most widely-applied extraction procedures proposed by Tessier et al.⁴⁶ distributes metals into five operationally – defined chemical fractions:

Exchangeable fraction

Metals extracted are weakly-sorbed species, retained on the soils surface by relatively weak electrostatic interactions or those released by ion-exchange processes, commonly extracted using dilute salt solutions of replacing cations (MgCl₂, CaCl₂, NH₄NO₃, NH₄-acetate).

Acid-soluble fraction

Metals bound to carbonates, susceptible to changes of pH, a buffered acetic acid/sodium acetate solution generally used.

Fraction bound to hydrous oxides of Fe, Mn and Al

Iron and manganese oxides exist in soil as nodules, concretions, cement between particles or coatings on them; these oxides bond trace metals and their dissolution rate is controlled by Eh and pH of reagents used; reducing agents such as ammonium oxalate, hydroxylamine and sodium dithionite have been mostly used to release metals bound in oxides.

Fraction bound to organic matter

Soil trace metals are bound to various form of soil organic matter, and organically bound fraction may be released using oxidising agents such as hydrogen peroxide, pyrophosphate or sodium hypochlorite.

Residual fraction

Residual fraction basically contain primary and secondary minerals holding metals within their crystal structure; strong, concentrated or boiling nitric acid, with or without hydrofluoric acid or perchloric acid, have been used to assess occluded metals in soil.

Selective sequential extraction was applied to investigate the potential of mobilizing trace metals in agricultural soils of Northwestern Croatia⁴⁷. In alluvial soils developed on Quaternary (Upper Pliocene to Holocene) deposits, extraction with 1M Mg(NO₃)₂ (pH 7)⁴⁸ indicated possible remobilization of elements from the solid phase into soil solution, particularly in the case of copper. There are several possible mechanisms that increase solubility of metals in the surface layer: 1) the soil mineral component is more susceptible to weathering in shallower than in deeper soil layers owing to faster infiltration of precipitation, higher biological activity and greater changes in temperature; 2) shallower soil horizons are richer in organic matter, which can stimulate metal desorption by formation of soluble organic complexes; and 3) exchangeable complex of shallower soil layers contains more basic cations (Na⁺, K⁺, Ca²⁺, Mg²⁺), which can also reduce sorption of metals by increasing the competition for exchange sites. All these processes are even more pronounced in the anthropogenic horizon of arable soils.

Table 2. The partitioning of metals among different extraction reagents in selective extraction of soil samples and comparison with *aqua regia* extraction

Metal	Soil depth, cm	Exchangeable Metal concentration, (EXC), mg kg ⁻¹	Carbonates, (CARB), %	Fe/Mn oxides, (OXD), %	Organic matter, (ORG), %	Residue, (RES), %	Total extract by aqua regia, %	Total extract, by SSE, %	RE ¹
Cr	0-25	n.d.	0,2	0,51	2,05	35,06	33,79	37,82	10,7
	25-40	n.d.	0,2	0,51	1,02	37,1	34,82	38,83	10,3
	40-100	n.d.	0,21	1,03	1,03	42,63	39,22	44,9	12,7
Cu	0-25	2,05	2,05	1,02	4,61	11,3	18,43	20,99	12,2
	25-40	2,25	2,25	1,02	1,54	13,3	17,41	20,37	14,5
	40-100	1,86	2,89	1,03	0,52	17,5	21,67	23,84	9,1
Ni	0-25	0,41	0,2	1,54	2,56	25,6	28,67	30,31	5,4
	25-40	0,2	n.d.	1,02	2,56	29,7	31,74	33,48	5,2
	40-100	0,62	0,21	1,55	2,58	36,1	39,22	41,08	4,5
Pb	0-25	0,82	3,28	4,61	5,12	20,48	35,84	34,31	-4,5
	25-40	0,82	1,64	2,05	0,51	18,43	26,62	23,45	-13,5
	40-100	0,62	1,86	3,61	1,55	19,61	28,9	27,25	-6,1
Zn	0-25	4,3	5,94	5,63	4,1	64,5	78,85	84,48	6,7
	25-40	4,3	2,66	2,05	3,07	58,4	69,63	70,45	1,2
	40-100	3,51	2,68	2,58	3,1	56,8	71,21	68,63	-3,8

¹RE (%) = (Total extracted by SSE – Total extracted by *aqua regia*) * 100 / Total extracted by *aqua regia*

Table 2 shows the distribution of metals among the defined geochemical fractions of the studied soil. Only a small portion of metals (less than 6% for zinc and less than 4% for copper) was in the exchangeable fraction. A significant portion of copper and lead was associated with the organic fraction, in agreement with the known affinity of Cu for organic matter. Metal fractions of Pb and Zn associated with the oxides reflect the dynamic of eluviation processes within the soil profile. Metals were mostly associated with the residual fraction.

Table 2. The partitioning of metals among different extraction reagents in selective extraction of soil samples and comparison with *aqua regia* extraction

The authors concluded from this study that the relative mobility of the metals is as followed: Cu>Zn>Pb>Ni>Cr.

Conclusions

The most common observation in most of the articles that study sequential or partial extraction of soil trace metals is that they are not completely specific to metals or chemical phases. The complexity of bioavailability phenomenon comes out from an array of matrix-related⁴⁹, species-related⁵⁰ and metal-related⁵¹ issues.

Generally, most of the laboratory methods for evaluating bioavailability of metals in soil overestimate actual available fraction. Therefore, further studies using biota have to be performed to understand the contribution of biological factors that control bioaccumulation and toxicity of trace metals.

References

- ^{1,21}Zovko, M., Romić, M., *Earth and Environmental Sciences*, **2011**, InTech, 437.
- ²Osborn, I., Edwards, A.C., Witter, E., Oenema, O., Ivarsson, K., Witherse, P.J.A., Nilssona, S.I., Richert Stinzing, A., *Eur J Agron*, 2003, 20 211.
- ³Chaignon, V., Sanchez-Neira, I., Herrmann, P., Jaillard, B., Hinsinger, P., *Environ. Pollut*, 2003, 123, 229.
- ^{4,33,34}Romic, M., Romic, D., Ondrasek, G., *Agriculturae Conspectus Scientificus*, 2004, 69, 35.
- ⁵Hung-Yu, L., Kai-Wei, J., Bo-Ching, Ch., *Soil Sci Plant Nutr*, 2010, 56, 601.
- ⁶Romic, M., Zovko, M., Romic, D., Bakic, H., *Commun Soil Sci Plan*. 2011, 43, 209.
- ⁷Chen, W., Krage, N., Wu, L., Pan, G., Khosrivafard, M., Chang, A.C., *J Environ Qual* 2008, 37, 689.
- ⁸Romic, D., Romic, M., Zovko, M., Bakic, H., Ondrasek, G., *Environ Geochem Hlth*, 2012, 34, 399.
- ^{9, 11,40,44,49}Peijnenburg, W.J.G.M., Jager, T., *Ecotox Environ Safe*, 2003, 56, 63.
- ¹⁰McLean, J.E. and B.E. Bledsoe (1992). *Behavior of materials in soils*. U.S. EPA, EPA/540/S-92/018. Robert S. Kerr Laboratory, Ada, OK
- ¹²Manouchehri, N., Besancon, S., Bermond, A., *Anal Chim Acta*, 2006, 559, 105.
- ¹³Wang, G., Su, M., Chen, Y., Lin, F., Luo, D., Gao, S., *Environ Poll*, 2006, 144: 127–135
- Davranche, M., Bollinger, J.C., *J Environ Qual*, 2001, 30, 1581.
- ¹⁴Cavallaro, N., McBride, M.B., *Soil Sc Soc Am J*, 1980, 44, 729.
- ¹⁵Green, C. H., Heil, D. M., Cardon, G.E., Butters, G.L., and Kelly, E.F. *J Environ Qual*, 2003, 32, 1323.
- ¹⁷Kuo, S., *Soil Sci Soc Am J*, 1986, 50, 1412.
- ¹⁸Lindroos, A.J., Brugger, T., Derome, J., Derome, K., *Water Air Soil Poll*, 2003, 149, 269.
- ¹⁹Ziper, C., Komarneni, S., Baker, D.E., *Soil Sci Soc Am J*, 1988, 52, 49.
- ²⁰Neuman, G., *Nutrient Cycling in Terrestrial Ecosystems, Series: Soil Biology*, 2007, 10, 123.
- ²²McLean, J.E., B.E., Bledsoe, U.S. EPA, EPA/540/S-92/018., 1992, Robert S. Kerr Laboratory, Ada, OK
- ^{23,45,51}Leleyter, L., Rousseau, Ch., Biree, L., Baraud F., *J Geochem Explor*, 2012,116-117: 51-59.
- ²⁴ Yu, S., He, Z.L., Huang, C.Y., Chen, G.C., Calvert, D.V., *Geoderma*, 2004, 23, 163.
- ²⁵Menzies, N.W., Donn, M.J., Kopittke, P.M., *Environ Pollut*, 2007, 145, 121.
- ²⁶Spijker, J., Mol G., Posthuma, L. Regional ecotoxicological hazards associated with anthropogenic enrichment of heavy metals. *Environ Geochem Hlth*, 2011, 33, 409.
- ²⁷Quevauviller, Ph., *Trends Anal Chem*, 1998, 17, 289.
- ²⁸Lindsay, W.L., Norvell, W.A., *Soil Soil Sci Soc Am J*, 1978, 42, 421.
- ²⁹Haq, A.U., Miller, M.H., *Agron J*, 1972, 64, 779.
- ³⁰O'Connor, G.A., *J Environ Qual*, 1988, 17, 715.
- ³¹Singh, B.R., Myhr, K., *Geoderma*, 1998, 84, 185.
- ³²ISO/DIS 14870, International Organisation for Standardisation, 1997.
- ³³Amacher, M.C., *Methods of Soil Analysis. Part 3-Chemical Methods*. SSSA-ASA Publ., Madison, USA, 1996, 739.
- ^{34,35}Romic, M., Romic, D., Ondrasek, G., *Agriculturae Conspectus Scientificus*, 2004, 69, 35.
- ^{36,39}Brun, L.A., Maillet, J., Richarte, J., Herrmann, P., Remy, J.C., *Environ Pollut*, 1998, 102, 151.
- ³⁷Novozamsky, I., Lexmond, T.H.M., Houba, V.J.G., *Int J Environ An Ch*, 1993, 51, 47.
- ³⁸Pueyo M., López-Sánchez J.F., Rauret G., *Anal Chim Acta*, 2004, 504: 217–226.
- ⁴¹Sutherland, R. A., Tack, F. M. G., Tolosa C. A., Verloo, M. G., *J Environ Qual*, 2000, 29, 1431.
- ^{42,46}Tessier, A., Campbell P.G.C., Bisson M., *Anal Chem*, 1979, 51, 844.
- ⁴³Shiowatana, J., Tantidanaib, N., Nookabkaewb S., Nacapricha D., *J Environ Qual*, 2001, 30:1195.
- Romic M., *Land and water management for sustained agriculture*. Course book. University of Zagreb Faculty of Agriculture. Zagreb. 2009, (in Croatian).
- ⁴⁷Romić M., Romić D., *Environ Geol*, 2003, 43, 795.
- ⁴⁸Shuman, L.M., *Soil Sci*, 1985, 140, 11.
- ⁵⁰Morera, M.T., Echeverría, J.C., Mazkiarán, C., Garrido, J.J., *Environ Pollut*, 2001, 113, 135.

Received: 19.10.2012.
Accepted: 21.11.2012.

